

JPTM

Journal of Pathology
and Translational Medicine

July 2021
Vol. 55 / No.4
jpatholtm.org
pISSN: 2383-7837
eISSN: 2383-7845



*Standardized Pathologic
Diagnosis of Appendiceal
Mucinous Neoplasm*

Aims & Scope

The *Journal of Pathology and Translational Medicine* is an open venue for the rapid publication of major achievements in various fields of pathology, cytopathology, and biomedical and translational research. The Journal aims to share new insights into the molecular and cellular mechanisms of human diseases and to report major advances in both experimental and clinical medicine, with a particular emphasis on translational research. The investigations of human cells and tissues using high-dimensional biology techniques such as genomics and proteomics will be given a high priority. Articles on stem cell biology are also welcome. The categories of manuscript include original articles, review and perspective articles, case studies, brief case reports, and letters to the editor.

Subscription Information

To subscribe to this journal, please contact the Korean Society of Pathologists/the Korean Society for Cytopathology. Full text PDF files are also available at the official website (<https://jpatholtm.org>). *Journal of Pathology and Translational Medicine* is indexed by Emerging Sources Citation Index (ESCI), PubMed, PubMed Central, Scopus, KoreaMed, KoMCI, WPRIM, Directory of Open Access Journals (DOAJ), and CrossRef. Circulation number per issue is 50.

Editors-in-Chief

Jung, Chan Kwon, MD (*The Catholic University of Korea, Korea*) <https://orcid.org/0000-0001-6843-3708>

Park, So Yeon, MD (*Seoul National University, Korea*) <https://orcid.org/0000-0002-0299-7268>

Associate Editors

Shin, Eunah, MD (*Yongin Severance Hospital, Yonsei University, Korea*) <https://orcid.org/0000-0001-5961-3563>

Kim, Haeryoung, MD (*Seoul National University, Korea*) <https://orcid.org/0000-0002-4205-9081>

Bychkov, Andrey, MD (*Kameda Medical Center, Japan; Nagasaki University Hospital, Japan*) <https://orcid.org/0000-0002-4203-5696>

Editorial Board

Avila-Casado, Maria del Carmen, MD (*University of Toronto, Toronto General Hospital UHN, Canada*)

Bae, Young Kyung, MD (*Yeungnam University, Korea*)

Bongiovanni, Massimo, MD (*Lausanne University Hospital, Switzerland*)

Bova, G. Steven, MD (*University of Tampere, Finland*)

Choi, Joon Hyuk, MD (*Yeungnam University, Korea*)

Chong, Yo Sep, MD (*The Catholic University of Korea, Korea*)

Chung, Jin-Haeng, MD (*Seoul National University, Korea*)

Fadda, Guido, MD (*Catholic University of Rome-Foundation Agostino Gemelli University Hospital, Italy*)

Fukushima, Noriyoshi, MD (*Jichi Medical University, Japan*)

Go, Heounjeong, MD (*University of Ulsan, Korea*)

Hong, Soon Won, MD (*Yonsei University, Korea*)

Jain, Deepali, MD (*All India Institute of Medical Sciences, India*)

Kakudo, Kennichi, MD (*Izumi City General Hospital, Japan*)

Kim, Jang-Hee, MD (*Ajou University, Korea*)

Kim, Jung Ho, MD (*Seoul National University, Korea*)

Kim, Se Hoon, MD (*Yonsei University, Korea*)

Komuta, Mina, MD (*Keio University, Tokyo, Japan*)

Kwon, Ji Eun, MD (*Ajou University, Korea*)

Lai, Chiung-Ru, MD (*Taipei Veterans General Hospital, Taiwan*)

Lee, C. Soon, MD (*University of Western Sydney, Australia*)

Lee, Hye Seung, MD (*Seoul National University, Korea*)

Lee, Sung Hak, MD (*The Catholic University, Korea*)

Liu, Zhiyan, MD (*Shanghai Jiao Tong University, China*)

Lkhagvadorj, Sayamaa, MD (*Mongolian National University of Medical Sciences, Mongolia*)

Moran, Cesar, MD (*MD Anderson Cancer Center, U.S.A.*)

Paik, Jin Ho, MD (*Seoul National University, Korea*)

Park, Jeong Hwan, MD (*Seoul National University, Korea*)

Ro, Jae Y., MD (*Cornell University, The Methodist Hospital, U.S.A.*)

Sakhuja, Puja, MD (*Govind Ballabh Pant Hospital, India*)

Shahid, Pervez, MD (*Aga Khan University, Pakistan*)

Song, Joon Seon, MD (*University of Ulsan, Korea*)

Tan, Puay Hoon, MD (*National University of Singapore, Singapore*)

Than, Nandor Gabor, MD (*Semmelweis University, Hungary*)

Tse, Gary M., MD (*The Chinese University of Hong Kong, Hong Kong*)

Yatabe, Yasushi, MD (*Aichi Cancer Center, Japan*)

Zhu, Yun, MD (*Jiangsu Institution of Nuclear Medicine, China*)

Ethic Editor

Choi, In-Hong, MD (*Yonsei University, Korea*)

Huh, Sun, MD (*Hallym University, Korea*)

Statistics Editors

Kim, Dong Wook, MD (*National Health Insurance Service Ilsan Hospital, Korea*)

Lee, Hye Sun, MD (*Yonsei University, Korea*)

Manuscript Editor

Chang, Soo-Hee, MD (*InfoLumi Co., Korea*)

Layout Editor

Kim, Haeja, MD (*iMiS Company Co., Ltd., Korea*)

Website and JATS XML File Producers

Cho, Yoonsang, MD (*M2Community Co., Korea*)

Im, Jeonghee, MD (*M2Community Co., Korea*)

Administrative Assistants

Jung, Ji Young, MD (*The Korean Society of Pathologists*)

Jeon, Anmi, MD (*The Korean Society for Cytopathology*)

Contact the Korean Society of Pathologists/the Korean Society for Cytopathology

Publishers: Cho, Nam Hoon, MD, Gong, Gyungyub, MD

Editors-in-Chief: Jung, Chan Kwon, MD, Park, So Yeon, MD

Published by the Korean Society of Pathologists/the Korean Society for Cytopathology

Editorial Office

Room 1209 Gwanghwamun Officia, 92 Saemunan-ro, Jongno-gu, Seoul 03186, Korea

Tel: +82-2-795-3094 Fax: +82-2-790-6635 E-mail: office@jpatholtm.org

#1508 Renaissancetower, 14 Mallijae-ro, Mapo-gu, Seoul 04195, Korea

Tel: +82-2-593-6943 Fax: +82-2-593-6944 E-mail: office@jpatholtm.org

Printed by iMiS Company Co., Ltd. (JMC)

Jungang Bldg. 18-8 Wonhyo-ro 89-gil, Yongsan-gu, Seoul 04314, Korea

Tel: +82-2-717-5511 Fax: +82-2-717-5515 E-mail: ml@smileml.com

Manuscript Editing by InfoLumi Co.

210-202, 421 Pangyo-ro, Bundang-gu, Seongnam 13522, Korea

Tel: +82-70-8839-8800 E-mail: infolumi.chang@gmail.com

Front cover image: Histologic feature of low-grade appendiceal mucinous neoplasm (p250).

© Copyright 2021 by the Korean Society of Pathologists/the Korean Society for Cytopathology

© Journal of Pathology and Translational Medicine is an Open Access journal under the terms of the Creative Commons Attribution Non-Commercial License (<https://creativecommons.org/licenses/by-nc/4.0>).

© This paper meets the requirements of KS X ISO 9706, ISO 9706-1994 and ANSI/NISO Z.39.48-1992 (Permanence of Paper).

CONTENTS

REVIEWS

- 239 **Distinctive morphological and molecular features of urothelial carcinoma with an inverted growth pattern**
Francesca Sanguedolce, Beppe Calò, Marco Chirico, Ugo Falagario, Gian Maria Busetto, Magda Zanelli, Alessandra Bisagni, Maurizio Zizzo, Stefano Ascani, Giuseppe Carrieri, Luigi Cormio
- 247 **Standardization of the pathologic diagnosis of appendiceal mucinous neoplasms**
Dong-Wook Kang, Baek-hui Kim, Joon Mee Kim, Jihun Kim, Hee Jin Chang, Mee Soo Chang, Jin-Hee Sohn, Mee-Yon Cho, So-Young Jin, Hee Kyung Chang, Hye Seung Han, Jung Yeon Kim, Hee Sung Kim, Do Youn Park, Ha Young Park, So Jeong Lee, Wonae Lee, Hye Seung Lee, Yoo Na Kang, Younghee Choi, The Gastrointestinal Pathology Study Group of the Korean Society of Pathologists
- 265 **Palmar and plantar fibromatosis: a review**
Brian D. Stewart, Alessandra F. Nascimento

ORIGINAL ARTICLES

- 271 **Potential of AKT2 expression as a predictor of lymph-node metastasis in invasive breast carcinoma of no special type**
Primariadewi Rustamadji, Elvan Wiyarta, Kristina Anna Bethania, Kusmardi Kusmardi
- 279 **Correlation of TTF-1 immunexpression and EGFR mutation spectrum in non-small cell lung carcinoma**
Tripti Nakra, Varsha Singh, Aruna Nambirajan, Prabhat Singh Malik, Anant Mohan, Deepali Jain
- 289 **Clinicopathologic features of cutaneous metastases from internal malignancies**
Hyeong Mok Kwon, Gyu Yeong Kim, Dong Hoon Shin, Young Kyung Bae

CASE REPORTS

- 298 **Sarcomatoid urothelial carcinoma arising in the female urethral diverticulum**
Heae Sung Park
- 303 **Metastatic gastric cancer of the testis diagnosed through urine cytology**
Mee Sook Roh, Song-Hee Han

Distinctive morphological and molecular features of urothelial carcinoma with an inverted growth pattern

Francesca Sanguedolce¹, Beppe Calò², Marco Chirico³, Ugo Falagario³, Gian Maria Busetto³, Magda Zanelli⁴,
 Alessandra Bisagni⁴, Maurizio Zizzo^{5,6}, Stefano Ascani⁷, Giuseppe Carrieri³, Luigi Cormio²

¹Pathology Unit, University of Foggia, Foggia;

²Urology Unit, University of Foggia, Bonomo Teaching Hospital, Foggia;

³Urology and Renal Transplantation Unit, University of Foggia, Foggia;

⁴Pathology Unit, Azienda USL-IRCCS di Reggio Emilia, Reggio Emilia;

⁵Surgical Oncology Unit, Azienda USL-IRCCS di Reggio Emilia, Reggio Emilia;

⁶Clinical and Experimental Medicine PhD Program, University of Modena and Reggio Emilia, Modena;

⁷Pathology Unit, Azienda Ospedaliera S. Maria di Terni, University of Perugia, Terni, Italy

Urothelial carcinoma with an inverted growth pattern (UC-IGP) is a peculiar entity within the spectrum of urothelial lesions. While efforts have been made over the last few decades to unravel its carcinogenesis and relationship with conventional urothelial carcinoma, the exact classification of inverted urothelial lesions is a matter of debate. The morphological features of UC-IGP pose several issues in differential diagnosis with other mostly benign lesions. Various techniques, including immunohistochemistry, UroVysion, and many molecular methods, have been employed to study the exact nature of this lesion. The aim of this review is to provide a comprehensive overview of the morphological and immunophenotypical aspects of UC-IGP. Moreover, we present and discuss the immunohistochemical and molecular markers involved in diagnosis and prognosis of UC-IGP lesions.

Key Words: Urothelial carcinoma; Inverted growth pattern; Immunohistochemistry; Molecular markers

Received: March 4, 2021 **Revised:** April 2, 2021 **Accepted:** April 20, 2021

Corresponding Author: Francesca Sanguedolce, MD, PhD, Pathology Unit, University Hospital OO.RR., University of Foggia, Viale Pinto 1, 71122 Foggia, Italy
 Tel: +39-0881736315, Fax: +39-0881736334, E-mail: francesca.sanguedolce@unifg.it

The majority of urothelial neoplasms has an exophytic growth pattern, yet some show an inverted architecture [1-3]. A systematic approach to classification of inverted/endophytic urothelial lesions was made in 2012 by the International Consultation on Urologic Disease (ICUD). According to the existing World Health Organization (WHO)/International Society of Urologic Pathology (ISUP) system criteria for exophytic papillary neoplasms and on the basis of the presence and degree of atypia (including assessment of polarity), inverted neoplasms are graded as (1) inverted papilloma (IP), (2) inverted papillary urothelial neoplasm of low malignant potential (PUNLMP), (3) inverted papillary urothelial carcinoma (PUC), (4) low-grade, non-invasive, inverted PUC, (5) high-grade, non-invasive, inverted PUC, or (6) high-grade, invasive [4]. Due to the frequent occurrence of both exophytic and endophytic patterns in the same urothelial lesion, such terminology should apply only to malignant lesions with promi-

nent inverted architecture [5]. However, this approach has been criticized for not considering other architectural and cytological features, namely presence of exophytic papillary structures, type of endophytic pattern (i.e., nests and trabeculae), number of cellular layers, and mitotic index [2,5].

Urothelial carcinoma (UC) with an inverted growth pattern (UC-IGP) is a malignant entity within this spectrum of lesions. Findings from the literature point out that these lesions carry peculiar histological and molecular features; however, issues in differential diagnosis can arise and affect the possibility of a proper diagnosis and subsequent adequate treatment. The aim of this review is to provide a comprehensive overview of the morphological and immunophenotypical aspects of UC-IGP. Moreover, we discuss the molecular evidence shedding light on the putative pathogenesis of this disease related to urothelial carcinogenesis.

MORPHOLOGICAL FEATURES

According to the current WHO classification, papillary urothelial carcinoma with an inverted growth pattern (PUC-IGP) is a variant of non-invasive PUC and is staged as pTa [6]. Unlike conventional PUC, PUC-IGP shows an endophytic architectural pattern with branching and anastomosing cords of urothelium, some of which have an expansile appearance [7,8]. The stromal-epithelial interface has a smooth profile with delicate vascular architecture. The cytological and architectural features lead similar grading as for conventional UCs, namely low-grade (LG) and high-grade (HG) [8], featuring nuclear atypia, architectural abnormality, and mitotic activity [9,10]. Such changes are present at the surface of the lesion in most cases, further supporting a diagnosis of UC. An exophytic papillary element has been reported in association with the inverted component [1,11], as well as a pseudoexophytic pattern resulting from artifactual fragmentation of the specimen.

The presence of prominent endophytic growth can be misdiagnosed as a pushing border of invasion, yet occasional true lamina propria invasion is supported by a stromal reaction [1,5,7,12] and/or neoplastic cords interweaving with fibers of muscularis mucosae [1,13]. Features such as irregularity of the endophytic nest profile, architectural complexity, and occurrence of single-cell invasion can be useful and should raise suspicion of an invasive lesion [14]. Transurethral resection (TUR)-related artifacts, namely tangential sectioning, cauterization, and crush effect, represent further issues in assessing stromal and/or muscular invasion [1,13].

In a recent large series of invasive HG-UC arising in a background of UC-IGP from various sites, Gutierrez et al. [15] reported on bladder tumors presenting at earlier stages (81% pT1) than those involving the upper urinary tract (80% and 43% \geq pT2 in the renal pelvis and ureter, respectively). UC in situ and variant histology were described in approximately 40% and 20% of all cases, respectively [15], the latter being associated with a more aggressive clinical behavior. Conversely, a previous study on 81 non-invasive LG-UC of the bladder, including eight UC-IGP, reported a lower recurrence risk in the inverted group [16]. A first attempt to classify PUC-IGP was conducted in 1997 by Amin et al. [13], who described two main histologic patterns featuring interanastomosing cords and trabeculae (IP-like pattern) and broad bulbous borders (broad-front pattern), respectively [13,17].

LG-PUC-IGP shows mild nuclear atypia in terms of irregular chromatin distribution, enlarged irregular nucleoli, expansile

growth with inverted nests and clusters, and increased mitoses [8,18]. HG-PUC-IGP has predominant inverted growth with higher architectural disorder in terms of marked loss of polarity with respect to the basement membrane [4], along with significant nuclear pleomorphism and increased mitotic activity with occasional atypical figures. However, many reported cases of “atypical inverted urothelial papilloma” are described with an exophytic papillary component and significant atypia and/or mitoses, which would best be considered UC with inverted growth [5,19].

IMMUNOHISTOCHEMICAL MARKERS

CD44

CD44 is a stem cell surface marker typically present in the basal layer of normal urothelium; however, UC in situ and the luminal subtype of invasive UC lack CD44 expression [8]. In their recent study on UC-IGPs of various grade, Bang et al. [2] described CD44 expression in two-thirds of their LG cases, while all HG tumors were negative. Further studies are needed to assess the potential of CD44 as a diagnostic and prognostic marker in this setting.

Cytokeratin 20

Cytokeratin 20 (CK20) is a low-molecular weight cytokeratin with diagnostic and prognostic potential in urothelial lesions [20]. CK20 is expressed commonly by superficial cells only in the normal urothelium; therefore, it is a marker of urothelial maturation and differentiation [5]. The immunohistochemical expression of CK20 is of diagnostic value in differentiating IP from UC-IGP [1-3] (Table 1). Moreover, Sun et al. [3] reported that combining Ki67 and CK20 assessment by immunohistochemistry with UroVysion fluorescence in situ hybridization (FISH) showed sensitivity and specificity as high as 89.5% and 100%, respectively.

Cyclin D1

Cyclin D1 is a key regulator of the cell cycle, and its alterations have been implicated in bladder carcinogenesis [21]. Cyclin D1 status has been studied as a prognostic marker in nonmuscle invasive bladder cancer (NMIBC), with conflicting results [21] (Table 1). The LG-IP-like UC reported by Sudo et al. [22] showed cytoplasmic expression of cyclin D1 along with other immunohistochemical markers. Interestingly, Bang et al. [2] found that 28 of 60 (47%) inverted urothelial neoplasms were positive for nuclear cyclin D1, in the absence of significant difference in stain-

Table 1. Expression of selected immunohistochemical markers in UC-IGP

Study	Site (No.)	CK20		Cyclin D1		HER2		Ki67		p16		p53	
		LG	HG	LG	HG	LG	HG	LG	HG	LG	HG	LG	HG
Cheon et al. [29]	Bladder (2)	-	-	-	-	2/2 (100)		-	-	-	-	-	-
Eiber et al. [31]	Bladder (22)	9/22 (41)		-	-	-	-	18/22 (82)		-	-	6/22 (27)	
Jones et al. [1]	Bladder (29)	17/29 (59)		-	-	-	-	19/29 (66)		-	-	17/29 (59)	
Terada [32]	Bladder (3)	-	-	-	-	-	-	3/3 (100)		-	-	3/3 (100)	
Ehsani et al. [30]	Renal pelvis (23)	-	-	-	-	15/23 (65)		-	-	-	-	-	-
McDaniel et al. [18]	Bladder (8), renal pelvis (1)	-	-	-	-	-	-	-	-	3/5 (60)	2/4 (50)	-	-
Sun et al. [3]	-	14/38 (36.8)		-	28/38 (73.7)	-	-	18/38 (47.4)	-	-	-	16/38 (42.1)	-
Bang et al. [2]	Bladder (19)	4/15 (27)	3/4 (75)	7/15 (47)	2/4 (50)	1/15 (7)	1/4 (25)	1/15 (7)	2/4 (50)	3/15 (20)	3/4 (75)	4/15 (27)	3/4 (75)

Values are presented as number (%).

UC-IGP, urothelial carcinoma with an inverted growth pattern; CK20, cytokeratin 20; HER2, human epidermal growth factor receptor 2; HG, high-grade; LG, low-grade.

ing levels between benign and malignant lesions. Accordingly, cyclin D1 nuclear expression was higher in LG-UC-IGP than in IP (73.7% vs. 69.4%, respectively) in the study by Sun et al. [3], but the difference did not achieve statistical significance ($p = .798$). Based on these findings, cyclin D1 seems not to be helpful in differential diagnosis of benign and malignant inverted lesions.

Human epidermal growth factor receptor 2

Human epidermal growth factor receptor 2 (HER2) is a tyrosine kinase receptor with oncogenic potential that is overexpressed in 5%–10% of UC, including nonmuscle invasive lesions [23–25]. HER2 expression has prognostic and therapeutic implications, since anti-HER2 targeted drugs are the standard-of-care for patients with HER2+ breast and gastroesophageal cancer [26,27]. However, analytical and pre-analytical issues can affect the reliability of HER2 assessment through current methods, especially with TUR specimens [28]. Cheon et al. [29] found moderate to strong HER2 overexpression (defined as distinct membrane staining) in two malignant bladder lesions with inverted pattern compared to five IP, which were negative for HER2. Similarly, significantly higher levels of HER2 expression ($p = .0465$) were described in UC-IGP compared with IP and PUNLMP-IGP using a 10% cutoff in a recent study by Bang et al. [2]. In addition, Ehsani and Osunkoya [30] reported a HER2 positivity rate (defined as strong complete membrane staining in > 30% cells) as high as 74% in their series of 46 renal pelvis UC cases; of them, 23 UC-IGP showed HER2 overexpression in 65% of cases, mostly HG-UC. Based on these results (Table 1), HER2 might be useful in differentiating malignant from benign lesions with an inverted growth pattern.

Ki67

The proliferative index assessed by scoring Ki67 nuclear an-

tigen has been studied extensively in both NMIBC and muscle invasive bladder cancer (MIBC) [21] and in inverted lesions as well. Overall, it has been reported as diffusely expressed in UC-IGP [1,2,22,31,32] with significantly higher level compared to that in benign inverted lesions [1–3,31]. Consistent with these results, assessment of proliferative activity using proliferating cell nuclear antigen antibody and AgNOR silver colloid staining yielded higher expression rates of both markers in malignant inverted lesions compared to IPs [29]. Eiber et al. [31] suggest that a combined assessment of fibroblast growth factor receptor 3 (FGFR3) mutation status and Ki67 proliferation index can yield a specificity as high as > 90% in differentiating UC-IGP from IP within a consistent histological setting, with a Ki67 labeling index < 5% and wild-type FGFR3 being associated with a benign lesion. It has been suggested that the rate of Ki67 positive cells tends toward constant growth and expansion at the center of the lesion as grade increases [1,33]; therefore, this marker might be an adjunct in disease grading (Table 1).

p16

In bladder cancer, p16 has been analyzed either in association with other cell cycle proteins as a prognostic/predictive factor or as an indirect marker of human papillomavirus–induced carcinogenesis [21]. The two studies assessing p16 expression in UC-IGP yielded overlapping results, with higher expression of p16 in malignant compared to benign lesions, without statistical significance (Table 1). Furthermore, in both studies, a more diffuse staining pattern was described in HG-UC versus LG-UC [2,18].

p53

The gene encoding tumor suppressor protein p53 is the most common target for mutations in human cancer, and alterations of p53 at a molecular level are found in early bladder carcinogenesis

events. p53 status seems to have a prognostic role in both NMIBC and MIBC, yet with contradictory results [21,34,35]. Although usually overexpressed in UC-IGP [22,32], no significant difference in p53 expression between benign and malignant inverted lesions was reported using different cutoffs (10%–50%) [2,31]. Conversely, Sun et al. [3] reported significantly higher p53 staining (cutoff, 10%) in a series of LG-UC-IGP compared to IP ($p = .001$). Similarly, Jones et al. [1] described a steady increase in p53 expression in UC-IGP versus IP (59% vs. 7%) using a 1% cutoff, suggesting that p53 should be part of a multi-marker panel (along with Ki67 and CK20) to distinguish benign from malignant inverted lesions. Interestingly, there were no statistically significant differences in p53 protein staining between IPs in patients with and without a history of UC [36] and between IPs with and without atypia [37] in two previous studies (Table 1). The use of different cutoffs can impair the reproducibility of immunohistochemical results among studies.

MOLECULAR FEATURES

RAS genes

HRAS and KRAS are prototype RAS oncoproteins that have been shown to infrequently incur mutations in conventional UC [21,35]. Conversely, HRAS mutations have been reported in inverted tumors [18], along with mutations in other members of the RAS pathway, namely mutations encoding the KRAS G12R and BRAF G469A mutants in LG-UC-IGP and HG-UC-IGP cases, respectively [18]. Moreover, an oncogenic HRAS or KRAS missense mutation was present in nearly all cases of IP and urothelial papilloma according to a recent series [38–40], compared to two of 25 UC-IGP cases (8%). In both cases, further oncogenic mutations in chromatin-modifying genes and/or cell cycle regulators were present. Based on such findings, it has been suggested that an altered RAS pathway supplies the growth and/or progression of inverted urothelial lesions [18].

Loss of heterozygosity

Chromosomal aberrations, namely changes of copy numbers of various genetic regions, can occur at several points along the UC pathway that can be detected by cytogenetic studies, including loss of heterozygosity (LOH) analysis [21]. Sung et al. [41] found a very low incidence of LOH at genetic loci, which are frequently lost in both UCs and PNULMPs, by examining four polymorphic microsatellite markers [42] in their series of 39 IPs. LOH analysis performed by Eiber et al. [31] on 62 IPs and 23 UC-IGPs using microsatellite markers at chromosomal loci

9p21, 9q, and 17p13.1 identified statistically significant differences in 9q LOH (13.2% of IPs vs. 36.4% of UC-IGPs, $p = .03$).

Telomere shortening

Telomeres are repetitive DNA sequences that protect chromosome ends. A process known as telomere shortening (TS) occurs with every iteration of DNA replication and cell division. Telomerase is a DNA polymerase that counteracts TS by repairing chromosome ends, and the expression of its catalytic subunit telomerase reverse transcriptase (TERT) is correlated with telomerase activity [35]. TS and telomerase activity are involved in cancer development and progression at different sites, including the bladder [43]. Williamson et al. [44] reported that relative telomere length, as assessed by FISH analysis with a telomere-specific peptide nucleic acid probe, was significantly reduced in UC-IGP compared to IP ($p < .001$). Interestingly, analysis of relative telomere signal intensity in normal urothelium, non-neoplastic lesions (cystitis glandularis), and IP yielded similar results [44]. Based on these results, the authors argued that IPs do not have premalignant potential, and that benign and malignant inverted lesions develop through different carcinogenetic pathways despite their morphological similarity.

TERT promoter mutations have been detected infrequently in IPs [39,45,46]. Similarly, Cheng et al. [10] identified a significantly lower rate of TERT mutations in IP compared with UC-IGP (15% vs. 58%, $p = .003$). Interestingly, the same C228T mutation was found in inverted lesions as well as in the majority of conventional UC, suggesting that a subset of IP might share a molecular pathway of carcinogenesis with UC-IGP and conventional UC [47]. Such findings suggest the use of TERT mutation analysis in the differential diagnosis of benign and malignant lesions [38,40,47–49].

UroVysion

UroVysion is a multicolor FISH-based urine assay with higher sensitivity than urine cytology in the setting of UC screening and follow-up [21]. This assay assesses amplification of chromosomes 3, 7, and 17 along with deletion of 9p21. Such alterations have been detected in up to 79% of UC-IGPs through different studies [1,5,7,33]. In their multimethod study on a series of 15 IPs and 29 UC-IGPs, Jones et al. [1] yielded normal results for all cases of IP, while UC-IGP demonstrated chromosomal abnormalities typical of conventional UC, including gains of chromosomes 3 and 7. Accordingly, UroVysion positivity, defined as a gain of at least two of chromosomes 3, 7, or 17 or a homozygous loss of 9p21, yielded increased sensitivity and specificity rates

compared to the immunohistochemical markers Ki67 and CK20 [3], and even higher accuracy was accomplished by a combination of the three tests, further highlighting the role of UroVysion in distinction between IP and UC-IGP.

Microsatellite instability

Microsatellite instability (MSI) resulting from errors in DNA replication is a distinctive feature of several tumors, including BC, where it has been reported to be associated with increased grade and stage [21] and to have a predictive role, especially in NMIBC [25]. MSI status can be assessed either directly by microsatellite analysis, a PCR-based technique, or indirectly by assessing the MSI factors MutL homologue 1 (MLH1), MutS homologue 2 (MSH2), and MutS homologue 6 (MSH6).

A frequent association between MSI positive status and inverted growth pattern in tumors of the upper urinary tract has been described [50,51], mostly highlighted by MSH2 and/or MSH6 protein loss. Eiber et al. [31] investigated MSI in their series of IPs and UC-IGPs through both microsatellite analysis and MLH1, MSH2, and MSH6 immunostaining; however, they failed to find a significant correlation between MSI status and diagnosis [31]. Based on these findings, they argued that microsatellite unstable inverted tumors of the upper urinary tract represent a distinct subgroup of inverted urothelial tumors.

FGFR3

FGFR3 is a member of the family of fibroblast growth factor tyrosine kinase receptors that is involved in urothelial carcinogenesis through a papillary pathway associated with low cellular grade and lack of invasion [52]. Alterations of the FGFR3 gene have been described in UC-IGP, namely activating mutations encoding S249C, R248C, and G370C [18]. Since such alterations have been detected in both LG-UC-IGP and HG-UC-IGP, a possible explanation could be the non-invasive nature of inverted lesions overall, despite their grade of differentiation [18].

Distinct molecular alterations in inverted urothelial lesions

Evidence from molecular genetic studies has shown that IPs have additional distinct molecular features compared to their malignant counterparts, such as low tumor mutational burden, mutations in the mitogen-activated protein kinase/ERK pathway, along with a lack of the prevalent *APOBEC* mutation signature [1,7,31,36,38-41]. On the other hand, both conventional UC and UC-IGP carry overlapping genetic alterations [53], namely mutations in *FGFR3*, *TP53*, *CDKN1A*, *PIK3CA*, *FBXW7*, *ERBB2*, and *NOTCH1* [18,40]. Interestingly, the specific point

mutations at *FBXW7* R505, *ERBB2* V842, and *NOTCH1* R1594 have not been reported in conventional urothelial cancers [54]. UC-IGP arising in the upper urinary tract has been described in association with hereditary non-polyposis colorectal cancer syndrome/Lynch syndrome, with DNA mismatch repair gene abnormalities and MSI [55], and the latter are more frequent in tumors of the renal pelvis and ureter than in bladder primaries and can be used as prognostic markers [25].

Differential diagnosis

Several authors have highlighted the high potential for misinterpretation of UC-IGP as IP due to overlapping morphological features [1,7,11-15,22,44]; however, a combination of morphologic, immunohistochemical, and molecular genetic assessments can be helpful in achieving a correct diagnosis [1]. This task is particularly challenging when the cystoscopy-obtained biopsy tissue is limited, extensively fragmented, heavily inflamed, and/or obscured by crush or cautery artifacts [15]. IPs are relatively less frequent than conventional urothelial benign papillary neoplasms, can be encountered anywhere throughout the urinary tract, and do not undergo malignant transformation [56].

Amin et al. [13] analyzed 18 UC-IGPs and established several morphologic criteria to distinguish them from IPs. UC-IGP tends to have an exophytic papillary surface, thick irregular cords or trabeculae, grade-dependent cytological atypia, and decrease to lack of maturation, spindling, or peripheral palisading [2,3,5,10,18,32]. Cytologic atypia presents in the form of nuclear pleomorphism, irregular chromatic structure, and/or enlarged uneven nucleoli [57]. Furthermore, UC-IGPs tend to have greater mitotic activity above the basal layer with occasionally atypical mitotic figures [3,57]. The presence of UC in situ in the surface urothelium is a further hint to diagnosis of UC-IGP [7].

Conversely, IPs have a smooth, dome-shaped surface due to the endophytic growth of uniform cords and trabeculae, usually lack an exophytic element, are more circumscribed, feature palisading at the periphery and spindling or streaming in the center of the trabeculae, and cytologic atypia is weak to absent [3,31]. It is clear that IPs lack stromal invasion; however, IPs with foamy/clear or vacuolated cytoplasm have been described occasionally [19]. At cystoscopy, IP usually appears as a single peduncle mass with smooth surface, while UC-IGP presents as wide-based, cauliflower-like multiple masses with an uneven surface [5] (Fig. 1).

It has been suggested that most lesions diagnosed in the past as IP with concurrent UC were actually UC-IGPs [58], and some IPs were labeled as LG-UC-IGPs [59], resulting in confusion regarding the actual incidence of each disease. Moreover, a cate-

	UC-IGP	IP
Major features		
Anastomosing cord and trabeculae	Large irregular	Thin uniform
Exophytic component	Usually present	Rare
Nuclear atypia	Present	Mild, if present
Mitoses	Often present at any layer sometimes atypical mitotic figures	Rare to absent at basal layer atypical mitoses absent
Minor features		
Fibrovascular cores	May be present	Absent
Cellular layers	>5	3–5
Polarity	Altered	Normal
Immunohistochemistry		
Ki67	↑	↓ to absent
p53	↑	↓
CK20	↑	↓
HER2	↑	↓
UroVysion	+	–

Fig. 1. Summary of the main morphological, immunohistochemical, and molecular differential features of urothelial carcinoma with an inverted growth pattern (UC-IGP) and inverted papilloma (IP). CK20, cytokeratin 20; HER2, human epidermal growth factor receptor 2.

gory of “IP with atypia” or “atypical IP” was introduced by some authors, referring to a subset of IP with malignant potential [36,37]. Compared to UC-IGP, IP with atypia has lower mitotic index and proliferative activity. Interestingly, Brimo et al. reported on a series of 12 UC-IGPs encompassing areas within the tumor whose morphological features were identical to those of IP in each case [17]. Immunohistochemically, higher rates of p53 and CK20 expression and increased Ki67 proliferative index were seen in UC-IGP compared to IP [1,7,14,44]. Sun et al. [3] described higher Ki67 and CK20 expression in LG-UC-IGP than IP. Interestingly, Broussard et al. [37] found a higher incidence of Ki67 and p53 in IPs with atypia compared to conventional IPs. Moreover, 24 of 38 (63.2%) LG-UC-IGP cases were positive for UroVysion FISH, whereas all IPs showed no gains of chromosomes 3, 7, or 17 and absence of 9p21 loss, suggesting that IP arises from pathogenetic mechanisms that differ from those that produce UC (Fig. 1).

As a lesion with an endophytic growth pattern, a large-nested variant of invasive UC enters the differential diagnosis with UC-IGP. However, involvement of the detrusor muscle as well as the high variability of size and shape, irregular profile, and infiltra-

tive architecture of large-nested UC allow distinction between the two [60].

CONCLUSION

In conclusion, UC-IGP and IP are distinct entities with peculiar biologic behaviors and clinical outcomes that can be difficult to distinguish due to their morphological commonalities. However, misdiagnosis should be avoided since IP is a benign disease, while UC-IGP can warrant further treatment or surveillance depending on grade [2,7,56]. Data from the literature assess the role of ancillary techniques, namely immunohistochemistry and FISH, in supporting a proper diagnosis [3]. However, studies on large case series are warranted to further elucidate the molecular mechanisms and diagnostic and prognostic markers of UC-IGP.

Ethics Statement

Not applicable.

Availability of Data and Material

Data sharing not applicable to this article as no datasets were generated or analyzed during the study.

Code Availability

Not applicable.

ORCID

Francesca Sanguedolce	https://orcid.org/0000-0001-7459-3521
Beppe Calò	https://orcid.org/0000-0001-9285-9426
Marco Chirico	https://orcid.org/0000-0002-0637-1481
Ugo Falagarò	https://orcid.org/0000-0002-1152-3005
Gian Maria Busetto	https://orcid.org/0000-0002-7291-0316
Magda Zanelli	https://orcid.org/0000-0002-8733-9933
Alessandra Bisagni	https://orcid.org/0000-0001-8484-7871
Maurizio Zizzo	https://orcid.org/0000-0001-9841-7856
Stefano Ascani	https://orcid.org/0000-0002-4516-9040
Giuseppe Carrieri	https://orcid.org/0000-0002-6609-6434
Luigi Cormio	https://orcid.org/0000-0002-1126-5368

Author Contributions

Conceptualization: FS. Project administration: FS, MZ (Magda Zanelli), LC. Supervision: GC, LC. Writing—original draft: FS, BC, MC, UF, GMB, MZ (Magda Zanelli), AB, MZ (Maurizio Zizzo), SA. Writing—review & editing: FS, SA, GC, LC. Approval of final manuscript: all authors.

Conflicts of Interest

The authors declare that they have no potential conflicts of interest.

Funding Statement

No funding to declare.

References

- Jones TD, Zhang S, Lopez-Beltran A, et al. Urothelial carcinoma with an inverted growth pattern can be distinguished from inverted

- papilloma by fluorescence in situ hybridization, immunohistochemistry, and morphologic analysis. *Am J Surg Pathol* 2007; 31: 1861-7.
2. Bang H, Park H, Park S, et al. Clinicopathologic study of 60 cases of urothelial neoplasms with inverted growth patterns: reclassification by international consultation on urologic disease (ICUD) recommendations. *Ann Diagn Pathol* 2020; 44: 151433.
 3. Sun JJ, Wu Y, Lu YM, et al. Immunohistochemistry and fluorescence in situ hybridization can inform the differential diagnosis of low-grade noninvasive urothelial carcinoma with an inverted growth pattern and inverted urothelial papilloma. *PLoS One* 2015; 10: e0133530.
 4. Amin MB, Smith SC, Reuter VE, et al. Update for the practicing pathologist: The International Consultation on Urologic Disease-European association of urology consultation on bladder cancer. *Mod Pathol* 2015; 28: 612-30.
 5. Guo A, Liu A, Teng X. The pathology of urinary bladder lesions with an inverted growth pattern. *Chin J Cancer Res* 2016; 28: 107-21.
 6. Lopez-Beltran A, Cheng L. Stage T1 bladder cancer: diagnostic criteria and pitfalls. *Pathology* 2021; 53: 67-85.
 7. Hodges KB, Lopez-Beltran A, MacLennan GT, Montironi R, Cheng L. Urothelial lesions with inverted growth patterns: histogenesis, molecular genetic findings, differential diagnosis and clinical management. *BJU Int* 2011; 107: 532-7.
 8. Moch H, Humphrey PA, Ulbright TM, Reuter VE. WHO classification of tumours of the urinary system and male genital organs. 4th ed. Lyon: IARC, 2016; 100-2.
 9. Lopez-Beltran A, Montironi R, Cheng L. Pathology of the urinary bladder: an algorithmic approach. Cambridge: Cambridge University Press, 2016; 1-163.
 10. Cheng L, MacLennan GT, Bostwick DG. Urologic surgical pathology. 4th ed. Philadelphia: Elsevier, 2020; 230-63.
 11. Terai A, Tamaki M, Hayashida H, Tomoyosh T, Takeuchi H, Yoshida O. Bulky transitional cell carcinoma of bladder with inverted proliferation. *Int J Urol* 1996; 3: 316-9.
 12. Lopez-Beltran A, Cheng L. Histologic variants of urothelial carcinoma: differential diagnosis and clinical implications. *Hum Pathol* 2006; 37: 1371-88.
 13. Amin MB, Gomez JA, Young RH. Urothelial transitional cell carcinoma with endophytic growth patterns: a discussion of patterns of invasion and problems associated with assessment of invasion in 18 cases. *Am J Surg Pathol* 1997; 21: 1057-68.
 14. Montironi R, Cheng L, Lopez-Beltran A, et al. Inverted (endophytic) noninvasive lesions and neoplasms of the urothelium: the Cinderella group has yet to be fully exploited. *Eur Urol* 2011; 59: 225-30.
 15. Gutierrez CM, Alemezaffar M, Osunkoya AO. Invasive high-grade urothelial carcinoma of the bladder, renal pelvis, ureter, and prostatic urethra arising in a background of urothelial carcinoma with an inverted growth pattern: a contemporary clinicopathological analysis of 91 cases. *Hum Pathol* 2019; 92: 18-24.
 16. Arslankoz S, Kulac I, Ertoy Baydar D. The influence of inverted growth pattern on recurrence for patients with non-invasive low grade papillary urothelial carcinoma of bladder. *Balkan Med J* 2017; 34: 464-8.
 17. Brimo F, Dauphin-Pierre S, Aprikian A, et al. Inverted urothelial carcinoma: a series of 12 cases with a wide morphologic spectrum overlapping with the large nested variant. *Hum Pathol* 2015; 46: 1506-13.
 18. McDaniel AS, Zhai Y, Cho KR, et al. *HRAS* mutations are frequent in inverted urothelial neoplasms. *Hum Pathol* 2014; 45: 1957-65.
 19. Fine SW, Epstein JI. Inverted urothelial papillomas with foamy or vacuolated cytoplasm. *Hum Pathol* 2006; 37: 1577-82.
 20. Sanguedolce F, Russo D, Calo B, Cindolo L, Carrieri G, Cormio L. Diagnostic and prognostic roles of CK20 in the pathology of urothelial lesions: a systematic review. *Pathol Res Pract* 2019; 215: 152413.
 21. Sanguedolce F, Bufo P, Carrieri G, Cormio L. Predictive markers in bladder cancer: do we have molecular markers ready for clinical use? *Crit Rev Clin Lab Sci* 2014; 51: 291-304.
 22. Sudo T, Irie A, Ishii D, Satoh E, Mitomi H, Baba S. Histopathologic and biologic characteristics of a transitional cell carcinoma with inverted papilloma-like endophytic growth pattern. *Urology* 2003; 61: 837.
 23. Lae M, Couturier J, Oudard S, Radvanyi F, Beuzeboc P, Vieillefond A. Assessing *HER2* gene amplification as a potential target for therapy in invasive urothelial bladder cancer with a standardized methodology: results in 1005 patients. *Ann Oncol* 2010; 21: 815-9.
 24. Cormio L, Sanguedolce F, Cormio A, et al. Human epidermal growth factor receptor 2 expression is more important than Bacillus Calmette Guerin treatment in predicting the outcome of T1G3 bladder cancer. *Oncotarget* 2017; 8: 25433-41.
 25. Sanguedolce F, Cormio A, Massenio P, et al. Altered expression of HER-2 and the mismatch repair genes *MLH1* and *MSH2* predicts the outcome of T1 high-grade bladder cancer. *J Cancer Res Clin Oncol* 2018; 144: 637-44.
 26. Sanguedolce F, Russo D, Mancini V, et al. Prognostic and therapeutic role of HER2 expression in micropapillary carcinoma of the bladder. *Mol Clin Oncol* 2019; 10: 205-13.
 27. Oh DY, Bang YJ. HER2-targeted therapies-a role beyond breast cancer. *Nat Rev Clin Oncol* 2020; 17: 33-48.
 28. Sanguedolce F, Russo D, Mancini V, et al. Human epidermal growth factor receptor 2 in non-muscle invasive bladder cancer: issues in assessment methods and its role as prognostic/predictive marker and putative therapeutic target: a comprehensive review. *Urol Int* 2019; 102: 249-61.
 29. Cheon J, Kim HK, Kim JJ, Yoon DK, Koh SK, Kim IS. Malignant inverted papilloma of the urinary bladder: the histopathological aspect of malignant potential of inverted papilloma. *J Korean Med Sci* 1995; 10: 103-10.
 30. Ehsani L, Osunkoya AO. Human epidermal growth factor receptor 2 expression in urothelial carcinoma of the renal pelvis: correlation with clinicopathologic parameters. *Int J Clin Exp Pathol* 2014; 7: 2544-50.
 31. Eiber M, van Oers JM, Zwarthoff EC, et al. Low frequency of molecular changes and tumor recurrence in inverted papillomas of the urinary tract. *Am J Surg Pathol* 2007; 31: 938-46.
 32. Terada T. Inverted variant of urothelial carcinoma of the urinary bladder: a report of three cases and a proposal for a new clinicopathologic entity. *Int J Clin Exp Pathol* 2013; 6: 766-70.
 33. Urakami S, Igawa M, Shirakawa H, Shiina H, Ishibe T. Inverted papilloma of the urinary bladder: a case evaluated for malignant potential. *Int Urol Nephrol* 1997; 29: 181-7.
 34. Cormio L, Tolve I, Annese P, et al. Altered p53 and pRb expression is predictive of response to BCG treatment in T1G3 bladder cancer. *Anticancer Res* 2009; 29: 4201-4.
 35. Sanguedolce F, Cormio A, Bufo P, Carrieri G, Cormio L. Molecular markers in bladder cancer: Novel research frontiers. *Crit Rev Clin Lab Sci* 2015; 52: 242-55.
 36. Cheville JC, Wu K, Sebo TJ, et al. Inverted urothelial papilloma: is

- ploidy, MIB-1 proliferative activity, or p53 protein accumulation predictive of urothelial carcinoma? *Cancer* 2000; 88: 632-6.
37. Broussard JN, Tan PH, Epstein JI. Atypia in inverted urothelial papillomas: pathology and prognostic significance. *Hum Pathol* 2004; 35: 1499-504.
 38. Akgul M, MacLennan GT, Cheng L. Distinct mutational landscape of inverted urothelial papilloma. *J Pathol* 2019; 249: 3-5.
 39. Isharwal S, Hu W, Sarungbam J, et al. Genomic landscape of inverted urothelial papilloma and urothelial papilloma of the bladder. *J Pathol* 2019; 248: 260-5.
 40. Almassi N, Pietzak EJ, Sarungbam J, et al. Inverted urothelial papilloma and urothelial carcinoma with inverted growth are histologically and molecularly distinct entities. *J Pathol* 2020; 250: 464-5.
 41. Sung MT, Eble JN, Wang M, Tan PH, Lopez-Beltran A, Cheng L. Inverted papilloma of the urinary bladder: a molecular genetic appraisal. *Mod Pathol* 2006; 19: 1289-94.
 42. Junker K, Boerner D, Schulze W, Utting M, Schubert J, Werner W. Analysis of genetic alterations in normal bladder urothelium. *Urology* 2003; 62: 1134-8.
 43. Zhu X, Han W, Xue W, et al. The association between telomere length and cancer risk in population studies. *Sci Rep* 2016; 6: 22243.
 44. Williamson SR, Zhang S, Lopez-Beltran A, Montironi R, Wang M, Cheng L. Telomere shortening distinguishes inverted urothelial neoplasms. *Histopathology* 2013; 62: 595-601.
 45. Wang CC, Huang CY, Jhuang YL, Chen CC, Jeng YM. Biological significance of TERT promoter mutation in papillary urothelial neoplasm of low malignant potential. *Histopathology* 2018; 72: 795-803.
 46. Kurtis B, Zhuge J, Ojaimi C, et al. Recurrent *TERT* promoter mutations in urothelial carcinoma and potential clinical applications. *Ann Diagn Pathol* 2016; 21: 7-11.
 47. Cheng L, Davidson DD, Wang M, et al. Telomerase reverse transcriptase (*TERT*) promoter mutation analysis of benign, malignant and reactive urothelial lesions reveals a subpopulation of inverted papilloma with immortalizing genetic change. *Histopathology* 2016; 69: 107-13.
 48. Warrick JI, Knowles MA, Yves A, et al. Report From the International Society of Urological Pathology (ISUP) Consultation Conference on Molecular Pathology of Urogenital Cancers. II. Molecular pathology of bladder cancer: progress and challenges. *Am J Surg Pathol* 2020; 44: e30-46.
 49. Cheng L, Montironi R, Lopez-Beltran A. *TERT* promoter mutations occur frequently in urothelial papilloma and papillary urothelial neoplasm of low malignant potential. *Eur Urol* 2017; 71: 497-8.
 50. Catto JW, Azzouzi AR, Amira N, et al. Distinct patterns of microsatellite instability are seen in tumours of the urinary tract. *Oncogene* 2003; 22: 8699-706.
 51. Harper HL, McKenney JK, Heald B, et al. Upper tract urothelial carcinomas: frequency of association with mismatch repair protein loss and lynch syndrome. *Mod Pathol* 2017; 30: 146-56.
 52. Ertl IE, Shariat SF, Mostafaei H, Ilijazi D, Loriot Y. Fibroblast growth factor receptors across urothelial carcinoma landscape. *Curr Opin Urol* 2020; 30: 557-65.
 53. Pietzak EJ, Bagrodia A, Cha EK, et al. Next-generation sequencing of nonmuscle invasive bladder cancer reveals potential biomarkers and rational therapeutic targets. *Eur Urol* 2017; 72: 952-9.
 54. Cancer Genome Atlas Research Network. Comprehensive molecular characterization of urothelial bladder carcinoma. *Nature* 2014; 507: 315-22.
 55. Hartmann A, Dietmaier W, Hofstadter F, Burgart LJ, Chevillat JC, Blaszyk H. Urothelial carcinoma of the upper urinary tract: inverted growth pattern is predictive of microsatellite instability. *Hum Pathol* 2003; 34: 222-7.
 56. Sweeney MK, Rais-Bahrami S, Gordetsky J. Inverted urothelial papilloma: a review of diagnostic pitfalls and clinical management. *Can Urol Assoc J* 2017; 11: 66-9.
 57. Raspollini MR, Lopez-Beltran A. *Urothelium*. Cham: Springer, 2020; 158-61.
 58. Epstein JI, Reuter VE, Amin MB. *Biopsy interpretation of the bladder*. 3rd ed. Philadelphia: Wolters Kluwer, 2017; 164-96.
 59. Risio M, Coverlizza S, Lasaponara F, Vercesi E, Giaccone G. Inverted urothelial papilloma: a lesion with malignant potential. *Eur Urol* 1988; 14: 333-8.
 60. Cox R, Epstein JI. Large nested variant of urothelial carcinoma: 23 cases mimicking von Brunn nests and inverted growth pattern of noninvasive papillary urothelial carcinoma. *Am J Surg Pathol* 2011; 35: 1337-42.

Standardization of the pathologic diagnosis of appendiceal mucinous neoplasms

Dong-Wook Kang¹, Baek-hui Kim², Joon Mee Kim³, Jihun Kim⁴, Hee Jin Chang⁵, Mee Soo Chang⁶, Jin-Hee Sohn⁷,
 Mee-Yon Cho⁸, So-Young Jin⁹, Hee Kyung Chang¹⁰, Hye Seung Han¹¹, Jung Yeon Kim¹², Hee Sung Kim¹³,
 Do Youn Park¹⁴, Ha Young Park¹⁵, So Jeong Lee¹⁶, Wonae Lee¹⁷, Hye Seung Lee¹⁸, Yoo Na Kang¹⁹, Younghee Choi²⁰,
 The Gastrointestinal Pathology Study Group of the Korean Society of Pathologists

¹Department of Pathology, Chungnam National University Sejong Hospital, Chungnam National University College of Medicine, Daejeon;

²Department of Pathology, Korea University Guro Hospital, Korea University College of Medicine, Seoul;

³Department of Pathology, Inha University School of Medicine, Incheon;

⁴Department of Pathology, Asan Medical Center, University of Ulsan College of Medicine, Seoul;

⁵Department of Pathology, Research Institute and Hospital, National Cancer Center, Goyang;

⁶Department of Pathology, Seoul National University Boramae Hospital, Seoul National University College of Medicine, Seoul;

⁷Department of Pathology, Kangbuk Samsung Hospital, Sungkyunkwan University School of Medicine, Seoul;

⁸Department of Pathology, Yonsei University Wonju College of Medicine, Wonju;

⁹Department of Pathology, Soonchunhyang University Seoul Hospital, Seoul;

¹⁰Department of Pathology, Kosin University Gospel Hospital, Kosin University College of Medicine, Busan;

¹¹Department of Pathology, Konkuk University School of Medicine, Seoul;

¹²Department of Pathology, Inje University Sanggye Paik Hospital, Seoul;

¹³Department of Pathology, Chung-Ang University School of Medicine, Seoul;

¹⁴Department of Pathology, St. Maria Pathology, Busan;

¹⁵Department of Pathology, Busan Paik Hospital, Inje University College of Medicine, Busan;

¹⁶Department of Pathology, Pusan National University Hospital and Pusan National University School of Medicine, Busan;

¹⁷Department of Pathology, Dankook University College of Medicine, Cheonan;

¹⁸Department of Pathology, Seoul National University College of Medicine, Seoul;

¹⁹Department of Forensic Medicine, Kyungpook National University School of Medicine, Daegu;

²⁰Department of Pathology, Hallym University Dongtan Sacred Heart Hospital, Hwaseong, Korea

Although the understanding of appendiceal mucinous neoplasms (AMNs) and their relationship with disseminated peritoneal mucinous disease have advanced, the diagnosis, classification, and treatment of AMNs are still confusing for pathologists and clinicians. The Gastrointestinal Pathology Study Group of the Korean Society of Pathologists (GPSG-KSP) proposed a multicenter study and held a workshop for the “Standardization of the Pathologic Diagnosis of the Appendiceal Mucinous Neoplasm” to overcome the controversy and potential conflicts. The present article is focused on the diagnostic criteria, terminologies, tumor grading, pathologic staging, biologic behavior, treatment, and prognosis of AMNs and disseminated peritoneal mucinous disease. In addition, GPSG-KSP proposes a checklist of standard data elements of appendiceal epithelial neoplasms to standardize pathologic diagnosis. We hope the present article will provide pathologists with updated knowledge on how to handle and diagnose AMNs and disseminated peritoneal mucinous disease.

Key Words: Appendiceal mucinous neoplasm; Disseminated peritoneal mucinous disease; Standardization; Pathologic diagnosis

Received: April 13, 2021 **Revised:** May 21, 2021 **Accepted:** May 28, 2021

Corresponding Author: Joon Mee Kim, MD, PhD, Department of Pathology, Inha University School of Medicine, 27 Inhang-ro, Jung-gu, Incheon 22332, Korea
 Tel: +82-32-890-3987, Fax: +82-32-890-3464, E-mail: jmkpath@inha.ac.kr

Appendiceal mucinous neoplasms (AMNs) are rare appendiceal epithelial tumors, characterized by mucinous epithelial proliferation with extracellular mucin and a common cause of disseminated peritoneal mucinous disease, pseudomyxoma peritonei

[1-3]. The accurate diagnosis of AMNs is clinically important because management may include a long-term follow-up to radical innovative therapy, such as cytoreductive surgery with hyperthermic intraperitoneal chemotherapy (CRS-HIPEC) and

systemic chemotherapy [1-5]. However, the definition and classification of AMNs have been inconsistent, which causes potential confusion when diagnosing and managing patients [5-11]. Recently, an international working group, Peritoneal Surface Oncology Group International (PSOGI), reached a modified Delphi consensus on classifications and diagnostic terminologies [12]. Although this was a global effort, the terminology of AMNs is still contentious. To establish a tumor staging system, the 8th edition of the American Joint Committee on Cancer (AJCC 8th) *Cancer Staging Manual* applied pT staging to low-grade appendiceal mucinous neoplasms (LAMNs) for the differentiation of high-grade diseases [13,14]. However, the biologic behaviors of AMNs and disseminated peritoneal mucinous disease are still controversial among the pathologists who perform diagnoses without adequate guidelines.

The Gastrointestinal Pathology Study Group of the Korean Society of Pathologists (GPSG-KSP) has contributed to the establishment of standard pathologic guidelines for gastrointestinal neoplasms [15-21]. However, there are no well-established or consensus guidelines for diagnosing and evaluating AMNs, leading to confusion and potential conflict in daily practice and medical insurance compensation. There is a need to assess cancer registration because of changes in the newly published 5th edition of the World Health Organization Classification (WHO 5th) of *Digestive System Tumors* and the AJCC 8th *Cancer Staging Manual*. AMNs are uncommon appendiceal epithelial neoplasm, and there are many limitations in a single institution study. The GPSG-KSP proposed a multicenter study to overcome the limitations and held a workshop entitled “Standardization of the Pathologic Diagnosis of the Appendiceal Mucinous Neoplasm.” The GPSG-KSP recruited institutions and pathologists and collected cases diagnosed as AMNs and related diseases in each institution from 2011 to 2015. Expert pathologists of the GPSG-KSP selected typical cases with AMNs and disseminated peritoneal mucinous disease according to the PSOGI consensus guidelines [12], the College of American Pathologists (CAP) protocol [22], the AJCC 8th *Cancer Staging Manual* [13], and the WHO 5th *Digestive System Tumors* [1]. Expert pathologists reached the consensus in the collected cases through a live microscopic examination using a 12-head microscope if conflicting cases were presented. One hundred and twenty-one members of the KSP participated in the workshop. Virtual slides provided a total of 23 cases during the workshop. Before the workshop, we asked several questions about the basic information of the participants and diagnostic terminologies and stagings of the AMNs (Supplementary Data S1). After a lecture on updates, we surveyed several issues

about the diagnostic criteria, biologic behavior codes, and tumor gradings of the AMNs and disseminated peritoneal mucinous disease (Supplementary Data S2). We collected their responses and discussed differing opinions with members of the GPSG-KSP. In addition, we propose an essential checklist of standard data elements of the appendiceal epithelial neoplasms for the standardization of pathologic diagnosis of AMNs and disseminated peritoneal mucinous disease.

APPENDICEAL MUCINOUS NEOPLASMS

Definition and characteristics of appendiceal mucinous neoplasms

Appendiceal epithelial neoplasms, over 70% of the mucin-producing type, account for most primary appendiceal tumors [1-3]. The classification of appendiceal epithelial tumors of the WHO 5th *Digestive System Tumors* is listed in Table 1. The WHO 5th *Digestive System Tumors* defined the AMN as a mucinous epithelial proliferation with extracellular mucin and pushing invasion pattern or pushing tumor margins [1]. Most AMNs de-

Table 1. Classification of appendiceal epithelial tumors based on the 5th edition of the *WHO Classification of Digestive System Tumors* [1]

ICD-O3	Epithelial tumors
-	Hyperplastic polyp
-	Sessile serrated lesion without dysplasia
8213/0	Serrated dysplasia, low grade
8213/2	Serrated dysplasia, high grade
8480/1	Low-grade appendiceal mucinous neoplasm
8480/2	High-grade appendiceal mucinous neoplasm
8140/3	Adenocarcinoma, NOS
8480/3	Mucinous adenocarcinoma (>50% mucin)
8490/3	Signet-ring cell carcinoma (>50% signet-ring cells)
8020/3	Carcinoma, undifferentiated, NOS
8243/3	Goblet cell adenocarcinoma
8240/3	Neuroendocrine tumor, NOS
8240/3	Neuroendocrine tumor, grade 1
8249/3	Neuroendocrine tumor, grade 2
8249/3	Neuroendocrine tumor, grade 3
8152/3	L-cell tumor
8152/3	Glucagon-like peptide producing tumor
8152/3	PP/PYY-producing tumor
8241/3	Enterochromaffin-cell carcinoid
8241/3	Serotonin-producing carcinoid
8246/3	Neuroendocrine carcinoma
8013/3	Large cell neuroendocrine carcinoma
8041/3	Small cell neuroendocrine carcinoma
8154/3	Mixed neuroendocrine-non-neuroendocrine carcinoma (MiNEN)

WHO, World Health Organization; ICD-O3, International Classification of Diseases for Oncology, 3rd edition; NOS, not otherwise specified.

velop in middle-aged or elderly patients and present with non-specific symptoms or signs, such as acute abdominal pain [1-5,12]. AMNs can exhibit variable clinical behaviors, ranging from a relatively slow-growing and low-grade tumor, but with considerable risk of recurrence, to a high-grade and aggressive neoplasm that produces eventual peritoneal metastasis [1-7]. AMNs can be divided into LAMN and high-grade appendiceal mucinous neoplasm (HAMN) by cytological grading. The classification, grading, biologic behavior codes, diagnostic criteria, and microscopic features are listed in Table 2.

Pushing invasion in appendiceal mucinous neoplasms

Pushing invasion is defined as a tongue-like protrusion, diverticulum-like growing, or broad-front spread of the epithelium into the appendiceal wall [1,3,12]. Pushing invasion can cause the attenuation of lamina propria and muscularis mucosae, and this is not associated with the destructive invasion or desmoplastic infiltration, characteristics of invasive carcinoma [1,3,12,23]. Moreover, pushing invasion through the appendiceal wall presents extra-appendiceal mucin accumulation, leading to diagnostic difficulty or misdiagnosis. Extracellular mucin can lead to the dissection of the wall and rupture with the potential for intra-peritoneal dissemination [24,25].

LOW-GRADE APPENDICEAL MUCINOUS NEOPLASM

Definition and histologic findings of low-grade appendiceal mucinous neoplasm

The AJCC 8th *Cancer Staging Manual* defined a LAMN as a mucinous neoplasm with low-grade cytology associated with the obliteration of the muscularis mucosae without overt features of the invasion [13]. The lamina propria is frequently effaced, and mucosal lymphoid tissues are decreased or absent. Mucinous cystadenoma and mucocele were histologically used as synonyms for LAMN but are no longer recommended in pathologic reports due to their ambiguous and misleading nature. The essential histologic finding of LAMN is low-grade cytology with pushing invasion; however, there is no destructive invasion in the appendiceal wall. Fig. 1 demonstrates the microscopic features of LAMNs, displaying pushing invasion and broad-front spreading by a mucin-rich epithelium. Notably, when regarding whether pushing invasion is necessary for the diagnosis of LAMN, most of the survey responders diagnosed Fig. 1A, B as LAMN. In typical LAMNs, there is a loss of the normal mucosal architectures, at least focally, such as obliteration of the lamina propria and muscularis mucosa, fibrosis of the submucosa, and atrophy of the lymphoid follicles. Although the epithelium may show a papillary, villous, undulating, or flat architecture, lining epithelial cells are generally arranged in a monolayer (Fig. 1C, D). The micro-

Table 2. Classification, grading, biologic behavior codes, and diagnostic criteria and microscopic features of appendiceal mucinous tumors

Classification	Grading ^a	ICD-O3	KCD-8	Diagnostic criteria and microscopic features [3,12]
Low-grade appendiceal mucinous neoplasm	Low/G1	8480/1	D37.3	Mucinous neoplasm with low-grade cytology and any of the following (by PSOGI criteria) Loss of muscularis mucosae Fibrosis of submucosa "Pushing invasion" (expansile or diverticulum-like growth) Dissection of acellular mucin in wall Undulating or flattened epithelial growth Rupture of appendix Mucin and/or cells outside appendix
High-grade appendiceal mucinous neoplasm	High/G2	8480/2	D01.7	Mucinous neoplasm with the architectural features of LAMN and no infiltrative invasion, but with high-grade cytologic atypia
Mucinous adenocarcinoma	High/G2	8480/3	C18.1	Malignant glandular neoplasm, comprising of >50% extracellular mucin, characterized by infiltrative invasion. The pattern of infiltrative invasion as follows: Infiltrative glands, or single infiltrative tumor cells associated with extracellular mucin and desmoplastic stroma Small dissecting mucin pools containing floating nests, glands, or single neoplastic cells
Mucinous adenocarcinoma with signet-ring cells	High/G3	8480/3	C18.1	Mucinous adenocarcinoma, comprising of ≤50% signet-ring cells
Signet-ring cell carcinoma	High/G3	8490/3	C18.1	Adenocarcinoma, comprising up to >50% signet-ring cells

ICD-O3, International Classification of Diseases for Oncology, 3rd edition; KCD-8, Korean Classification of Disease, 8th edition; PSOGI, Peritoneal Surface Oncology Group International; LAMN, low-grade appendiceal mucinous neoplasm.

^aGrading divide into low- and high-grade by the two-tier system and G1 to G3 by three-tiered system.

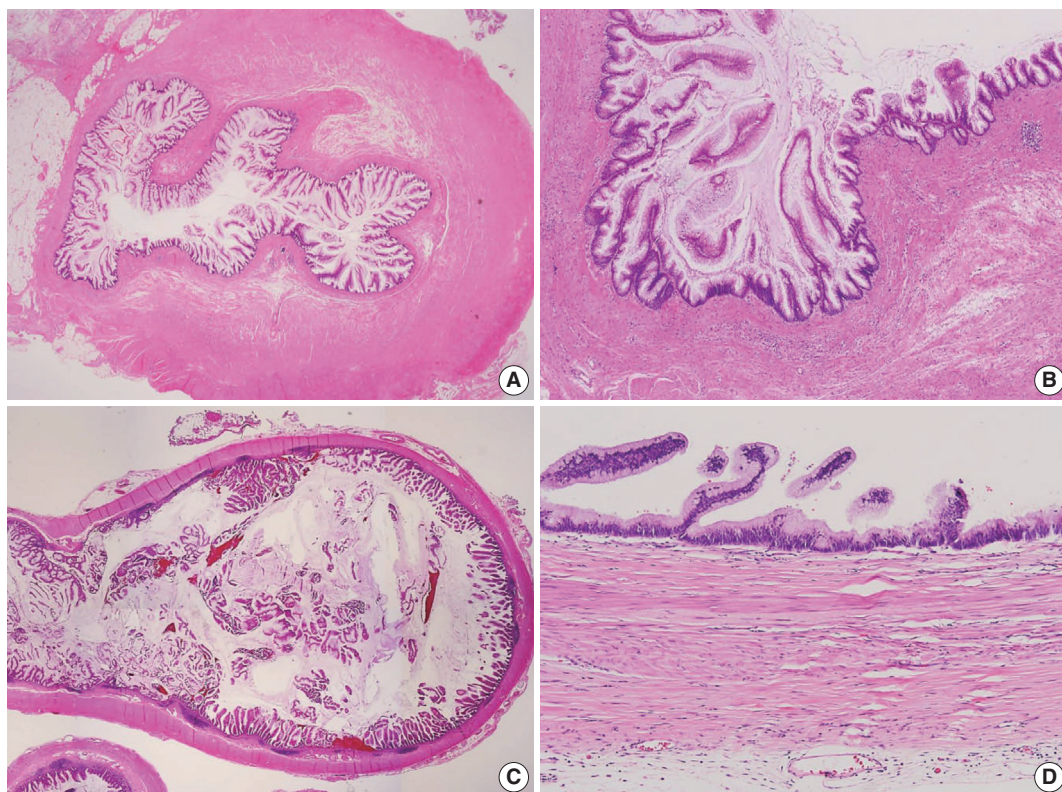


Fig. 1. Low-grade appendiceal mucinous neoplasm (LAMN). (A) A LAMN demonstrates a “pushing invasion” or tongue-like protrusion into the appendiceal wall. (B) A LAMN reveals a pushing growth by the mucinous epithelium into the appendiceal wall, which should not be considered as infiltrative invasion. (C) A LAMN shows a “pushing border” or broad-front border by the epithelium. (D) A LAMN reveals a flat or papillary epithelium associated with the loss of the lamina propria, obliteration of muscularis mucosae, and atrophy of submucosa and muscularis propria.

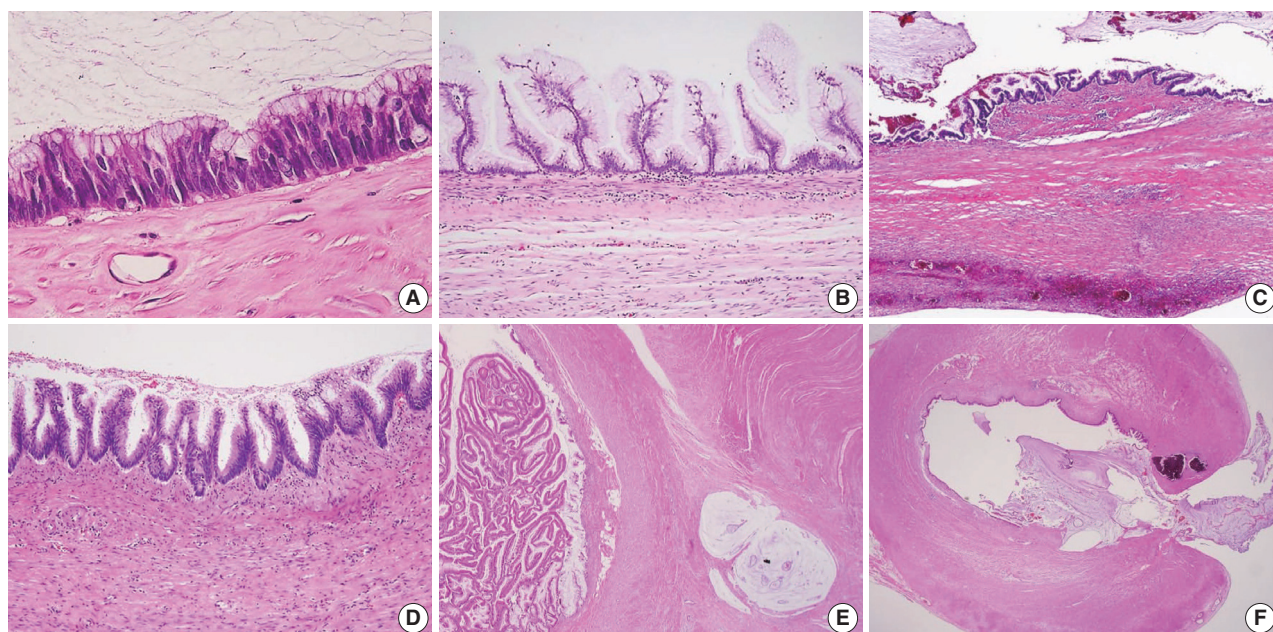


Fig. 2. Various microscopic features of a low-grade appendiceal mucinous neoplasm. (A) Low-grade cytologic features with pencil-like nuclei maintaining the nuclear polarity. (B) The neoplastic mucinous epithelium may have a villous architecture with loss of lamina propria and muscularis mucosae. (C) The appendiceal wall exhibits extensive fibrosis. (D) The neoplastic epithelium displays an undulating or short wave-like architecture. (E) The appendiceal wall is dissected by mucin. (F) Rupture of the wall by mucin and/or cells outside the appendix.

scopic features essential for LAMN proposed by the PSOGI panel are illustrated in Fig. 2. It is not surprising that LAMN with intact muscularis mucosae may develop disseminated peritoneal mucinous disease. For this reason, there is hesitancy in diagnosing a lesion with intact muscularis mucosae as adenoma because adenomas should be limited to benign lesions that have no potential for peritoneal dissemination. Patients with LAMN often present symptoms like acute appendicitis. Typical LAMNs usually have thin fibrotic walls and abundant intraluminal mucin, and less commonly, calcification of the wall. Grossly apparent rupture with mucin extrusion is generally manifested in patients with disseminated peritoneal mucinous disease.

Mimickers of low-grade appendiceal mucinous neoplasm

Because LAMNs show benign-looking cytology, they can mimic several benign lesions associated with mucinous epithelial proliferation. The appendiceal diverticulum is perhaps the most common mimicker of LAMN due to their pushing growing pattern, specifically when related to abundant mucin exposed to the serosal surface. A preserved lamina propria is an indication of the diagnosis of a diverticulum. Careful examination of the

entire appendix at lower magnification often leads to identifying a diverticulum. Sometimes, Schwann cell hyperplasia expands the lamina propria, possibly because of the obliteration effects [26,27]. If a histologic examination of the entire appendix fails to reveal a lining epithelium, the possibility of a retention cyst may be considered. Appendiceal retention cysts are rare and mostly small-sized; thus, lesions more than 2 cm in diameter are much more likely to be LAMNs. Appendiceal endometriosis with intestinal metaplasia is uncommon and can resemble a LAMN. The epithelial component acquires an intestinal phenotype characterized by columnar mucin-secreting cells, sometimes with goblet cells. Recognition of the endometrial stroma surrounding the glands and CD10 immunohistochemical stain will lead to a diagnosis. Mucosal hyperplasia can be seen in acute appendicitis. Mucosal hyperplasia tends to be more pronounced toward the luminal side and is frequently observed in areas of intense inflammation. Occasionally, reactive cellular atypia in the acute suppurative appendicitis may approximate the neoplastic atypia in LAMN. Fig. 3 reveals various mimickers of LAMN.

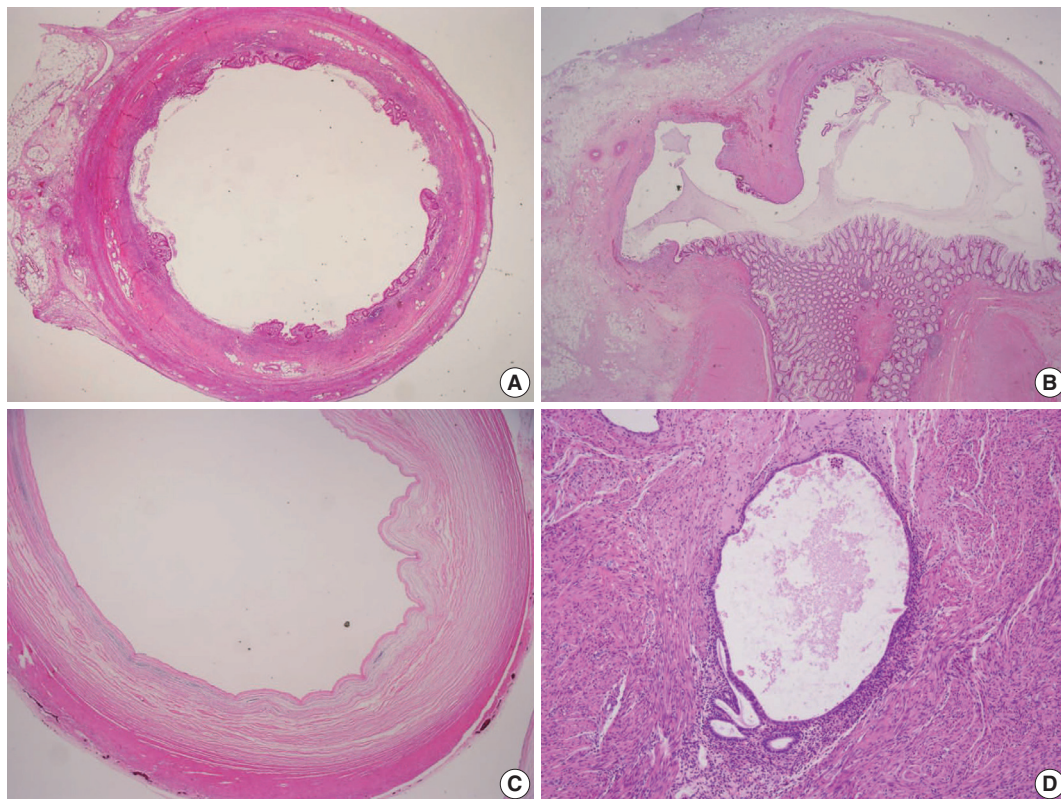


Fig. 3. Mimickers of appendiceal mucinous neoplasm. (A) Acute suppurative appendicitis. (B) An appendiceal diverticulum presents pushing growth by abundant mucin and acute suppurative inflammation. Note that a lower magnification often leads to the identification of the diverticulum. (C) Retention cyst without a lining epithelium. (D) Appendiceal endometriosis.

HIGH-GRADE APPENDICEAL MUCINOUS NEOPLASM

Definition and histologic of HAMN

HAMN was proposed for the lesion with similar architectures of LAMN having high-grade cytologic features but no infiltrative invasion [13]. Fig. 4 demonstrates the histologic findings of HAMN. The microscopic findings include cribriform, loss of nuclear polarity, high-grade cytology (i.e., enlarged, hyperchromatic, pleomorphic nuclei, and atypical mitotic figures), frequent single-cell necrosis and may present sloughing of necrotic cells into the lumen [23]. HAMNs are suggested to reveal an intermediate risk between LAMNs and mucinous adenocarcinomas.

Biologic behavior code of HAMN

According to the WHO 5th *Digestive System Tumors*, the *International Classification of Diseases for Oncology*, 3rd edition (ICD-O3) behavior codes for LAMN and HAMN were proposed as 8480/1 and 8480/2, respectively (Table 2). The response of the ICD-O3 of the HAMN was varied at the workshop because the questionnaire for the suspected ICD-O3 behavior code of the HAMN was conducted before the publication of the WHO 5th *Digestive System Tumors*. However, there was a consensus that the behavior code should be 8480/2 to avoid confusion in the following GPSG meeting. Misdraji et al. [7] reported that HAMNs show more aggressive clinical behavior than LAMNs, but the prognosis is still not unveiled because HAMNs are extremely rare. Therefore, nothing of the HAMNs prognosis is known. Yantiss et al. [11] reported that HAMN was more likely to be associated with aggressive clinical course and extra-appendiceal mucin spreading than LAMN. Carr et al. [23] proposed that

HAMN should include lesions with high-grade cytologic atypia that is seen only focally, provided it is unequivocal; however, there has been no accepted consensus on the quantification of focal lesions yet. We surveyed the “focal” concept at the workshop, and the responses are shown in Supplementary Data S2.

SERRATED LESIONS

Classification of appendiceal serrated lesions

The WHO 5th *Digestive System Tumors* defined an appendiceal serrated lesion as a mucinous epithelial lesion characterized by a serrated (sawtooth or stellate) architecture of the luminal crypt [1]. Serrated lesions are classified as a hyperplastic polyp, sessile serrated lesion without dysplasia, and serrated lesion with dysplasia or serrated dysplasia [1,14]. Polyps that lack a luminal crypt of serrated architecture and dysplasia are classified as hyperplastic polyps. Sessile serrated lesions are commonly deficient in cytological dysplasia. They often involve mucosa in a diffuse circumferential fashion. Serrated dysplasia refers to conventional adenoma-like dysplasia, traditional serrated adenoma-like dysplasia, and mixed morphological patterns of dysplasia [14]. LAMNs are heterogeneous, with typical LAMN in some areas and serrated lesions in others, raising the possibility that some LAMNs could arise from serrated lesions.

Pathologic findings and pathogenesis of appendiceal serrated lesions

Occasionally, LAMNs simulate a serrated lesion and are challenging to diagnose, particularly if the muscularis mucosae is intact. By the diagnostic criteria of the PSOGI classification, a serrated lesion should be confined to the lesion with intact mus-

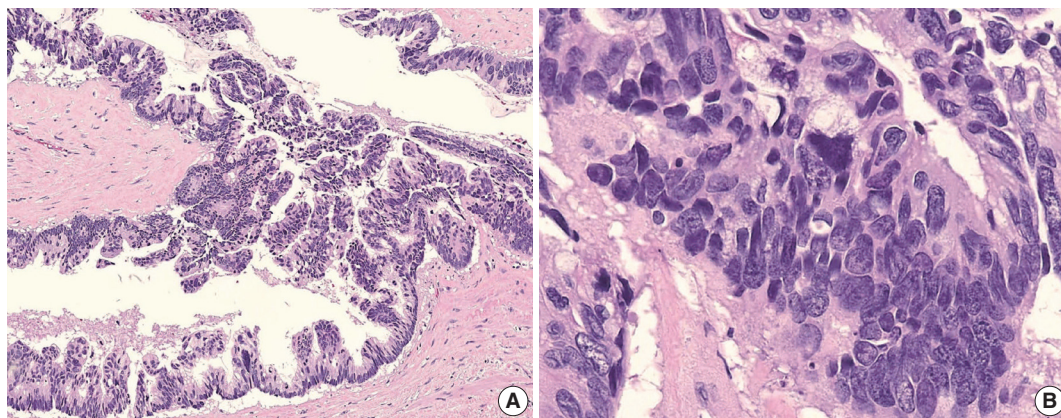


Fig. 4. High-grade appendiceal mucinous neoplasm (HAMN). (A) A HAMN shows the same low-power architectural features as low-grade appendiceal mucinous neoplasm without infiltrative invasion. (B) A HAMN is characterized by high-grade cytology, including enlarged and vesicular nuclei with full-thickness stratification, loss of nuclear polarity, prominent nucleoli, and sometimes mitotic figures.

cularis mucosae, no mucin in the wall or outside, and no expansile growth pattern or pushing invasion [12]. Although appendiceal serrated lesions have similar microscopic features to their colorectal counterparts, they commonly harbor *KRAS* mutations but lack *BRAF* mutations, indicating that the serrated pathway in the appendix is likely to be different from those of the colorectum [14,23,28]. However, serrated lesions remain incompletely studied and are not fully understood. The serrated lesions of the appendix are demonstrated in Fig. 5.

STAGING OF APPENDICEAL MUCINOUS NEOPLASMS

AJCC 8th TNM staging

The AJCC 7th *Cancer Staging Manual* was not clear on applying the staging criteria of AMNs [29]. However, the AJCC 8th *Cancer Staging Manual* showed significant changes to the staging

criteria of AMNs, particularly for LAMN [13]. In addition, the role of acellular mucin or a mucinous epithelium outside of the appendix is also addressed and included in the staging [1,13]. A summary of the AJCC pT classification of LAMN and prognostic significance from the AJCC 8th *Cancer Staging Manual* is listed in Table 3. In non-mucinous appendiceal tumors, the pTis category includes high-grade dysplasia, carcinoma in situ, and intramucosal carcinoma [13]. Notably, LAMNs confined to the appendiceal wall are classified as pTis. The staging of pTis reflects the excellent outcome when limited to the appendiceal wall [13]. In most LAMNs, there is no well-preserved mucosal architecture; hence, assessing the involvement of the mucosa and submucosa is impossible, resulting in the inability to apply pT1 designation to the LAMNs. In addition, studies evaluating the outcomes in LAMN have determined that pushing invasion into the appendiceal wall is not associated with tumor recurrence [7,11,30]. Thus, pT2 designation does not apply to LAMN [13].

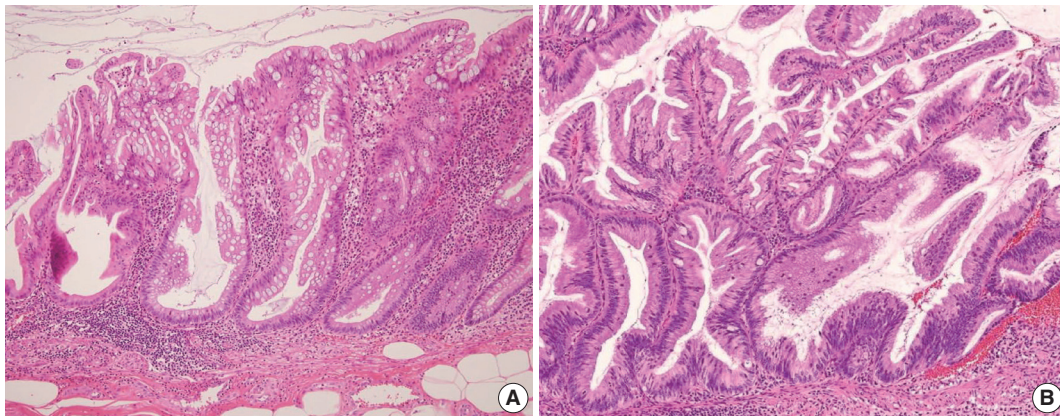


Fig. 5. Appendiceal serrated lesions. (A) A sessile serrated lesion without dysplasia is a common microscopic finding to the colorectum counterpart, displaying deep crypt serration and dilated bases. Note that the muscularis mucosae are intact. (B) Serrated dysplasia, low grade presents adenoma-like dysplasia in the crypt base.

Table 3. Summary of pT stages of LAMN and prognostic significance from the AJCC *Cancer Staging Manual*, 8th edition [3,13]

pT stage	Definition and lesions	Prognostic significances
pTis(LAMN)	LAMN confined to the appendiceal wall after histologic examination of the entire appendix. Acellular mucin or mucinous epithelium may interrupt the muscle propria.	pTis(LAMN) has essentially no risk of recurrence. pTis(LAMN) designation requires correlation with the intraoperative findings and an evaluation by the operator.
pT3(LAMN)	LAMN with acellular mucin or mucinous epithelium extending into the subserosa or mesoappendix but no involvement of the serosa after histologic examination of the entire appendix.	Unknown risk of peritoneal recurrence. Long-term follow-up for 10 yr is suggested until additional data on recurrence risk becomes available.
pT4(LAMN)	LAMN invades the visceral peritoneum, including the acellular mucin or mucinous epithelium involving the serosa of the appendix or mesoappendix (pT4a), and/or directly invades adjacent organs or structures (pT4b).	Low risk (acellular mucin) and high risk (mucinous epithelium) of peritoneal recurrence. Long-term follow-up for 10 yr with periodic imaging is required. Additional surgery or CRS-HIPEC is uncertain but is used in some centers.

Note that pT1 and pT2 do not apply to LAMN.

LAMN, low-grade appendiceal mucinous neoplasm; AJCC, American Joint Committee on Cancer; CRS-HIPEC, cytoreductive surgery with hyperthermic intraperitoneal chemotherapy.

Staging of low-grade appendiceal mucinous neoplasm

Various pT stagings of LAMN were presented in the workshop and are illustrated in Fig. 6. In a questionnaire for suspected pTis or other stages, many pathologists were unaware of the new concept of pTis(LAMN). Because mucinous tumors can frequently extend into the muscularis propria by pushing invasion in LAMN, mucin extending into the muscularis propria should be classified as pTis(LAMN) as long as it does not extend into the mesoappendix or serosa (Fig. 6A, B). LAMNs showing either acellular mucin or mucinous epithelium involvement to subserosa or mesoappendix are classified as pT3 (Fig. 6C). Perforation of the appendix by LAMN is associated with a high risk of peritoneal dissemination. Given the risk of disseminated peritoneal mucinous disease, pT4 includes assessing both acellular mucin and the mucinous epithelium and is designated as T4a (penetration of the serosa) (Fig. 6D) and T4b (directly invades adjacent organs or structures) (Fig. 6E). Notably, pT4a does not include luminal or mural spreading into the cecum. Most cases of LAMNs are associated with luminal mucin. This mucin can frequently contaminate the serosa during the gross examination, histologic processing, and even operation. These cases should not be diagnosed as pT4a. Indeed, mucinous deposits on the appendiceal serosa are associated with a granulation tissue-like response and neo-vascularization; numerous small capillaries containing red blood cells are seen coursing through the mucin (Fig. 6F). When the peritoneal dissemination is limited to acellular mucin only, it is classified as M1a. Other metastatic categories are M1b, which refers to metastases confined to the peritoneum only, and M1c which refers to metastases outside the peritoneum, such as pleuropulmonary metastasis.

larization; numerous small capillaries containing red blood cells are seen coursing through the mucin (Fig. 6F). When the peritoneal dissemination is limited to acellular mucin only, it is classified as M1a. Other metastatic categories are M1b, which refers to metastases confined to the peritoneum only, and M1c which refers to metastases outside the peritoneum, such as pleuropulmonary metastasis.

Staging of HAMN

According to the Union for International Cancer Control staging system, LAMN and HAMN are considered as pTis, if confined to the appendiceal wall [1]. However, the AJCC 8th *Cancer Staging Manual* stated that the HAMN should be staged using the same staging system as invasive mucinous adenocarcinoma [13]. These two different opinions may bring confusion in daily practice. Valasek and Pai [3] proposed that HAMN with pushing invasion into the muscularis propria would be classified as pT2 using the same staging system for invasive adenocarcinoma. However, since there are very few cases of HAMN, the actual application of the staging for HAMNs will be determined after the results of large-scale survival analysis. We surveyed the expected pT stages of the HAMNs at the workshop, and the responses are shown in Supplementary Data S2.

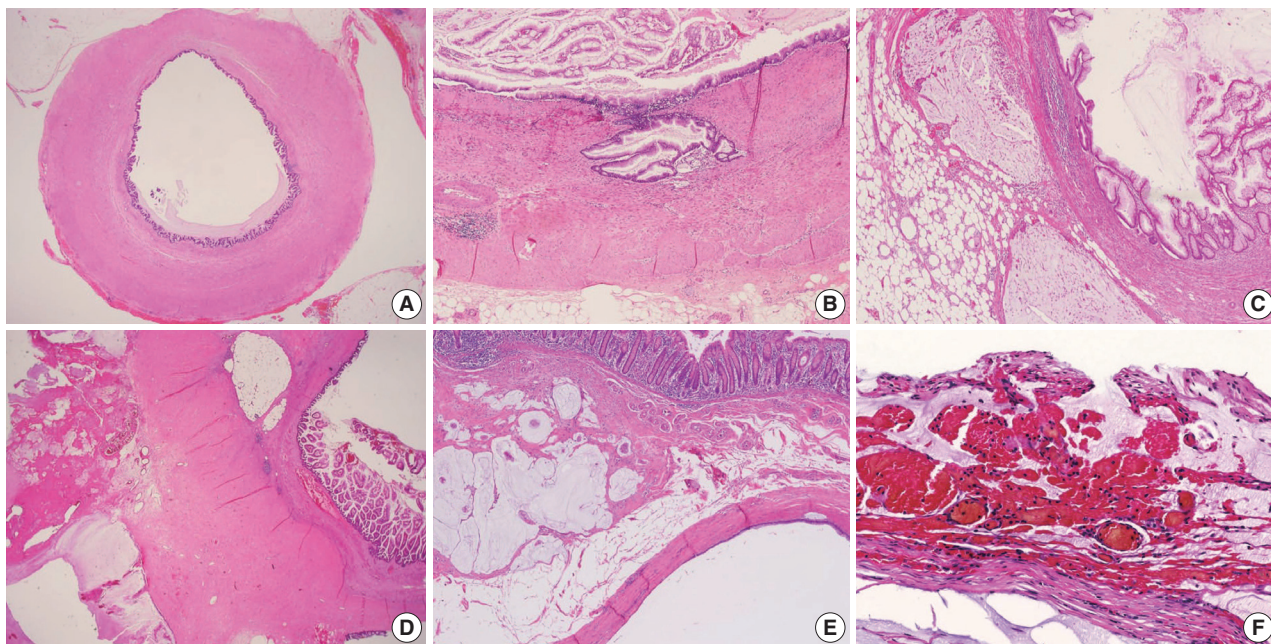


Fig. 6. Pathologic staging of low-grade appendiceal mucinous neoplasms (LAMNs). (A) A LAMN confined to the appendiceal wall is designated as pTis(LAMN). (B) Acellular mucin or mucinous epithelium may frequently extend into the muscularis propria; however, the pT stage is defined as pTis. Note that pT1 and pT2 do not apply to LAMN. (C) A LAMN extends to the subserosa or mesoappendix and is classified as pT3. (D) Acellular mucin or mucinous epithelium penetrating the serosal surface is classified as pT4a. (E) The tumor directly invades into the adjacent intestinal segment by way of the serosa, e.g., invasion of the ileum (pT4b). (F) Acellular mucin on the serosal surface with inflammatory reaction and neovascularization (pT4a).

APPENDICEAL MUCINOUS ADENOCARCINOMA

Definition and histologic findings of appendiceal mucinous adenocarcinoma

Appendiceal mucinous adenocarcinoma is defined as mucinous neoplasms showing infiltrative invasion comprised of > 50% extracellular mucin [1]. In contrast to the pushing invasion of the LAMN, the infiltrative invasion is confined to destructive stromal invasion into the appendiceal wall. The histologic features of infiltrative invasion include infiltrative tumor cells, which exhibit cribriform, small tubules, or single cells accompanied by mucin within the desmoplastic stroma, and small dissecting mucin containing floating tumor cells but inconspicuous desmoplastic reaction [1,3,12]. The neoplastic epithelium in mucinous adenocarcinoma demonstrates high-grade cytology that may be only seen focally, are characterized by enlarged nuclei, prominent nucleoli, increased mitotic figures, full-thickness stratification, and loss of nuclear polarity, which often extends to the luminal aspect of the epithelial cell.

Grading system of appendiceal mucinous adenocarcinoma

The PSOGI consensus panel has classified appendiceal mucinous adenocarcinomas and moderately and poorly differentiated mucinous adenocarcinoma, similar to the grading system of non-mucinous adenocarcinoma in other gastrointestinal tracts [12]. However, the PSOGI consensus classification was not easy to apply to appendiceal mucinous adenocarcinomas. The AJCC 8th *Cancer Staging Manual* classified the appendiceal mucinous tumors as a three-tier grading system: G1 (well-differentiated), G2 (moderately differentiated), and G3 (poorly differentiated), based on cytologic features, tumor cellularity, and signet-ring components [13].

Appendiceal G1 (well-differentiated) tumors are low-grade cytology, usually lacking infiltrative invasion, and essentially refers to LAMN. Given that mucinous adenocarcinoma is characterized by infiltrative invasion and almost always exhibits at least focal areas of high-grade cytologic features, typical mucinous adenocarcinomas should be classified as either G2 (moderately differentiated) or G3 (poorly differentiated) tumors [3]. Mucinous adenocarcinomas often show complex architecture, such as cribriform and complex papillary structures. The presence of signet-ring cells is an indication of infiltrative mucinous adenocarcinoma. Poorly differentiated (G3) mucinous adenocarcinoma demonstrates infiltrative invasion, with most having signet-ring cells. Signet-ring cells, characterized by prominent intracytoplasmic mucin displacing the nucleus, may infiltrate single cells or as

aggregates, classified as grade G3 (poorly differentiated). Most G3 tumors are almost entirely composed of signet-ring cells, while a minority of cases are composed of mixed signet-ring cells and glandular structures. If cancer comprises ≤ 50% signet-ring cells, the WHO terminology is mucinous adenocarcinoma with signet-ring cells or mucinous adenocarcinoma, poorly differentiated. If the tumor contains > 50% signet-ring cells, the WHO terminology is signet-ring cell carcinoma. The microscopic findings of high-grade (G2 and G3) appendiceal mucinous adenocarcinomas are demonstrated in Fig. 7.

Most mucinous adenocarcinomas have clinically aggressive behavior, infiltrating through the appendiceal wall (pT4), and frequently metastasize to the abdominal or pelvic peritoneum at diagnosis. After an appendectomy specimen, diagnosis of mucinous adenocarcinoma should result in subsequent right hemicolectomy to evaluate lymph node metastases.

Ancillary tests of appendiceal mucinous neoplasms

A limited number of studies have reported that the vast majority of *KRAS* mutations occurred in G1 and G2 tumors [4,31-35], and most *KRAS* mutations occur in 50% to 60% of Tis(LAMN) [4]. These data suggest that *KRAS* mutations are important in tumor initiation but may be less critical for aggressive high-grade tumor progression. *GNAS* mutations, known as essential in abundant mucin production, are also presented in G1 and G2 tumors but less commonly in G3 tumors [31-35]. The co-mutation of *GNAS* and *KRAS* is identified in between 65% to 85% of cases [35,36]. Other minor mutations, including *MET*, *PIK3CA*, *FAT4*, *AKT1*, *SMAD2*, *JAK3*, *STK11*, and *RB1* have been identified [33,37]. However, *BRAF* mutation, microsatellite instability (MSI), and DNA mismatch repair protein deficiency are rarely seen in LAMN [10,38].

DISSEMINATED PERITONEAL MUCINOUS DISEASE

Pseudomyxoma peritonei should be avoided in pathologic diagnosis

Pseudomyxoma peritonei, the clinical term for disseminated peritoneal mucinous disease, is a syndrome and applies to a neoplastic condition characterized by the grossly persistent accumulation of mucinous ascites in the peritoneal cavity [12]. The expansion of mucin within the abdominal cavity results from mucus following the normal flow of peritoneal fluid, redistribution of the mucin, and neoplastic cells [23]. Based on clinicopathological and immunohistochemical data, most cases are due to

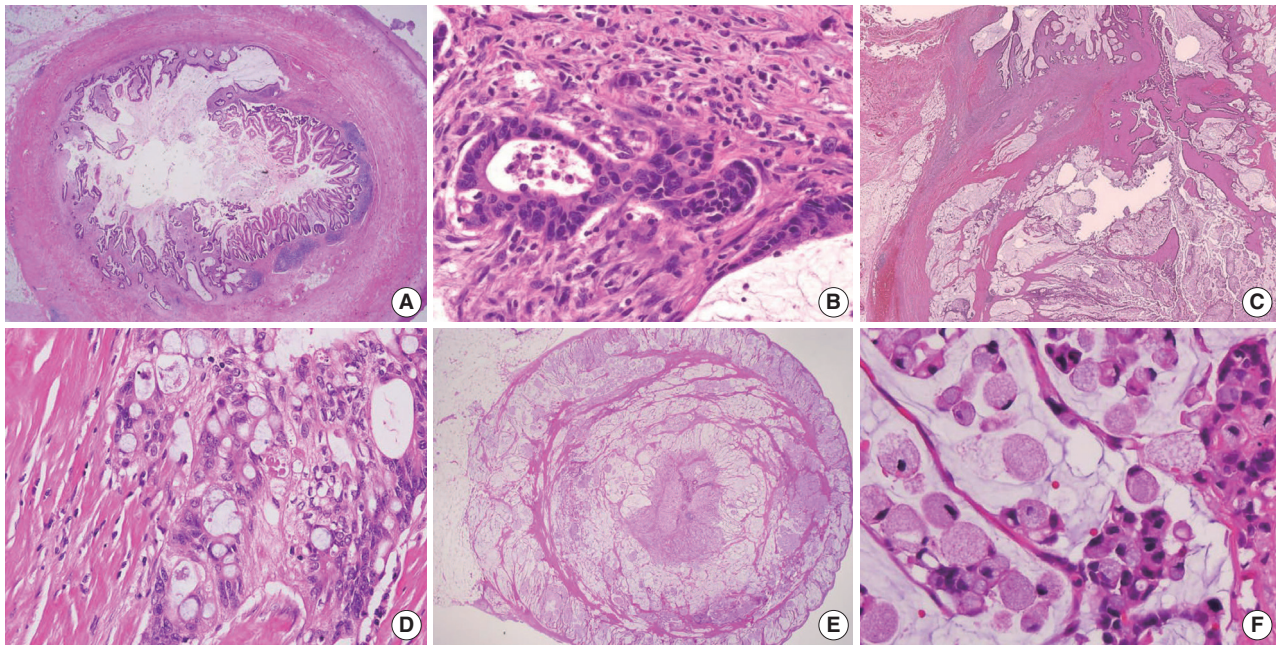


Fig. 7. Various histologic features of appendiceal mucinous adenocarcinoma and signet-ring cell carcinoma. (A) Mucinous adenocarcinoma presents within the appendiceal wall. (B) Moderately differentiated (G2) mucinous adenocarcinoma exhibits high-grade cytology and demonstrates infiltrating glands associated with desmoplastic stroma. (C) Mucinous adenocarcinoma markedly distorts the appendix with dissecting cellular pools present within the appendiceal wall. (D) Poorly differentiated (G3) mucinous adenocarcinoma demonstrates high-grade cytology and signet-ring cells. (E) Signet-ring cell carcinoma (G3, poorly differentiated) essentially replaces the entire wall of the appendix. (F) Neoplastic signet-ring cells are seen in single cells or small clusters within the dissecting mucin pools.

the perforation of AMNs [12,23,24,39,40]. Occasionally, mucinous neoplasms from other organs, including the colon, pancreas, ovary, and urachus, may also present with clinical appearances [12,23,24,39,40]. Immunohistochemical stains of cytokeratin 20 and CDX2 may be helpful in the diagnosis of the appendiceal origin (Supplementary Fig. S1). Clinically, abdominal discomfort, distention, intestinal obstruction, and often omental cake in which the omentum transforms into a firm mass can present within the intraabdominal cavity [4,9,41-43]. Given this, pseudomyxoma peritonei is a clinical term and used mainly by oncologists and radiologists; thus, it should not be used in histopathologic diagnosis [13]. The tendency of tumor cells from the appendix to produce abundant extracellular mucin shows slow infiltration into the peritoneum and underlying tissues with rare lymphovascular invasion relative to the overall tumor bulk [5]. Accurate diagnosis of AMNs and disseminated peritoneal mucinous disease is essential because management may include follow-up or radical treatment such as CRS-HIPEC [23].

Diagnostic terminology and classification of disseminated peritoneal mucinous disease

Ronnett et al. [9] classified disseminated peritoneal mucinous

disease into three prognostically relevant categories: disseminated peritoneal adenomucinosis (DPAM), peritoneal mucinous carcinomatosis (PMCA), and PMCA with signet-ring cells [44]. However, the classification by Ronnett et al. [44] was not well established, leading to conflicting results. Given recent updates on diagnostic terminology, DPAM and PMCA are no longer recommended in pathology reports. Asare et al. [45] found that histologic grade was an independent predictor of survival in 25,992 patients with appendiceal cancer.

The PSOGI consensus panel has presented the diagnostic terminology for disseminated peritoneal mucinous disease: low-grade mucinous carcinoma peritonei, high-grade mucinous carcinoma peritonei, and high-grade mucinous carcinoma peritonei with signet-ring cells are equivalent to the alternative terminology of DPAM, PMCA, and PMCA with signet-ring cells, respectively. The AJCC 8th *Cancer Staging Manual* has proposed terminologies accompanying grading based on the criteria of Misdraji et al. [13,46,47]. Misdraji [46] used the diagnostic terms directly from the appendiceal neoplasm into the peritoneum: LAMN (G1) with peritoneal involvement, mucinous adenocarcinoma moderately differentiated (G2), and mucinous adenocarcinoma poorly differentiated (G3). In addition, acellular mucin is classi-

fied separately. Davison et al. [4] determined that the three-tiered grading is the most important predictive factor of overall survival in patients with stage IV AMNs.

Grading system of disseminated peritoneal mucinous disease

Low-grade (G1, well-differentiated) mucinous carcinoma peritonei, synonymous with a LAMN with peritoneal involvement, is defined as a mucinous neoplasm of low-grade cytology involving the peritoneum without infiltrative invasion or desmoplasia. Perineural and lymphovascular invasions are not seen. Typically, the neoplastic epithelial component accounts for less than 20% of the total mucin component. Low-grade (G1, well-differentiated) mucinous carcinoma peritonei almost always arises from a LAMN, so the AJCC 8th *Cancer Staging Manual* and Misdraji [46] proposed the term of LAMN with peritoneal involvement [13]. High-grade (G2, moderately differentiated) mucinous carcinoma peritonei, a synonym of moderately differentiated mucinous adenocarcinoma, is defined as a disseminated peritoneal

mucinous tumor by the presence of high-grade cytology in the absence of signet-ring cells. The high-grade cytology criteria correspond to moderately differentiated (G2) appendiceal mucinous adenocarcinoma or HAMN. These can demonstrate diffuse high-grade cytology or display a mixture of low- and high-grade cytology areas. The cytologic features may be heterogeneous with low-grade areas with high-grade cytology, and this heterogeneity needs generous sampling for histologic evaluation. Cribriform complex growth and infiltrating tubular structures associated with stromal desmoplasia can be seen. Davison et al. [4] defined the high tumor cellularity as > 20% of the mucinous component. High-grade mucinous carcinoma peritonei with signet-ring cells (G3 tumor) shows high-grade cytology and invasive tumors with a signet-ring cell component, equivalent to poorly differentiated mucinous adenocarcinoma. High-grade (G2 and G3) disseminated peritoneal mucinous disease can present destructive infiltrative invasion into the extra-appendiceal spread, peritoneum, or other organs, frequently associated with perineural and lympho-

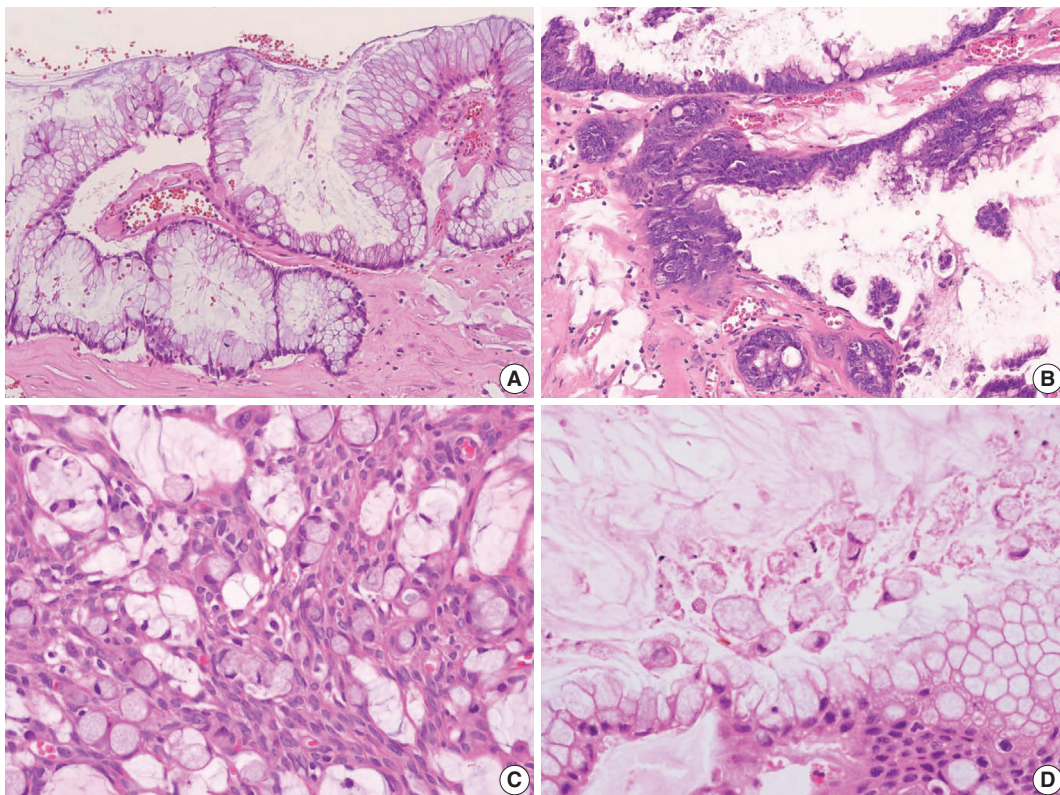


Fig. 8. Histologic features of disseminated peritoneal mucinous tumors. (A) A disseminated peritoneal mucinous tumor of low-grade (G1, well-differentiated) without destructive invasion. The tumor cells resemble those of low-grade appendiceal mucinous neoplasm. (B) A disseminated peritoneal mucinous tumor of high-grade (G2, moderately differentiated) cytology. High-grade cytology corresponds to moderately differentiated (G2) mucinous adenocarcinoma. (C) High-grade (G3) mucinous carcinoma peritonei with signet-ring cells presents high-grade cytology and invasive signet-ring cell component, equivalent to the poorly differentiated mucinous adenocarcinoma. (D) Isolated signet-ring-like cells float within mucin pools. Degenerating tumor cells or histiocytes may exhibit signet-ring-like morphology.

vascular invasion. The microscopic findings of a disseminated peritoneal mucinous tumor are presented in Fig. 8.

Diagnostic difficulty of disseminated peritoneal mucinous disease

The discordance grade may be presented between appendiceal and peritoneal tumors. The PSOGI consensus panel recommends that peritoneal grading should be used for staging purposes, as intraperitoneal grading is more likely to influence patient prognosis [3]. However, the CAP protocol advocates that more high-grade tumors between the appendix and peritoneum should be assigned to the tumor for staging. These diverse ideas can lead to diagnostic confusion and difficulty; thus, more advanced investigations concerning prognosis are required. Regarding the potential discrepancy between G2 and G3 tumors, Breadly and Carr [40] recommended that more than 10% of the signet-ring cell components should be identified in the diagnosis of G3 tumors. Because degenerating tumor cells or even histiocytes floating within mucin pools without destructive invasion may often exhibit signet-ring cell-like features (Fig. 8D). Sirintrapun et al. [48] reported that isolated signet cells within mucin pools are less prognostically significant than those found in invading tissue. We surveyed the best criterion of a focal lesion with signet-ring cells at the workshop, and the results are shown in Supplementary Data S2.

The pathologic grade is an independent prognostic factor in patients with stage IV mucinous appendiceal neoplasms. Pa-

tients with high-grade (G2 or G3) disseminated peritoneal mucinous tumors have significantly worse survival than patients with low-grade (G1) tumors. Therefore, for high-grade disseminated peritoneal mucinous tumors, systemic chemotherapy followed by the option of CRS-HIPEC is recommended according to the therapeutic response [4,45,49-52].

Biologic behavior codes of primary and metastatic tumors

The ICD-O3 code is 8480/6 in secondary disseminated peritoneal mucinous disease regardless of the grading; however, ICD-O3 is 8480/3 in the primary or unknown origin of disseminated peritoneal disease [53]. The histologic grade, behavior codes, diagnostic terminologies, and criteria for acellular mucin and disseminated peritoneal mucinous disease are summarized in Table 4. In addition, the checklist of standard data elements of the appendiceal epithelial tumors, including disseminated peritoneal mucinous disease, is presented in Table 5.

OTHER APPENDICEAL EPITHELIAL TUMORS

Non-mucinous adenocarcinoma and adenoma

Non-mucinous adenocarcinoma is less common than mucinous adenocarcinoma [1]. Uemura et al. [54] reported that non-mucinous adenocarcinoma is biologically distinct from the mucinous subtype and shows mostly moderate to poorly differentiated with frequent peritoneal metastasis. The histopathologic findings and tumor grading of non-mucinous adenocarcinoma are the

Table 4. Histologic grade, behavior codes, terminology, and diagnostic criteria for secondary disseminated peritoneal mucinous disease

Lesion	Grade	Behavior codes		Terminology		Criteria	Treatment
		ICD-O3	KCD-8	PSOGI/Carr [12]	AJCC/Misdraji [10]		
Mucin without tumor cells	-	8480/6	C78.6	Acellular mucin	Acellular mucin	Mucin within the peritoneal cavity without neoplastic epithelial cells	CRS-HIPEC
Mucinous tumor with low-grade histologic features	G1	8480/6	C78.6	Low-grade mucinous carcinoma peritonei	LAMN with peritoneal involvement	Scanty (≤20% cellularity) Strips, gland-like or small clusters Low-grade cytological atypia Not more than occasional mitosis Pushing invasion	CRS-HIPEC
Mucinous tumor with high-grade histologic features	G2	8480/6	C78.6	High-grade mucinous carcinoma peritonei	Mucinous adenocarcinoma, moderately differentiated	More cellular (>20% cellularity) Cribriform growth Mixed but mostly high-grade cytological atypia Numerous mitoses Destructive infiltrative invasion	Systemic chemotherapy ± CRS-HIPEC
Mucinous tumor with signet-ring cells	G3	8480/6	C78.6	High-grade mucinous carcinoma peritonei with signet-ring cells	Mucinous adenocarcinoma, poorly differentiated	Any lesion with signet-ring cells (degenerating cells within mucin that mimic signet-ring cells should be discounted)	Systemic chemotherapy ± CRS-HIPEC

Note that ICD-O3 and KCD-8 codes of primary or unknown origin disseminated peritoneal mucinous disease are 8480/3 and C80.0, respectively. ICD-O3, International Classification of Diseases for Oncology, 3rd edition; KCD-8, Korean Classification of Disease, 8th edition; PSOGI, Peritoneal Surface Oncology Group International; AJCC, American Joint Committee on Cancer; CRS-HIPEC, cytoreductive surgery with hyperthermic intraperitoneal chemotherapy; LAMN, low-grade appendiceal mucinous neoplasm.

same as conventional colorectal adenocarcinoma [1]. Non-mucinous adenocarcinoma demonstrates a high level of MSI. The frequency of *KRAS* mutation is similar in both colorectal ade-

nocarcinomas and appendiceal non-mucinous adenocarcinomas, but the molecular pathogenesis is different [38,55,56]. The PSO-GI panel prefers to confine “adenoma” to lesions that resemble

Table 5. Checklist of standard data elements of appendiceal epithelial tumors

Specimen type
<input type="checkbox"/> Appendectomy <input type="checkbox"/> Appendectomy and right colectomy <input type="checkbox"/> Other: (specify: _____)
Tumor size
_____ x _____ x _____ cm
Tumor site
<input type="checkbox"/> Proximal half of appendix <input type="checkbox"/> Distal half of appendix <input type="checkbox"/> Diffusely involving appendix <input type="checkbox"/> Other: (specify: _____)
Histologic types (WHO 5th Digestive System Tumors) [1]
<input type="checkbox"/> Low-grade appendiceal mucinous neoplasm (LAMN) <input type="checkbox"/> High-grade appendiceal mucinous neoplasm (HAMN) <input type="checkbox"/> Mucinous adenocarcinoma <input type="checkbox"/> Non-mucinous adenocarcinoma <input type="checkbox"/> Signet-ring cell carcinoma <input type="checkbox"/> Goblet cell adenocarcinoma <input type="checkbox"/> Large cell neuroendocrine carcinoma <input type="checkbox"/> Small cell neuroendocrine carcinoma <input type="checkbox"/> Mixed neuroendocrine-non-neuroendocrine carcinoma (MiNEN) <input type="checkbox"/> Medullary carcinoma <input type="checkbox"/> Adenosquamous carcinoma <input type="checkbox"/> Undifferentiated carcinoma <input type="checkbox"/> Other histologic type not listed (specify: _____)
Histologic grade
<input type="checkbox"/> G1: Well differentiated <input type="checkbox"/> G2: Moderately differentiated <input type="checkbox"/> G3: Poorly differentiated <input type="checkbox"/> GX: Cannot be assessed <input type="checkbox"/> Other: (specify: _____)
Disseminated peritoneal mucinous disease
<input type="checkbox"/> Not identified <input type="checkbox"/> Present <ul style="list-style-type: none"> <input type="checkbox"/> Low-grade mucinous carcinoma peritonei/LAMN (G1) with peritoneal involvement <input type="checkbox"/> High-grade mucinous carcinoma peritonei/Mucinous adenocarcinoma, moderately differentiated (G2) <input type="checkbox"/> High-grade mucinous carcinoma peritonei with signet-ring cells / Mucinous adenocarcinoma, poorly differentiated (G3)
Resection margins including proximal and mesenteric margins
<input type="checkbox"/> Cannot be assessed <input type="checkbox"/> Uninvolved by tumor <ul style="list-style-type: none"> <input type="checkbox"/> Distance of tumor from the closest margin: _____ mm <input type="checkbox"/> Involved by tumor <ul style="list-style-type: none"> <input type="checkbox"/> Involved by invasive carcinoma (<input type="checkbox"/> Proximal margin, <input type="checkbox"/> Mesenteric margin) <input type="checkbox"/> Involved by appendiceal mucinous neoplasm (<input type="checkbox"/> Proximal margin, <input type="checkbox"/> Mesenteric margin) <input type="checkbox"/> Involved by acellular mucin (<input type="checkbox"/> Proximal margin, <input type="checkbox"/> Mesenteric margin)
Lympho-vascular invasion
<input type="checkbox"/> Not identified <input type="checkbox"/> Present <input type="checkbox"/> Cannot be determined

(Continued to the next page)

Table 5. Continued

Perineural invasion
<input type="checkbox"/> Not identified <input type="checkbox"/> Present <input type="checkbox"/> Cannot be determined
Tumor deposits
<input type="checkbox"/> Not identified <input type="checkbox"/> Present <input type="checkbox"/> Cannot be determined
Regional lymph nodes
<input type="checkbox"/> No lymph nodes submitted or found
<input type="checkbox"/> Total number of lymph nodes examined: _____
<input type="checkbox"/> Number of lymph nodes involved with metastases: _____
Pathologic stage classification (pTNM, AJCC 8th edition) [13]
TNM Descriptors: <input type="checkbox"/> m (multiple) <input type="checkbox"/> r (recurrent) <input type="checkbox"/> y (post-neoadjuvant therapy)
Primary tumor (pT)
<input type="checkbox"/> pTX: Primary tumor cannot be assessed
<input type="checkbox"/> pTX0: No evidence of primary tumor
<input type="checkbox"/> pTis: Carcinoma in situ (high-grade dysplasia); intraepithelial carcinoma; invasion of lamina propria (intramucosal carcinoma)
<input type="checkbox"/> pTis(LAMN): LAMN confined to the appendix (defined as involvement by acellular mucin or mucinous epithelium that may extend into the muscularis propria)
<input type="checkbox"/> pT1: Tumor invades submucosa (does not apply to LAMN)
<input type="checkbox"/> pT2: Tumor invades muscularis propria (does not apply to LAMN)
<input type="checkbox"/> pT3: Tumor invades through the muscularis propria into the subserosa or mesoappendix
<input type="checkbox"/> pT4: Tumor invades the visceral peritoneum, including the acellular mucin or mucinous epithelium involving the serosa of the appendix or mesoappendix, and/or directly invades adjacent organs or structures
<input type="checkbox"/> pT4a: Tumor invades the visceral peritoneum, including the acellular mucin or mucinous epithelium involving the serosa of appendix or serosa of mesoappendix
<input type="checkbox"/> pT4b: Tumor directly invades other organs or structures
Regional lymph nodes (pN)
<input type="checkbox"/> pNX: Regional lymph nodes cannot be assessed
<input type="checkbox"/> pN0: No regional nodal metastasis
<input type="checkbox"/> pN1: One to three regional lymph nodes are positive (tumor in lymph nodes measuring ≥ 0.2 mm), or any number of tumor deposits is present, and all identifiable lymph nodes are negative
<input type="checkbox"/> pN1a: One regional lymph node is positive
<input type="checkbox"/> pN1b: Two or three regional lymph nodes are positive
<input type="checkbox"/> pN1c: No regional lymph node metastasis, but tumor deposits in the subserosa or mesentery
<input type="checkbox"/> pN2: Metastasis in 4 or more regional nodes
Distant metastasis (pM)
<input type="checkbox"/> Not applicable
<input type="checkbox"/> pM1: Distant metastasis
<input type="checkbox"/> pM1a: Intraperitoneal acellular mucin only
<input type="checkbox"/> pM1b: Intraperitoneal metastasis only, including mucinous epithelium
<input type="checkbox"/> pM1c: Non-peritoneal metastasis
Additional pathologic findings or pre-existing lesions
<input type="checkbox"/> None
<input type="checkbox"/> Other: (specify: _____)
Ancillary studies
<input type="checkbox"/> Specify: _____

conventional adenomas of the colorectum limited to the mucosa and intact muscularis mucosae without luminal dilatation or expansile growth pattern [12,23]. Based on this, appendiceal adenomas are uncommon, and many neoplasms that were previously reported as adenomas are now classified as LAMN or serrated lesions. For example, a villous lesion showing serration with conventional dysplasia and intact muscularis mucosae without

pushing invasion should be called a serrated dysplasia rather than a villous adenoma. The WHO 5th *Digestive System Tumors* and CAP protocol recommend that appendiceal adenoma should be restricted to the precursor lesion of non-mucinous adenocarcinoma [1,14,22]. The histologic findings of non-mucinous adenocarcinoma arising in adenoma are presented in Fig. 9A–C.

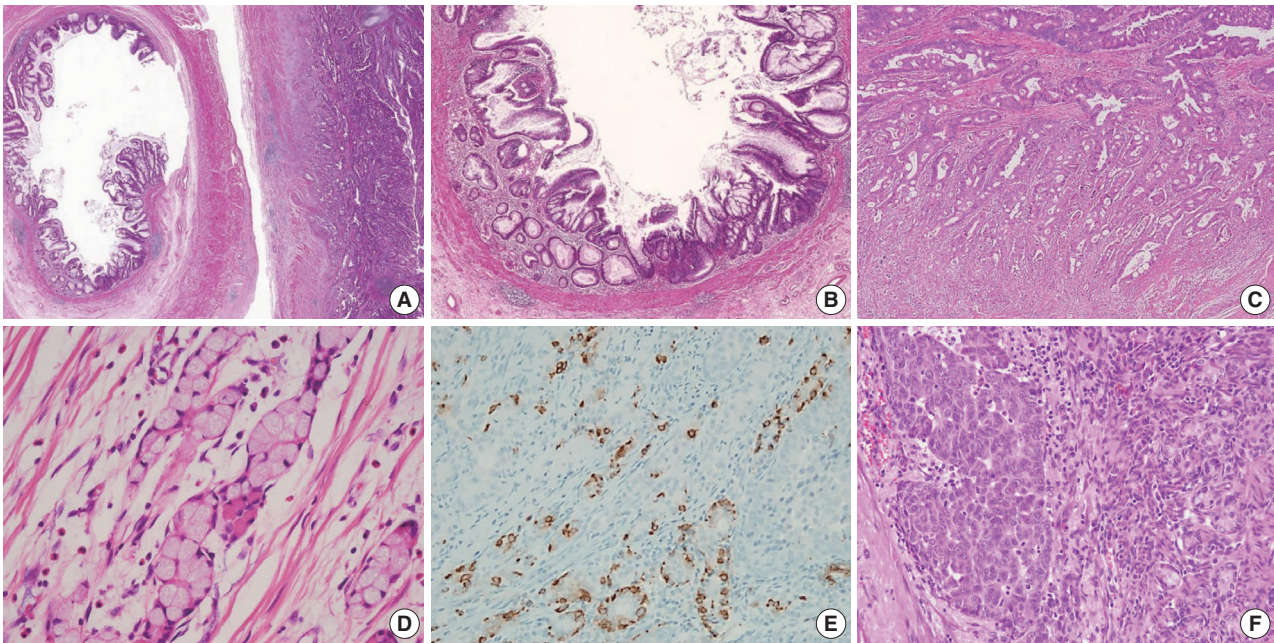


Fig. 9. Histologic features of non-mucinous adenocarcinoma and goblet cell adenocarcinoma. (A) Co-existing adenoma and non-mucinous adenocarcinoma of the appendix. (B) Low-grade adenoma of the appendix resembles conventional adenoma of the colorectum. The mucosal architecture is well preserved with intact muscularis mucosae without a pushing invasion pattern. (C) Non-mucinous adenocarcinoma displays moderately differentiated and 50% to 95% gland formation. (D) Low-grade (G1) goblet cell adenocarcinoma shows small clusters composed of cohesive goblet cells and a few Paneth-like cells, displaying mostly low-grade patterns. (E) Low-grade (G1) goblet cell adenocarcinoma, immunohistochemistry of synaptophysin shows positive expression in neuroendocrine cells. (F) High-grade (G3) goblet cell adenocarcinoma displays >50% high-grade patterns.

Goblet cell adenocarcinoma

Goblet cell adenocarcinoma can occur almost exclusively in the appendix and is sometimes difficult to differentiate from AMNs and non-mucinous appendiceal tumors. Goblet cell adenocarcinoma, previously called goblet cell carcinoid or mucinous carcinoid, is a rare and aggressive tumor [1]. The tumor components are goblet-like cells and variable numbers of neuroendocrine cells and Paneth-like cells, and it is characteristically arranged as tubules similar to intestinal crypts [1]. The classic low-grade tumor displays tubular or clustered growth and small groups of cohesive goblet cells, whereas the high-grade tumor shows infiltrating tumor cells, convoluted anastomosing tubules, cribriform masses, irregular solid pattern, and large aggregates of goblet cells or signet-ring cells [57]. Nonaka et al. [58] found that neuroendocrine cells are inconsistent and not essential in the tumor component. For this reason, pathologists must find at least a focal lesion of classical low-grade tumor component to diagnose as a goblet cell adenocarcinoma.

Several classification and grading systems have been described. Tang et al. [59] classified goblet cell adenocarcinomas into three groups based on the histopathologic features: group A (typical goblet cell carcinoid), group B (adenocarcinoma ex-goblet cell

carcinoid, signet-ring cell type), and group C (adenocarcinoma ex-goblet cell carcinoid, poorly differentiated type). Recently, the WHO 5th *Digestive System Tumors* classified goblet cell adenocarcinomas into a three-tiered grading system, based on the proportion of the tumor cells that consists of low-grade and high-grade patterns as follows: grade 1, > 75% of low-grade pattern or < 25% of high-grade pattern; grade 2, 50%–75% of low-grade pattern or 25%–50% of high-grade pattern; and grade 3, < 50% of low-grade pattern or > 50% of the high-grade pattern [1,60]. Nonaka et al. [58] reported that the high-grade component percentage was correlated with cancer-specific survival. The histological and immunohistochemical findings of goblet cell adenocarcinoma are presented in Fig. 9D–F. The pathogenesis remains entirely elusive. It is generally believed that it is derived from the pluripotent stem cells at the crypt base that can undergo dual glandular and neuroendocrine differentiation.

CONCLUSION

The GPSG-KSP presents a “Standardization of the Pathologic Diagnosis of the Appendiceal Mucinous Neoplasm.” This article focuses on the diagnostic criteria, terminology, grading, staging,

biologic behaviors, treatment, and prognosis of AMNs and disseminated peritoneal mucinous disease. In addition, we propose a checklist of standard data elements of the appendiceal epithelial neoplasms. We hope that the present article will lead to the standardization of the pathologic diagnosis of AMNs and disseminated peritoneal mucinous disease and improvement in the communication between pathologists and between pathologists and clinicians.

Supplementary Information

The Data Supplement is available with this article at <https://doi.org/10.4132/jptm.2021.05.28>

Ethics Statement

Not applicable.

Availability of Data and Material

Data sharing not applicable to this article as no datasets were generated or analyzed during the study.

Code Availability

Not applicable.

ORCID

Dong-Wook Kang	https://orcid.org/0000-0002-4300-3469
Baek-hui Kim	https://orcid.org/0000-0001-6793-1991
Joon Mee Kim	https://orcid.org/0000-0003-1355-4187
Jihun Kim	https://orcid.org/0000-0002-8694-4365
Hee Jin Chang	https://orcid.org/0000-0003-2263-2247
Mee Soo Chang	https://orcid.org/0000-0002-0948-799X
Jin-Hee Sohn	https://orcid.org/0000-0002-4735-3853
Mee-Yon Cho	https://orcid.org/0000-0002-7955-4211
So-Young Jin	https://orcid.org/0000-0002-9900-8322
Hee Kyung Chang	https://orcid.org/0000-0002-4843-5316
Hye Seung Han	https://orcid.org/0000-0002-3591-9995
Jung Yeon Kim	https://orcid.org/0000-0002-7539-9242
Hee Sung Kim	https://orcid.org/0000-0002-8154-2391
Do Youn Park	https://orcid.org/0000-0001-7641-1509
Ha Young Park	https://orcid.org/0000-0002-7192-2374
So Jeong Lee	https://orcid.org/0000-0002-6465-9811
Wonae Lee	https://orcid.org/0000-0001-9266-6640
Hye Seung Lee	https://orcid.org/0000-0002-1667-7986
Yoo Na Kang	https://orcid.org/0000-0003-3634-9127
Younghee Choi	https://orcid.org/0000-0002-3882-4000

Author Contributions

Conceptualization: MSC, JMK. Project administration: DWK, YNK, BHK, JYK, JMK, JK, HSK, DYP, HYP, JHS, SJL, WL, HSL, MSC, HKC, HJC, MYC, SYJ, YC, HSH. Supervision: BHK, JMK, JK, MSC, HJC. Writing—original draft: DWK. Writing—review & editing: JMK. Approval of final manuscript: all authors.

Conflicts of Interest

H.S.L., a contributing editor of the *Journal of Pathology and Translational Medicine*, was not involved in the editorial evaluation or decision to publish this article. All remaining authors have declared no conflicts of interest.

Funding Statement

This research was supported by The Korean Society of Pathologists Grant No. 2018.

Acknowledgments

We are thankful to Jae-Hyun Ahn (SeongKohn Traders' Company) for technical support of whole slide image scanning and online service. Whole slide images are available in online (http://dg.digitalpathology.co.kr/ExternalInterface/Viewlink?INST=INST_A&FA=FAC_B&ENC=Mq0sd5WKOFTGTWOpht1H8QhMt2fskenwse8wnOu3t9Rc5czHdfX3smwHgHd3_MghleGuQR2V9bkDxEmpPeX4HX2fEJuXWDILRYOAb_UuaUNQ).

References

- Misdraji J, Carr NJ, Pai RK. Appendiceal mucinous neoplasm. In: WHO Classification of Tumours Editorial Board, ed. WHO classification of tumours: digestive system tumours. 5th ed. Lyon: International Agency for Research on Cancer, 2019; 135-55.
- Misdraji J. Appendiceal mucinous neoplasms: controversial issues. *Arch Pathol Lab Med* 2010; 134: 864-70.
- Valasek MA, Pai RK. An update on the diagnosis, grading, and staging of appendiceal mucinous neoplasms. *Adv Anat Pathol* 2018; 25: 38-60.
- Davison JM, Choudry HA, Pingpank JF, et al. Clinicopathologic and molecular analysis of disseminated appendiceal mucinous neoplasms: identification of factors predicting survival and proposed criteria for a three-tiered assessment of tumor grade. *Mod Pathol* 2014; 27: 1521-39.
- Pai RK, Longacre TA. Pseudomyxoma peritonei syndrome: classification of appendiceal mucinous tumours. *Cancer Treat Res* 2007; 134: 71-107.
- Ronnett BM, Kurman RJ, Zahn CM, et al. Pseudomyxoma peritonei in women: a clinicopathologic analysis of 30 cases with emphasis on site of origin, prognosis, and relationship to ovarian mucinous tumors of low malignant potential. *Hum Pathol* 1995; 26: 509-24.
- Misdraji J, Yantiss RK, Graeme-Cook FM, Balis UJ, Young RH. Appendiceal mucinous neoplasms: a clinicopathologic analysis of 107 cases. *Am J Surg Pathol* 2003; 27: 1089-103.
- Lamps LW, Gray GF Jr, Dilday BR, Washington MK. The coexistence of low-grade mucinous neoplasms of the appendix and appendiceal diverticula: a possible role in the pathogenesis of pseudomyxoma peritonei. *Mod Pathol* 2000; 13: 495-501.
- Ronnett BM, Zahn CM, Kurman RJ, Kass ME, Sugarbaker PH, Shmookler BM. Disseminated peritoneal adenomucinosis and peritoneal mucinous carcinomatosis: a clinicopathologic analysis of 109 cases with emphasis on distinguishing pathologic features, site of origin, prognosis, and relationship to "pseudomyxoma peritonei". *Am J Surg Pathol* 1995; 19: 1390-408.
- Misdraji J, Burgart LJ, Lauwers GY. Defective mismatch repair in the pathogenesis of low-grade appendiceal mucinous neoplasms and adenocarcinomas. *Mod Pathol* 2004; 17: 1447-54.
- Yantiss RK, Shia J, Klimstra DS, Hahn HP, Odze RD, Misdraji J. Prognostic significance of localized extra-appendiceal mucin deposition in appendiceal mucinous neoplasms. *Am J Surg Pathol* 2009; 33: 248-55.
- Carr NJ, Cecil TD, Mohamed F, et al. A consensus for classification and pathologic reporting of pseudomyxoma peritonei and associated appendiceal neoplasia: the results of the Peritoneal Surface Oncology Group International (PSOGI) modified Delphi process.

- Am J Surg Pathol 2016; 40: 14-26.
13. Amin MB, Edge SB, Greene FL, et al. AJCC cancer staging manual. 8th ed. New York: Springer, 2017.
 14. Nagtegaal ID, Odze RD, Klimstra D, et al. The 2019 WHO classification of tumours of the digestive system. *Histopathology* 2020; 76: 182-8.
 15. Kim WH, Park CK, Kim YB, et al. A standardized pathology report for gastric cancer. *Korean J Pathol* 2005; 39: 106-13.
 16. Chang HJ, Park CK, Kim WH, et al. A standardized pathology report for colorectal cancer. *Korean J Pathol* 2006; 40: 193-203.
 17. Cho MY, Kang YK, Kim KM, et al. Proposal for creating a guideline for cancer registration of the gastrointestinal tumors (I). *Korean J Pathol* 2008; 42: 140-50.
 18. The Gastrointestinal Pathology Study Group of Korean Society of Pathologists; Cho MY, Sohn JH, et al. Proposal for a standardized pathology report of gastroenteropancreatic neuroendocrine tumors: prognostic significance of pathological parameters. *Korean J Pathol* 2013; 47: 227-37.
 19. Gastrointestinal Pathology Study Group of Korean Society of Pathologists; Cho MY, Kim JM, et al. Current trends of the incidence and pathological diagnosis of gastroenteropancreatic neuroendocrine tumors (GEP-NETs) in Korea 2000-2009: multicenter study. *Cancer Res Treat* 2012; 44: 157-65.
 20. Kang YK, Kim KM, Sohn T, et al. Clinical practice guideline for accurate diagnosis and effective treatment of gastrointestinal stromal tumor in Korea. *J Korean Med Sci* 2010; 25: 1543-52.
 21. Jung ES, Kang YK, Cho MY, et al. Update on the proposal for creating a guideline for cancer registration of the gastrointestinal tumors (I-2). *Korean J Pathol* 2012; 46: 443-53.
 22. Misdraji J, Oliva E, Goldblum JR, Lauwers GY, Compton CC; Members of the Cancer Committee, College of American Pathologists. Protocol for the examination of specimens from patients with invasive carcinomas of the appendix. *Arch Pathol Lab Med* 2006; 130: 1433-9.
 23. Carr NJ, Bibeau F, Bradley RF, et al. The histopathological classification, diagnosis and differential diagnosis of mucinous appendiceal neoplasms, appendiceal adenocarcinomas and pseudomyxoma peritonei. *Histopathology* 2017; 71: 847-58.
 24. Carr NJ, Finch J, Islesley IC, et al. Pathology and prognosis in pseudomyxoma peritonei: a review of 274 cases. *J Clin Pathol* 2012; 65: 919-23.
 25. Ramaswamy V. Pathology of mucinous appendiceal tumors and pseudomyxoma peritonei. *Indian J Surg Oncol* 2016; 7: 258-67.
 26. Altieri ML, Piozzi GN, Salvatori P, Mirra M, Piccolo G, Olivari N. Appendiceal diverticulitis, a rare relevant pathology: presentation of a case report and review of the literature. *Int J Surg Case Rep* 2017; 33: 31-4.
 27. Hsu M, Young RH, Misdraji J. Ruptured appendiceal diverticula mimicking low-grade appendiceal mucinous neoplasms. *Am J Surg Pathol* 2009; 33: 1515-21.
 28. Hara K, Saito T, Hayashi T, et al. A mutation spectrum that includes *GNAS*, *KRAS* and *TP53* may be shared by mucinous neoplasms of the appendix. *Pathol Res Pract* 2015; 211: 657-64.
 29. Milovanov V, Sardi A, Studeman K, Nieroda C, Sittig M, Gushchin V. The 7th edition of the AJCC staging classification correlates with biologic behavior of mucinous appendiceal tumor with peritoneal metastases treated with cytoreductive surgery and hyperthermic intraperitoneal chemotherapy (CRS/HIPEC). *Ann Surg Oncol* 2016; 23: 1928-33.
 30. Pai RK, Beck AH, Norton JA, Longacre TA. Appendiceal mucinous neoplasms: clinicopathologic study of 116 cases with analysis of factors predicting recurrence. *Am J Surg Pathol* 2009; 33: 1425-39.
 31. Pai RK, Hartman DJ, Gonzalo DH, et al. Serrated lesions of the appendix frequently harbor *KRAS* mutations and not *BRAF* mutations indicating a distinctly different serrated neoplastic pathway in the appendix. *Hum Pathol* 2014; 45: 227-35.
 32. Noguchi R, Yano H, Gohda Y, et al. Molecular profiles of high-grade and low-grade pseudomyxoma peritonei. *Cancer Med* 2015; 4: 1809-16.
 33. Liu X, Mody K, de Abreu FB, et al. Molecular profiling of appendiceal epithelial tumors using massively parallel sequencing to identify somatic mutations. *Clin Chem* 2014; 60: 1004-11.
 34. Nummela P, Saarinen L, Thiel A, et al. Genomic profile of pseudomyxoma peritonei analyzed using next-generation sequencing and immunohistochemistry. *Int J Cancer* 2015; 136: E282-9.
 35. Gleeson EM, Feldman R, Mapow BL, et al. Appendix-derived pseudomyxoma peritonei (PMP): molecular profiling toward treatment of a rare malignancy. *Am J Clin Oncol* 2018; 41: 777-83.
 36. Singhi AD, Davison JM, Choudry HA, et al. *GNAS* is frequently mutated in both low-grade and high-grade disseminated appendiceal mucinous neoplasms but does not affect survival. *Hum Pathol* 2014; 45: 1737-43.
 37. Pengelly RJ, Rowaiye B, Pickard K, et al. Analysis of mutation and loss of heterozygosity by whole-exome sequencing yields insights into pseudomyxoma peritonei. *J Mol Diagn* 2018; 20: 635-42.
 38. Zauber P, Berman E, Marotta S, Sabbath-Solitare M, Bishop T. *Ki-ras* gene mutations are invariably present in low-grade mucinous tumors of the vermiform appendix. *Scand J Gastroenterol* 2011; 46: 869-74.
 39. Bignell M, Carr NJ, Mohamed F. Pathophysiology and classification of pseudomyxoma peritonei. *Pleura Peritoneum* 2016; 1: 3-13.
 40. Bradley RF, Carr NJ. Pseudomyxoma peritonei: pathology, a historical overview, and proposal for unified nomenclature and updated grading. *AJSP Rev Rep* 2019; 24: 88-93.
 41. Ithemelandu C, Sugarbaker PH. Clinicopathologic and prognostic features in patients with peritoneal metastasis from mucinous adenocarcinoma, adenocarcinoma with signet ring cells, and adenocarcinoid of the appendix treated with cytoreductive surgery and perioperative intraperitoneal chemotherapy. *Ann Surg Oncol* 2016; 23: 1474-80.
 42. Morano WF, Gleeson EM, Sullivan SH, et al. Clinicopathological features and management of appendiceal mucocoeles: a systematic review. *Am Surg* 2018; 84: 273-81.
 43. LaFramboise WA, Pai RK, Petrosko P, et al. Discrimination of low- and high-grade appendiceal mucinous neoplasms by targeted sequencing of cancer-related variants. *Mod Pathol* 2019; 32: 1197-209.
 44. Ronnett BM, Yan H, Kurman RJ, Shmookler BM, Wu L, Sugarbaker PH. Patients with pseudomyxoma peritonei associated with disseminated peritoneal adenomucinosis have a significantly more favorable prognosis than patients with peritoneal mucinous carcinoma. *Cancer* 2001; 92: 85-91.
 45. Asare EA, Compton CC, Hanna NN, et al. The impact of stage, grade, and mucinous histology on the efficacy of systemic chemotherapy in adenocarcinomas of the appendix: analysis of the National Cancer Data Base. *Cancer* 2016; 122: 213-21.
 46. Misdraji J. Mucinous epithelial neoplasms of the appendix and

- pseudomyxoma peritonei. *Mod Pathol* 2015; 28 Suppl 1: S67-79.
47. Misdraji J, Lauwers GY, Irving JA, Batts KP, Young RH. Appendiceal or cecal endometriosis with intestinal metaplasia: a potential mimic of appendiceal mucinous neoplasms. *Am J Surg Pathol* 2014; 38: 698-705.
 48. Sirintrapun SJ, Blackham AU, Russell G, et al. Significance of signet ring cells in high-grade mucinous adenocarcinoma of the peritoneum from appendiceal origin. *Hum Pathol* 2014; 45: 1597-604.
 49. Baratti D, Kusamura S, Milione M, Bruno F, Guaglio M, Deraco M. Validation of the recent PSOGI pathological classification of pseudomyxoma peritonei in a single-center series of 265 patients treated by cytoreductive surgery and hyperthermic intraperitoneal chemotherapy. *Ann Surg Oncol* 2018; 25: 404-13.
 50. Narasimhan V, Wilson K, Britto M, et al. Outcomes following cytoreduction and HIPEC for pseudomyxoma peritonei: 10-year experience. *J Gastrointest Surg* 2020; 24: 899-906.
 51. Shaib WL, Goodman M, Chen Z, et al. Incidence and survival of appendiceal mucinous neoplasms: a SEER analysis. *Am J Clin Oncol* 2017; 40: 569-73.
 52. Kunduz E, Bektasoglu HK, Unver N, Aydogan C, Timocin G, Destek S. Analysis of appendiceal neoplasms on 3544 appendectomy specimens for acute appendicitis: retrospective cohort study of a single institution. *Med Sci Monit* 2018; 24: 4421-6.
 53. Ball HL. Conducting online surveys. *J Hum Lact* 2019; 35: 413-7.
 54. Uemura M, Qiao W, Fournier K, et al. Retrospective study of non-mucinous appendiceal adenocarcinomas: role of systemic chemotherapy and cytoreductive surgery. *BMC Cancer* 2017; 17: 331.
 55. Kabbani W, Houlihan PS, Luthra R, Hamilton SR, Rashid A. Mucinous and nonmucinous appendiceal adenocarcinomas: different clinicopathological features but similar genetic alterations. *Mod Pathol* 2002; 15: 599-605.
 56. Matson DR, Xu J, Huffman L, et al. *KRAS* and *GNAS* co-mutation in metastatic low-grade appendiceal mucinous neoplasm (LAMN) to the ovaries: a practical role for next-generation sequencing. *Am J Case Rep* 2017; 18: 558-62.
 57. Yozu M, Johncilla ME, Srivastava A, et al. Histologic and outcome study supports reclassifying appendiceal goblet cell carcinoids as goblet cell adenocarcinomas, and grading and staging similarly to colonic adenocarcinomas. *Am J Surg Pathol* 2018; 42: 898-910.
 58. Nonaka D, Papaxoinis G, Lamarca A, Fulford P, Valle J, Chakrabarty B. A study of appendiceal crypt cell adenocarcinoma (so-called goblet cell carcinoid and its related adenocarcinoma). *Hum Pathol* 2018; 72: 18-27.
 59. Tang LH, Shia J, Soslow RA, et al. Pathologic classification and clinical behavior of the spectrum of goblet cell carcinoid tumors of the appendix. *Am J Surg Pathol* 2008; 32: 1429-43.
 60. Taggart MW, Abraham SC, Overman MJ, Mansfield PF, Rashid A. Goblet cell carcinoid tumor, mixed goblet cell carcinoid-adenocarcinoma, and adenocarcinoma of the appendix: comparison of clinicopathologic features and prognosis. *Arch Pathol Lab Med* 2015; 139: 782-90.

Palmar and plantar fibromatosis: a review

Brian D. Stewart¹, Alessandra F. Nascimento²

¹Department of Pathology, Immunology and Laboratory Medicine, University of Florida College of Medicine, Gainesville, FL;

²CWRU School of Medicine, University Hospitals, Bone and Soft Tissue Pathology, Cleveland, OH, USA

Palmar fibromatosis (Dupuytren disease/contracture) is the most common type of fibromatosis, defined as a benign proliferation of fibroblasts and myofibroblasts. The disease process is most common in white, middle-aged and older men occurring at the distal palmar crease leading to nodules and contracture, which in many cases recur after surgical treatment. In a similar process, plantar fibromatosis (Ledderhose disease) is a proliferation of fibroblasts and myofibroblasts on the plantar aponeurosis of mostly middle-aged patients that may lead to painful nodules but usually does not lead to contracture. Both processes are histologically similar, composed of a bland cellular proliferation of spindle cells with a bluish appearance and with a variable amount of background collagen, depending on the age of the lesion. The etiology of both lesions is still uncertain, while treatment ranges from observation to surgery, with some pharmacologic agents being investigated with mixed success. In this paper we provide an overview of both processes with regards to clinical and radiologic findings, pathophysiology, diagnosis, treatment, and prognosis.

Key Words: Fibromatosis; Plantar; Palmar; Dupuytren; Ledderhose

Received: June 5, 2021 **Accepted:** June 14, 2021

Corresponding Author: Brian D. Stewart, MD, Department of Pathology, Immunology and Laboratory Medicine, University of Florida College of Medicine, P.O. Box 100275, 1600 SW Archer Road, Gainesville, FL 32610-0275, USA
 Tel: +1-352-627-9240, Fax: +1-352-627-9242, E-mail: bstewart@ufl.edu

This article has been published jointly, with consent, in both *Journal of Pathology and Translational Medicine* and *PathologyOutlines.com*.

Palmar and plantar fibromatoses are both benign, superficial, proliferative processes of the palmar and plantar aponeuroses, respectively, caused by the proliferation of fibroblasts and myofibroblasts. Other terms used for this in the clinical setting are Dupuytren disease or contracture for palmar fibromatosis and Ledderhose disease or morbus Ledderhose for plantar fibromatosis. This review will offer insights into the epidemiology, clinical features, pathophysiology, imaging characteristics, treatment, and prognosis of these common entities.

ETIOLOGY AND PATHOGENESIS

Palmar fibromatosis is the most common type of superficial fibromatosis affecting approximately 1%–2% of the population. The prevalence increases with the patient's age to where approximately 20% of the population at age 65 suffers from this disease. Males are more often affected, with a male to female ratio of 3–4:1. It can affect both the metacarpophalangeal and proximal interphalangeal joints [1]. Half of the cases affect both hands.

Patients of northern European ancestry are most commonly affected and the disease is rare in the black population.

Palmar fibromatosis is associated with diabetes, smoking, repetitive vibrational trauma and is thought to be caused by fibrogenic cytokines [2]. The process is characterized by a proliferation of fibroblasts followed by their differentiation into myofibroblasts and the production of extracellular matrix. Fibroblast growth factor, wntless/integrated (Wnt), and transforming growth factor β have all been proposed as having a role in disease progression [3–7].

The prevalence of plantar fibromatosis is not currently well characterized and is now on the National Institutes of Health list of rare diseases [8]. The disease process usually affects the medial and central bands of the plantar aponeurosis of middle-aged patients, although several reports of patients less than 16 years old to as young as 9 months have been published [9]. Approximately 25% of cases are bilateral with males being more affected than females [10]. A possible genetic predisposition has been suggested, as two genetic variants were found in a genome

wide association study where one indel (chr5:118704153:D) and one single nucleotide polymorphism (rs62051384) were detected [11].

The etiology of plantar fibromatosis is not currently understood, but has been associated with long-term phenobarbital use for epilepsy, frozen shoulder, smoking, alcohol addiction, diabetes, and repeated trauma [8,12]. The disease process advances through several phases. There is first the proliferative phase in which increased fibroblastic activity and cellular proliferation is seen. This is followed by the active phase where nodule formation occurs. Finally, there is the residual phase consisting of collagen deposition, scar formation and tissue contracture.

CLINICAL FEATURES AND RADIOLOGY

The diagnosis of both plantar and palmar fibromatosis is usually made clinically, although occasionally histologic confirmation may be necessary. Palmar fibromatosis often presents with subcutaneous nodules on the distal volar aspect which puckers the overlying skin as it ages. The process leads to painful flexion contracture, most commonly of digits 4 and 5, due to cord-like expansion of the digital aponeurotic slips (Fig. 1A, B). Deeper structures such as the tendons or skeletal muscle are not involved. Plantar disease is concurrently seen in 10% of patients, while an additional 1%–4% have penile fibromatosis (Peyronie disease). Ultrasound of the hand shows nodules superficial to the flexor tendons in superficial fascia. The early lesions are hypochoic with hypervascularity while more chronic lesions become more hyperechoic without vascularity [13]. The subcutaneous nodules on magnetic resonance imaging (MRI) are typically uniformly of low signal intensity on both T1 and T2 [14].

Plantar fibromatosis presents with single or multiple slow

growing subcutaneous nodules located in the medial or central plantar aponeurosis measuring 0.5 to 3.0 cm in diameter. These are initially painless but are later associated with pain after standing or walking, typically on the medial aspect of the sole. Plantar disease is associated with concomitant palmar and penile fibromatoses, along with keloids. Unlike palmar disease, plantar fibromatosis is usually not associated with contractures [15]. Radiographs of the foot are usually normal. Ultrasonography is seen as superior to MRI, where hypochoic to mixed lesions are embedded on the plantar fascia and less reflective to the much brighter plantar fascia surrounding it with sharp juxtaposition [16]. The plantar fascia shows discrete, fusiform, multinodular thickening [17]. Alternating linear bands of hypochoic and isochogenicity relative to the plantar fascia, known as the Comb sign, is seen in 51% of cases [18]. MRI demonstrates nodules that appear as focal oval-shaped areas of disorganization embedded in the plantar fascia [16]. T1-weighted images show isometric to low signal intensity as compared to muscle, while T2-weighted MRI shows low to intermediate signal [17,19].

PATHOLOGIC FINDINGS

Palmar fibromatosis presents macroscopically as small nodules or nodular masses associated with aponeuroses and subcutaneous fat (Fig. 2) with a gray to yellow to white cut surface, the exact nature of the color depending on the amount of collagen content. Cytologic examination is usually limited to touch preparations made during the rare specimen sent for frozen section (Fig. 3A, B). These are usually hypocellular with clusters of bland spindle cells with oval to elongated nuclei. Nuclear atypia and mitotic activity are not present. The microscopic features depend on the age of the lesion. In the proliferative phase, there are uniform,

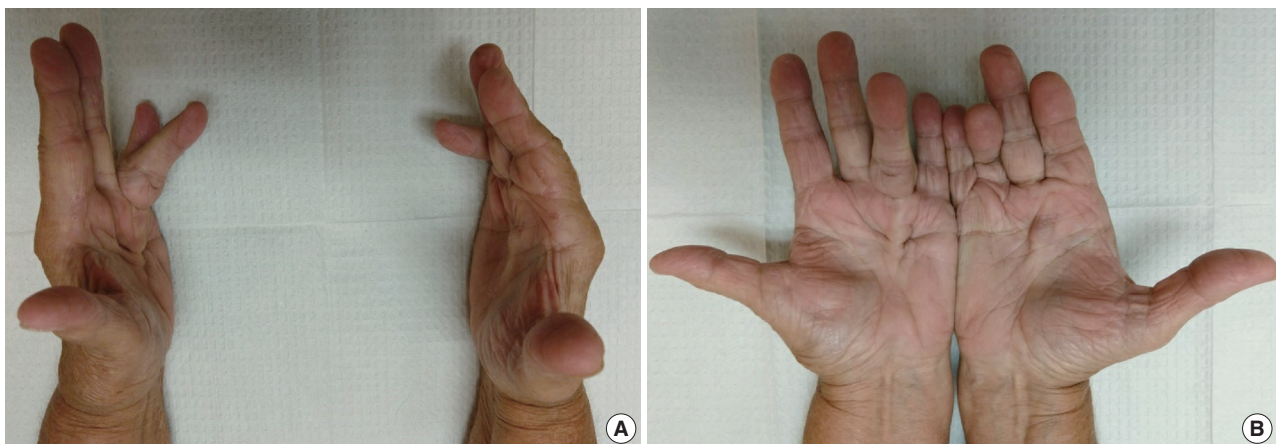


Fig. 1. (A, B) Bilateral nodules in the distal palmar crease and contractures involving the fourth digit.

plump, spindle cells (myofibroblasts and fibroblasts) with bland nuclei and indistinct nucleoli, usually with a “bluer” appearance than the surrounding aponeurotic tissue (Figs. 4–6). The stroma contains a moderate amount of collagen and elongated vessels. In older, less cellular lesions, the collagenous content is denser. Occasionally, attachment to the overlying dermis or cartilaginous metaplasia can be seen. There is usually no infiltration into surrounding tissue beyond the subcutis.

The gross and microscopic characteristics of plantar fibromatosis are similar to its palmar counterpart (Figs. 7–9). Evans described the presence of a variable number of multinucleated giant cells found during the proliferative phase [20]. The formation of nodules is seen during the active phase while the less cellular, more collagenous residual phase often has a prominent chronic inflammatory component and hemosiderin deposition.

Immunohistochemical studies are usually not necessary for di-



Fig. 2. Excised contraction band of palmar fibromatosis with surrounding soft tissue.

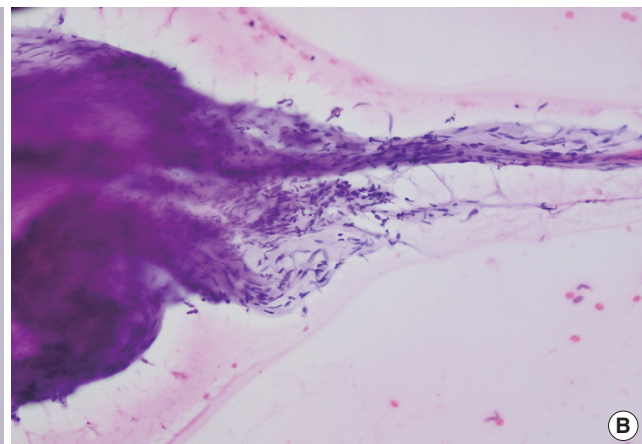
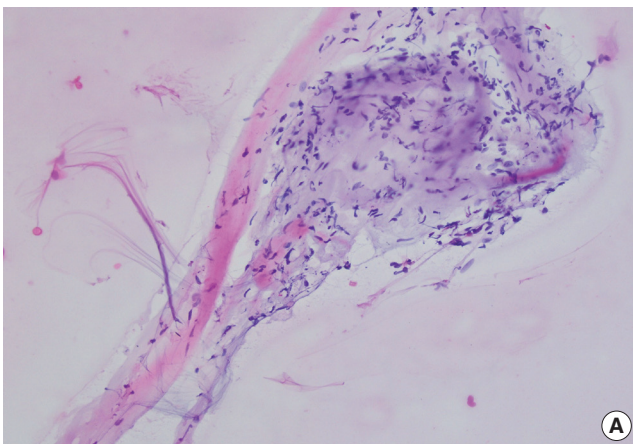


Fig. 3. (A, B) Touch prep of a specimen sent for frozen section showing clusters of loosely arranged spindle cells with bland fusiform nuclei without atypia or mitotic figures.

agnosis due to the characteristic histology of these lesions. Vimentin is uniformly reactive while muscle specific and smooth muscle actins are variable. Infrequently, desmin may show reactivity. Keratins, CD34, epithelial membrane antigen, and S-100 should all be negative. Beta-catenin is negative in plantar fibromatosis, but aberrant nuclear staining in palmar fibromatosis is common [21,22].

MOLECULAR AND CYTOGENETICS

Palmar fibromatosis is usually considered a reactive, as opposed to neoplastic, lesion [23]. The lesions are near diploid, often with trisomy 7 or 8, and show no gene amplifications or deletions [24]. Loss of the Y chromosome may be seen [25]. Aberrations in the Wnt signaling pathway are common; however, no somatic mutations of beta-catenin genes, as seen in desmoid fibromatosis, are present [6,22,26,27].

Like palmar fibromatosis, plantar fibromatosis is near diploid, often with trisomy 7 or 8, and does not contain somatic mutations of beta-catenin genes [22]. Trisomy 14 has also been reported, along with a case containing a clonal reciprocal $t(2;7)(p13;p13)$ [28,29].

DIFFERENTIAL DIAGNOSIS

The clinical, gross, and histologic features of palmar and plantar fibromatosis are quite characteristic and the diagnosis is usually straightforward. However, it is important to keep in mind some of the differential diagnoses. Spindle cell sarcomas, such as synovial sarcoma and malignant peripheral nerve sheath tumor (MPNST), and epithelioid sarcoma should not be missed as the

treatment and prognosis is vastly different. Epithelioid sarcoma commonly presents in the hand but cells will show a distinctive epithelioid appearance with abundant eosinophilic cytoplasm.

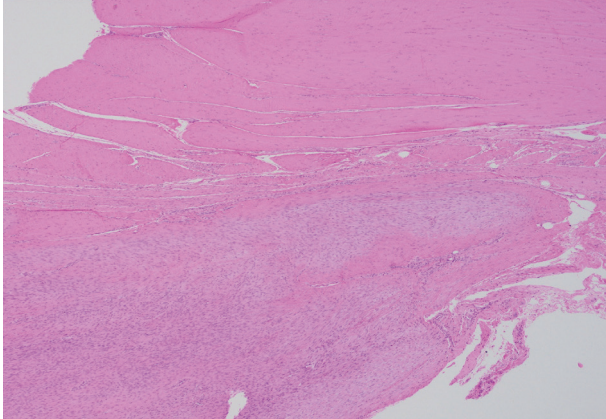


Fig. 4. Immature fibroblastic proliferation (lower 1/2) well-demarcated from the involved tendon (upper 1/2).

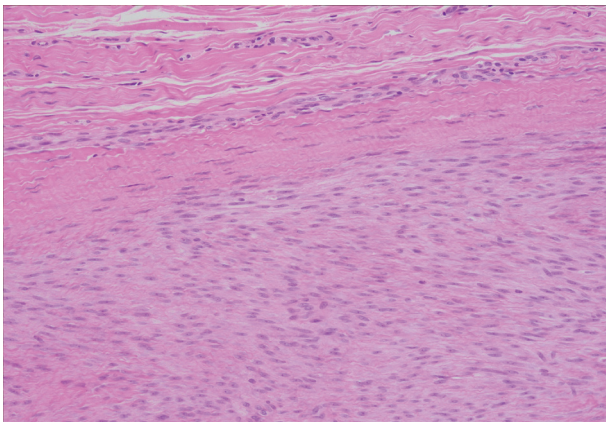


Fig. 5. Higher magnification showing the immature fibroblastic proliferation (lower 2/3 of the field) involving normal fibrous tissue (upper 1/3).

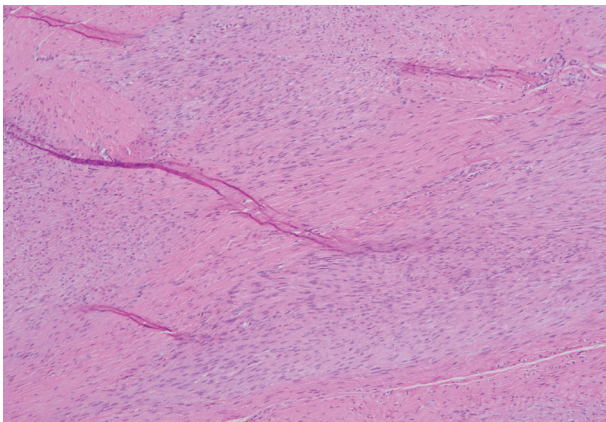


Fig. 6. Tendinous tissue with interspersed fascicles of a bland appearing immature spindle cell proliferation in both longitudinal and cross sections.

Central necrosis and/or hyalinization is often seen. Epithelioid sarcoma is characteristically reactive for cytokeratins and CD34 and shows a loss of nuclear staining for SMARCB1 (INI-1).

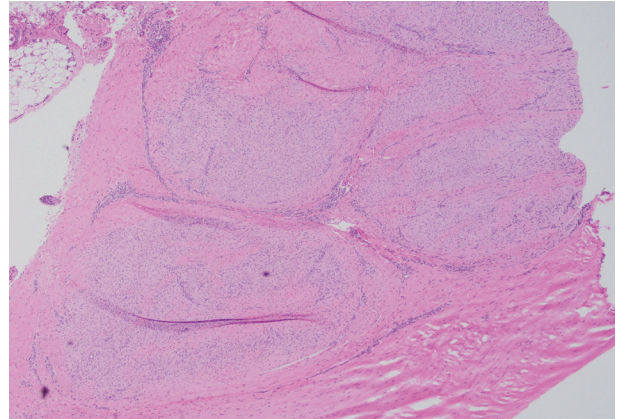


Fig. 7. Nodular proliferation of immature fibroblasts and myofibroblasts embedded within the plantar aponeurosis.

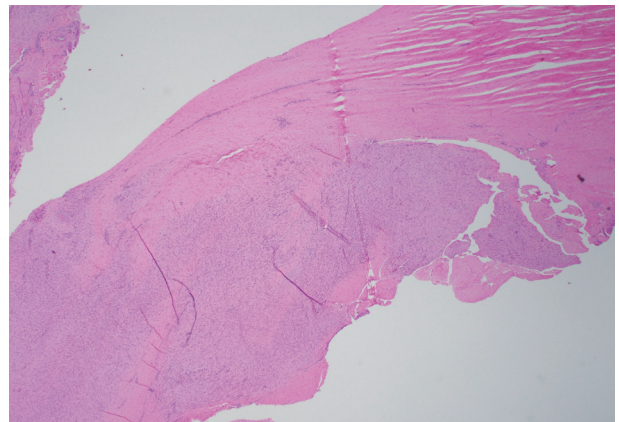


Fig. 8. Large nodule of immature fibroblasts and myofibroblasts (lower 1/2) with pushing and locally infiltrating borders into the plantar aponeurotic tissue (upper 1/2).

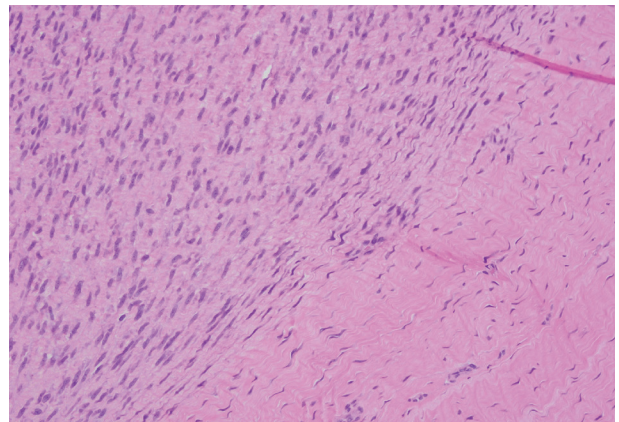


Fig. 9. Cellular proliferation of immature fibroblasts and myofibroblasts with plump to fusiform nuclei (left) well demarcated from the less cellular and more collagenous plantar fascia (right).



Fig. 10. (A, B) Patient from Fig. 1 after removal of the contraction band and resolution of the contracture of the fourth digits.

Clinically, plantar fibromatosis that has not formed nodules may be confused with a calcaneal stress fracture, tarsal tunnel syndrome, or plantar fasciitis [10]. With the development of nodules, malignancies such as melanoma, synovial sarcoma, and Kaposi sarcoma may be of concern. On a histologic level, calcifying aponeurotic fibroma can be excluded as plump or epithelioid fibroblasts palisading around cartilage and spotty calcification is seen in this entity and not in plantar fibromatosis. As in the hand, desmoid-type fibromatosis is rare in the feet and infiltrates skeletal muscle. These lesions are also usually greater than 3 cm and often shows nuclear beta-catenin reactivity in more than 80% of cases. Plantar fibromatosis also may raise the differential diagnoses of synovial sarcoma and MPNST. If these are of concern, fluorescence in situ hybridization (SS18) and immunohistochemistry (i.e., S-100, SOX-10, H3K27me3) may be employed to assist in this differential.

TREATMENT AND PROGNOSIS

Observation is an option for palmar fibromatosis, while excision or incision of the contracture band may be necessary if the contracture results in functional disability and the total flexion deformity is greater than 30 degrees [30] (Figs. 10A, B). Unfortunately, the lesion often recurs. Collagenase (*Clostridium histolyticum*) has been recently investigated as a treatment option [8,30,31]. The disease course seems to cause greater morbidity for white men with a strong family history, those with bilateral involvement, severe disease and ectopic manifestations [32].

As with palmar fibromatosis, conservative measures should be used for plantar fibromatosis prior to recommending surgery. If surgery is performed for symptomatic lesions, complete fasciectomy has fewer recurrences than local and wide excisions

[8,10,33]. Along with collagenase, several nonoperative treatments such as steroid injections, verapamil, radiation therapy, extracorporeal shock wave therapy, and tamoxifen have all had variable scientific support [10]. Those with bilateral involvement, multiple nodules, and a positive family history have a worse prognosis [34].

CONCLUSION

Palmar and plantar fibromatoses are related entities that together form a relatively common diagnostic group encountered in surgical pathology. Further study is needed to ascertain the etiology of these diseases as treatment options currently are limited with a high rate of recurrence. Recognizing the basic clinical, radiographic, and pathologic features is important to arrive at the correct diagnosis.

Ethics Statement

Not applicable.

Availability of Data and Material

Data sharing not applicable to this article as no datasets were generated or analyzed during the study.

Code Availability

Not applicable.

ORCID

Brian D. Stewart

<https://orcid.org/0000-0002-6126-1154>

Alessandra F. Nascimento

<https://orcid.org/0000-0001-6285-4827>

Author Contributions

Investigation: BDS. Project administration: BDS. Visualization: BDS, AFN. Writing—original draft: BDS. Writing—review & editing: BDS, AFN. Approval of final manuscript: all authors.

Conflicts of Interest

The authors declare that they have no potential conflicts of interest.

Funding Statement

No funding to declare.

Acknowledgments

The authors would like to thank Chung M. Chan, M.D., for the contribution of the clinical photos of palmar fibromatosis.

References

- Dibenedetti DB, Nguyen D, Zografos L, Ziemiecki R, Zhou X. Prevalence, incidence, and treatments of Dupuytren's disease in the United States: results from a population-based study. *Hand (N Y)* 2011; 6: 149-58.
- Cordova A, Tripoli M, Corradino B, Napoli P, Moschella F. Dupuytren's contracture: an update of biomolecular aspects and therapeutic perspectives. *J Hand Surg Br* 2005; 30: 557-62.
- Follonier Castella L, Gabbiani G, McCulloch CA, Hinz B. Regulation of myofibroblast activities: calcium pulls some strings behind the scene. *Exp Cell Res* 2010; 316: 2390-401.
- Krause C, Kloen P. Concurrent inhibition of TGF-beta and mitogen driven signaling cascades in Dupuytren's disease: non-surgical treatment strategies from a signaling point of view. *Med Hypotheses* 2012; 78: 385-8.
- Ratkaj I, Bujak M, Jurisic D, et al. Microarray analysis of Dupuytren's disease cells: the profibrogenic role of the TGF-beta inducible p38 MAPK pathway. *Cell Physiol Biochem* 2012; 30: 927-42.
- Dolmans GH, Werker PM, Hennies HC, et al. Wnt signaling and Dupuytren's disease. *N Engl J Med* 2011; 365: 307-17.
- Sayadi LR, Alhunayan D, Sarantopoulos N, et al. The molecular pathogenesis of Dupuytren disease: review of the literature and suggested new approaches to treatment. *Ann Plast Surg* 2019; 83: 594-600.
- Carroll P, Henshaw RM, Garwood C, Raspovic K, Kumar D. Plantar fibromatosis: pathophysiology, surgical and nonsurgical therapies: an evidence-based review. *Foot Ankle Spec* 2018; 11: 168-76.
- Godette GA, O'Sullivan M, Menelaus MB. Plantar fibromatosis of the heel in children: a report of 14 cases. *J Pediatr Orthop* 1997; 17: 16-7.
- Young JR, Sternbach S, Willinger M, Hutchinson ID, Rosenbaum AJ. The etiology, evaluation, and management of plantar fibromatosis. *Orthop Res Rev* 2019; 11: 1-7.
- Kim SK, Ioannidis JPA, Ahmed MA, et al. Two genetic variants associated with plantar fascial disorders. *Int J Sports Med* 2018; 39: 314-21.
- Strzelczyk A, Vogt H, Hamer HM, Kramer G. Continuous phenobarbital treatment leads to recurrent plantar fibromatosis. *Epilepsia* 2008; 49: 1965-8.
- Teh J. Ultrasound of soft tissue masses of the hand. *J Ultrason* 2012; 12: 381-401.
- Yacoe ME, Bergman AG, Ladd AL, Hellman BH. Dupuytren's contracture: MR imaging findings and correlation between MR signal intensity and cellularity of lesions. *AJR Am J Roentgenol* 1993; 160: 813-7.
- Espert M, Anderson MR, Baumhauer JF. Current concepts review: plantar fibromatosis. *Foot Ankle Int* 2018; 39: 751-7.
- McNally EG, Shetty S. Plantar fascia: imaging diagnosis and guided treatment. *Semin Musculoskelet Radiol* 2010; 14: 334-43.
- Griffith JE, Wong TY, Wong SM, Wong MW, Metreweli C. Sonography of plantar fibromatosis. *AJR Am J Roentgenol* 2002; 179: 1167-72.
- Cohen BE, Murthy NS, McKenzie GA. Ultrasonography of plantar fibromatosis: updated case series, review of the literature, and a novel descriptive appearance termed the "Comb sign". *J Ultrasound Med* 2018; 37: 2725-31.
- Narvaez JA, Narvaez J, Ortega R, Aguilera C, Sanchez A, Andia E. Painful heel: MR imaging findings. *Radiographics* 2000; 20: 333-52.
- Evans HL. Multinucleated giant cells in plantar fibromatosis. *Am J Surg Pathol* 2002; 26: 244-8.
- Carlson JW, Fletcher CD. Immunohistochemistry for beta-catenin in the differential diagnosis of spindle cell lesions: analysis of a series and review of the literature. *Histopathology* 2007; 51: 509-14.
- Fausto de Souza D, Micaelo L, Cuzzi T, Ramos ESM. Ledderhose disease: an unusual presentation. *J Clin Aesthet Dermatol* 2010; 3: 45-7.
- Wang L, Zhu H. Clonal analysis of palmar fibromatosis: a study whether palmar fibromatosis is a real tumor. *J Transl Med* 2006; 4: 21.
- Kaur S, Forsman M, Ryhanen J, Knuutila S, Larramendy ML. No gene copy number changes in Dupuytren's contracture by array comparative genomic hybridization. *Cancer Genet Cytogenet* 2008; 183: 6-8.
- De Wever I, Dal Cin P, Fletcher CD, et al. Cytogenetic, clinical, and morphologic correlations in 78 cases of fibromatosis: a report from the CHAMP Study Group. *CHromosomes And Morphology. Mod Pathol* 2000; 13: 1080-5.
- Shih B, Tassabehji M, Watson JS, Bayat A. DNA copy number variations at chromosome 7p14.1 and chromosome 14q11.2 are associated with Dupuytren's disease: potential role for MMP and Wnt signaling pathway. *Plast Reconstr Surg* 2012; 129: 921-32.
- Michou L, Lermusiaux JL, Teyssedou JP, Bardin T, Beaudreuil J, Petit-Teixeira E. Genetics of Dupuytren's disease. *Joint Bone Spine* 2012; 79: 7-12.
- Breiner JA, Nelson M, Bredthauer BD, Neff JR, Bridge JA. Trisomy 8 and trisomy 14 in plantar fibromatosis. *Cancer Genet Cytogenet* 1999; 108: 176-7.
- Sawyer JR, Sammartino G, Gokden N, Nicholas RW. A clonal reciprocal t(2;7)(p13;p13) in plantar fibromatosis. *Cancer Genet Cytogenet* 2005; 158: 67-9.
- Denkler KA, Vaughn CJ, Dolan EL, Hansen SL. Evidence-based medicine: options for Dupuytren's contracture: incise, excise, and dissolve. *Plast Reconstr Surg* 2017; 139: 240e-55e.
- Sanjuan-Cervero R. Current role of the collagenase Clostridium histolyticum in Dupuytren's disease treatment. *Ir J Med Sci* 2020; 189: 529-34.
- Townley WA, Baker R, Sheppard N, Grobbelaar AO. Dupuytren's contracture unfolded. *BMJ* 2006; 332: 397-400.
- van der Veer WM, Hamburg SM, de Gast A, Niessen FB. Recurrence of plantar fibromatosis after plantar fasciectomy: single-center long-term results. *Plast Reconstr Surg* 2008; 122: 486-91.
- Kadir HK, Chandrasekar CR. Partial fasciectomy is a useful treatment option for symptomatic plantar fibromatosis. *Foot (Edinb)* 2017; 31: 31-4.

Potential of AKT2 expression as a predictor of lymph-node metastasis in invasive breast carcinoma of no special type

Primariadewi Rustamadji^{1*}, Elvan Wiyarta^{2*}, Kristina Anna Bethania¹, Kusmardi Kusmardi³

¹Department of Anatomic Pathology, Faculty of Medicine, Universitas Indonesia, Jakarta;

²Faculty of Medicine, Universitas Indonesia, Jakarta;

³Department of Anatomic Pathology, Drug Development Research Cluster, Human Cancer Research Center, IMERI, Faculty of Medicine, Universitas Indonesia, Jakarta, Indonesia

Background: Invasive breast carcinoma of no special type (IBC-NST) is the most common type of breast cancer and mainly causes regional lymph-node metastasis (LNM). We investigated the potential for AKT2 expression as a predictive biomarker for LNM in IBC-NST. **Methods:** Forty-eight paraffin blocks containing IBC-NST primary tumors were divided into two groups based on presence or absence of LNM. Age, tumor grade, tumor size, lymphovascular invasion (LVI), and AKT expression were assessed. AKT2 expression was assessed based on immunohistochemical staining, while other data were collected from archives. **Results:** Multiple logistic regression results showed that AKT2 expression and LVI were significantly associated with LNM (odds ratio [OR], 5.32; 95% confidence interval [CI], 1.42 to 19.93 and OR, 4.46; 95% CI, 1.17 to 16.97, respectively). AKT2 expression was able to discriminate against LNM (area under the receiver operating characteristic, 0.799 ± 0.063 ; 95% CI, 0.676 to 0.921) at an H-score cutoff of 104.62 (83.3% sensitivity, 62.5% specificity). **Conclusions:** AKT2 expression has potential as a predictor of LNM in IBC-NST. The H-score cutoff for AKT2 expression can be used as a classification guide in future studies.

Key Words: AKT2; Breast neoplasms; Metastasis; Immunohistochemistry

Received: March 13, 2021 **Revised:** April 11, 2021 **Accepted:** April 26, 2021

Corresponding Author: Elvan Wiyarta, MBBS, Faculty of Medicine, Universitas Indonesia, Salemba Raya No. 6. RW. 5, Kenari, Kec. Senen, Kota Jakarta Pusat, Jakarta 10430, Indonesia
 Tel: +62-81382222670, E-mail: elvan.wiyarta@ui.ac.id

*Primariadewi Rustamadji and Elvan Wiyarta contributed equally to this work.

Breast cancer is the most common and deadly type of cancer in women, accounting for 25% of all cancers in women. The 2018 global breast cancer incidence reached 2.09 million new cases [1]. Breast cancer results from a tumor that arises from uncontrolled proliferation of breast tissue. To improve identification, histological breast cancer classification is divided into two types based on the relationship to the basement membrane: non-invasive breast carcinoma (nIBC) and invasive breast carcinoma (IBC) [2]. IBC has faster progression, many subtypes, and is more common than nIBC. Among the IBC subtypes, 70% are invasive breast carcinoma of no special type (IBC-NST) [2]. Higher breast cancer grades indicate worse prognosis, and the likelihood of metastasis is greater in carcinomas with poor grading, such as with IBC-NST. Metastasis is a progression stage wherein cancer cells spread and invade other organs [3]. Metastasis occurs by forming new cancer cell colonies in other healthy

body tissues, further reducing patient prognosis [3]. In IBC-NST, the most common body tissue for metastases is axillary lymph nodes, hereinafter referred to as lymph-node metastasis (LNM).

Various efforts to improve LNM prediction have been made for tertiary prevention in breast cancer patients, one of which is identification of specific IBC-NST biomarkers [4]. Many studies have investigated potential IBC-NST biomarkers, including AKT, which is a protein involved in IBC-NST progression. AKT is located in the cell membrane, and cytoplasm activates various downstream protein substrates that instigate cancer progression [5]. However, according to a systematic review by Yang et al. [6], many studies have produced inconsistent findings regarding the role of AKT in breast cancer. These discrepancies might be because AKT is thought to have three isoforms—AKT1, AKT2, and AKT3—each of which has distinct

and opposing roles [7]. AKT3 has not been widely studied, but it is suspected to play a greater role in triple-negative breast cancer [7]. AKT1 plays a role in proliferation through upregulation of cyclin D1, but it is thought to inhibit cell migration and invasion through downregulation of β 1-integrin and focal adhesion kinase (FAK) [7]. In contrast, AKT2 is thought to induce cell migration and metastasis through induction of vimentin and F-actin [7]. Responding to this problem, we see the potential for AKT2 as a predictor of LNM in IBC-NST. AKT2 is one of the proteins involved in cancer invasion pathways and epithelial mesenchymal transition (EMT), both of which affect patient prognosis [8]. However, there are no studies into AKT2 as a predictor of LNM in IBC-NST. Therefore, this study investigates the role of AKT2 expression as a potential predictor of LNM in IBC-NST and assesses its potential as a predictive biomarker of IBC-NST.

MATERIALS AND METHODS

Study design and data collection

This is a cross-sectional study that was conducted in the Anatomical Pathology Laboratory of the Faculty of Medicine at the University of Indonesia from December 2019 to December 2020. The study conforms with The Code of Ethics of the World Medical Association (Declaration of Helsinki) [9]. Data retrieved from the 2019 and 2020 departmental archives were patient age, tumor subtype (limited to IBC-NST), tumor grade (based on Nottingham Grading System [10]), tumor size, lymphovascular invasion (LVI), and LNM. AKT2 expression data were obtained through quantification of immunohistochemistry (IHC) staining results.

Samples

The samples evaluated in this study were primary tumor paraffin blocks from breast mastectomy in Asian females that had been diagnosed histopathologically with IBC-NST, either with or without metastasis into adjacent lymph nodes. Samples having an additional histopathological diagnosis other than IBC-NST (e.g., invasive lobular carcinoma, medullary carcinoma, papillary carcinoma), systemic comorbidities (hypertension, diabetes mellitus, etc.), or damaged paraffin blocks (e.g., paraffin blocks with tumor masses cut or eaten by animals, etc.) were excluded.

Samples were classified according to presence or absence of LNM. The minimum sample size was calculated with $\alpha = 5\%$, confidence interval (CI) = 95%, and power = 80%. Consequently, a minimum of 23 samples was required for each group.

We obtained 24 samples for the metastatic lymph node group and 24 samples for the non-metastatic lymph node group. To avoid bias, grouping data were accessed by a single researcher (K.K.), and the other researchers were blind to patient groupings until the research process was complete.

Slide preparation and IHC staining

Slide preparation was performed by cutting the tissue in a paraffin block using a microtome to a thickness of 3–5 μ m. Next, the sample was heated on a slide warmer (30–60 minutes) at 58°C, deparaffinized using stratified xylol (Merck, Jakarta, Indonesia) for 5 minutes, rehydrated in alcohol (Merck) for 5 minutes, and rinsed with water for 5 minutes. Each slide was pre-treated with heat-induced retrieval antigen using 0.1 M NaOH citrate buffer pH 7.0 (Brataco Inc., Jakarta, Indonesia) in an autoclave at 121°C for 15 minutes and then washed in phosphate buffered saline (PBS) pH 7.4 (Brataco Inc.) for 5 minutes. Blocking was performed using hydrogen peroxide (Brataco Inc.) in 3% v/v methanol (Brataco Inc.) for 30 minutes at room temperature. Next, it was washed under running water for 5 minutes, followed by nonspecific protein blocking with universal Background Sniper (Abcam, Jakarta, Indonesia) for 15 minutes. After the blocking process, the slides were incubated for 1 hour with anti-AKT2 antibody (Abcam) at a 1:100 dilution and then washed in PBS for 5 minutes. Subsequently, the slides were incubated with biotinylated secondary antibody (Abcam) for 30 minutes and washed in PBS for 5 minutes. Diaminobenzidine tetrahydrochloride (Abcam) was dropped onto a slide and counterstained with Lillie-Mayer's hematoxylin (Abcam) for 2 minutes. Subsequently, the slides were immersed in lithium carbonate (Merck) for 2 minutes followed by graded alcohol dehydration (5 minutes) and graded xylol clearing (5 minutes). Finally, the sections were covered with a liquid cover, which is an aqueous mounting media. The stained sections were subsequently examined for AKT2 expression. Negative and positive controls were included for each staining. The negative control was established by eliminating the primary antibody administration step.

Quantification of AKT2 expression

Immunohistochemical staining assessment was performed by two experienced researchers (P.R. and K.A.B.). Each preparation was observed using a light microscope at 400x magnification and was documented using Leica LAZ EZ software (Jena, Germany) and a camera that was integrated with a Leica DM750 microscope. AKT2 expression was assessed in at least 500 tumor cells from 5 high-power visual fields (\times 400) that were chosen ran-

domly. Each region was represented by a minimum of 100 tumor cells. AKT2 positivity was represented by brown staining of the tumor cell membrane and cytoplasm.

Staining intensity was categorized into no staining (0), low positive (1+), positive (2+), and high positive (3+) based on the intensity of the brown color observed in each view field using the cell counter function in ImageJ [11]. The H-score was calculated to quantify AKT2 expression and was based on the following formula [12]:

$$\text{H-score} = (\% \text{ low positive} \times 1) + (\% \text{ positive} \times 2) + (\% \text{ high positive} \times 3) \quad (1)$$

Two observers (P.R. and K.A.B.) independently calculated the H-scores for all samples. To avoid bias, the results of the previously assessed calculations were reported to the statistician (E.W.) until the entire sample was assessed. The mean H-score of the two observers was used for statistical analyses.

Statistical analyses

Data were entered into a master table using Microsoft Excel 2013 (Microsoft Corp., Redmond, WA, USA), and the tabulated data were analyzed using the SPSS ver. 20 (IBM Corp., Armonk, NY, USA) and visualized using GraphPad Prism 8 (GraphPad

Software, Inc., La Jolla, CA, USA). Variability in H-score between the two observers was compared with the intraclass correlation coefficient (ICC) to assess data reliability. The ICC model used a two-way mixed average measurement with absolute agreement. ICC values were grouped according to 95% confident intervals of the ICC estimate: poor, < 0.5; moderate, 0.5–0.75; good, 0.75–0.9; and excellent, > 0.90.

H-scores of the two observers were averaged and grouped into high or low groups using the median H-score as the cutoff (median split approach) [13,14]. This grouping describes AKT2 expression in each sample. A bivariate analysis was performed to compare age (< 50 years or ≥ 50 years), tumor grade (high or low), tumor size (≤ 5 cm or > 5 cm), LVI (yes or no), and AKT2 expression (high or low) against LNM (yes or no). All variables that have a $p < .2$ in bivariate analysis will be included in multivariate multiple logistic regression models using the backward logistic regression method. The discrimination capacity of the model was calculated from the area under the receiver operating characteristic (AUROC) curve. A p -value less than .05 was considered statistically significant.

The receiver operating characteristic (ROC) curve for the AKT2 H-score was analyzed, for which we included H-score as a continuous variable. ROC was determined according to the area under the curve (AUC) that was grouped as follows: 0.5, no dis-

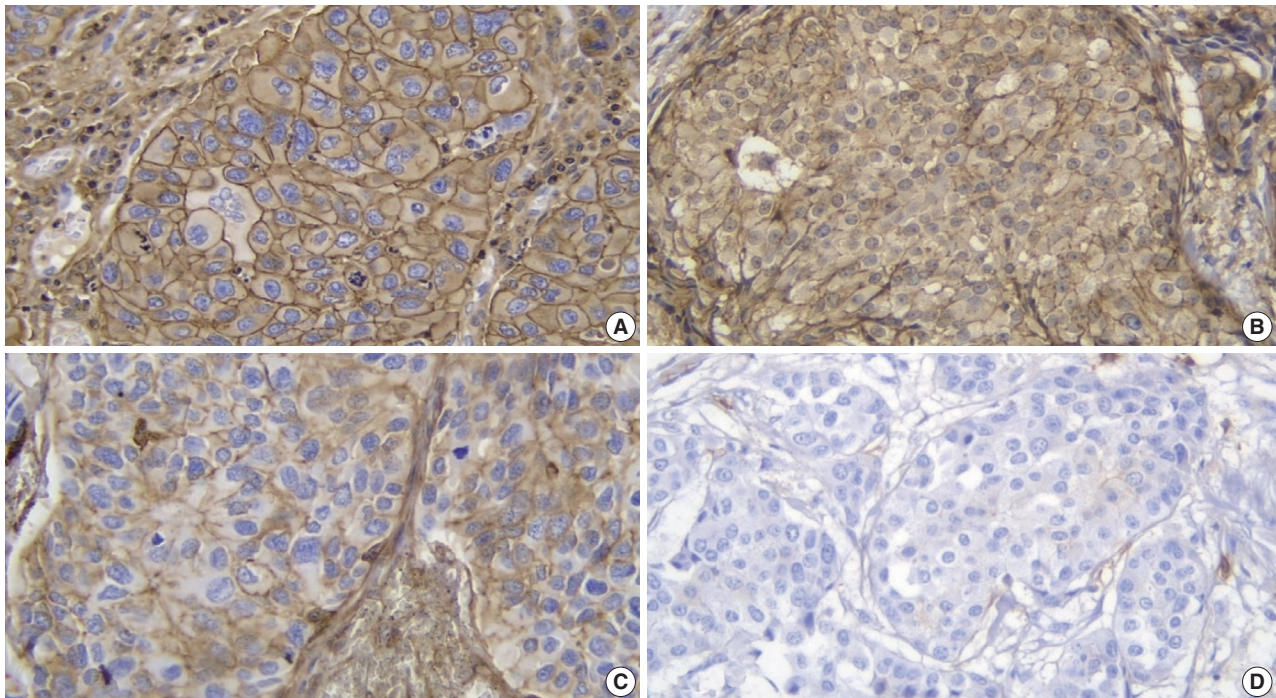


Fig. 1. Immunohistochemical staining for AKT2 expression in IBC-NST tumor cells: (A) high positive, (B) positive (C) low positive, and (D) no staining. IBC-NST, invasive breast carcinoma of no special type.

crimination; 0.7–0.8, acceptable; 0.8–0.9, excellent; and > 0.9, outstanding. The AKT2 expression cutoff value was assessed from the ROC curve based on the highest Youden Index [15] and the lowest K-Index [16]. The Youden Index uses the maximum vertical distance of the ROC curve from the (x, y) point on the diagonal (chance) line.

RESULTS

IHC staining and H-score reliability

All 48 samples underwent immunohistochemical staining for AKT2 expression. Representative immunohistochemical staining results are shown in Fig. 1A–D. Each image represents a sample of tumor cells with different staining groups: high positive (A), positive (B), low positive (C), and no staining (D). The images include several visual fields from the same slide. These photos also show that, in one slide, sometimes even in one visual field, several cells can be found with different intensities. AKT2 expression can be observed in the cell membrane and cytoplasm. The intensity of brown color in these areas was quantified into an H-score for further assessment.

Two observers (P.R. and K.A.B.) assessed all 48 samples independently. The distribution of H-scores within each sample can be seen in Fig. 2. Reliability between any two measurements was determined to be moderate. The average measure ICC was 0.726 (95% CI, 0.509 to 0.847; $F(47.47) = 3.593$; $p < .001$).

Association between AKT2 expression and LNM

The clinicopathologic characteristics of each sample are presented in Table 1. Each of these variables is a covariate that can have a role in LNM occurrence. Therefore, we considered the role of each variable by conducting bivariate tests to evaluate their relationships with LNM. Bivariate analyses of several variables were performed to assess their association with LNM (Table 2), including patient age (< 50 years or ≥ 50 years), tumor grade (grade III [high] or grade I–II [low]), tumor size (≤ 5 cm or > 5 cm), LVI (yes or no), and AKT2 expression (high or low).

Bivariate analysis results indicated a significant relationship

Table 1. Frequency distribution based on clinicopathological characteristics

Clinicopathological characteristic	No. (%)
Age (yr)	
≥ 50	27 (56.3)
< 50	21 (43.8)
Mean ± SD	50.9 ± 12.3
Median (min–max)	50 (29–75)
Tumor grade	
Grade I	5 (10.4)
Grade II	16 (33.3)
Grade III	27 (56.3)
Tumor size (cm)	
< 2	2 (4.2)
2–5	28 (58.3)
> 5	18 (37.5)
Lymphovascular invasion	
Yes	27 (56.3)
No	21 (43.8)

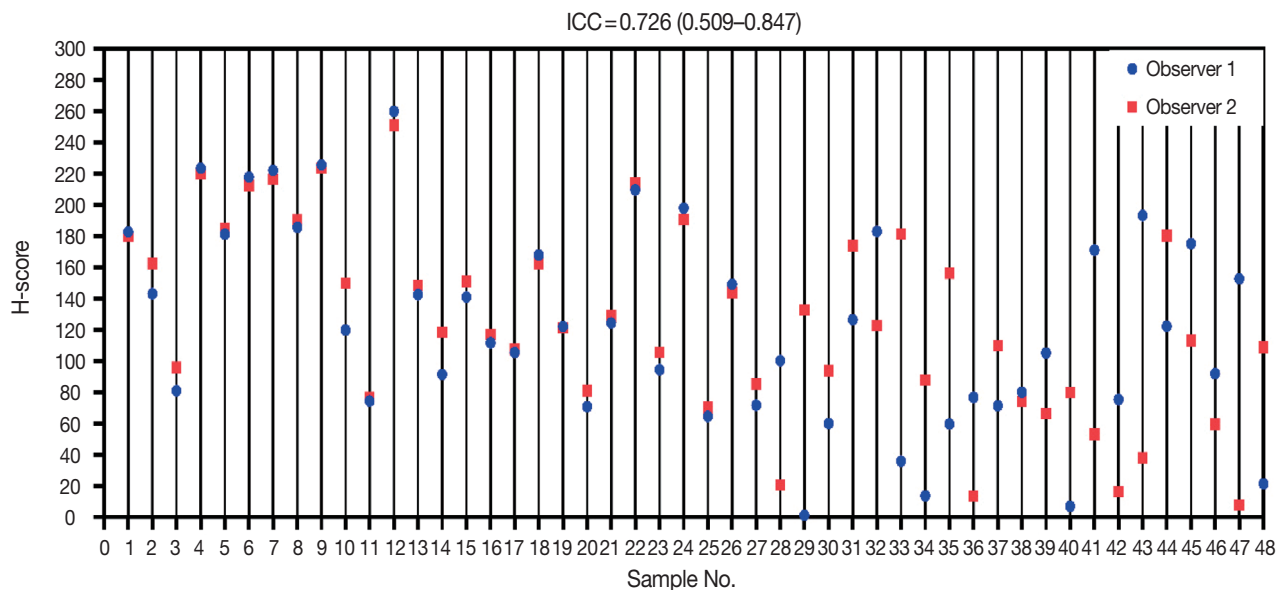


Fig. 2. Dot plot depicting the distribution of H-score between two observers over the entire sample.

Table 2. The results of bivariate analysis on several variables of LNM in IBC-NST

Variable	Lymph-node metastasis, n (%)			p-value	OR	95% CI	
	Yes	No	Total			Min	Max
Age (yr) ^a				>.990	1.19	0.38	3.71
≥50	14 (51.9)	13 (48.1)	27				
<50	10 (47.6)	11 (52.4)	21				
Tumor grade ^a				.561	1.67	0.53	5.27
High	15 (55.6)	12 (44.4)	27				
Low	9 (42.9)	12 (57.1)	21				
Tumor size (cm) ^a				.371	0.49	0.15	1.60
>5	7 (38.9)	11 (61.1)	18				
≤5	17 (56.7)	13 (43.3)	30				
Lymphovascular invasion ^a				.020	5.00	1.45	17.27
Yes	18 (66.7)	9 (33.3)	27				
No	6 (28.6)	15 (71.4)	21				
AKT2 expression ^a				.009	5.90	1.70	20.48
High	17 (70.8)	7 (29.2)	24				
Low	7 (29.2)	17 (70.8)	24				

LNM, lymph-node metastasis; IBC-NST, invasive breast carcinoma of no special type.
^aBivariate analysis was performed using the chi-square test with continuity correlation.

Table 3. Multiple logistic regression results for LNM in IBC-NST

Predictor	β	SE β	Wald's χ ²	df	p-value	e ^β (odds ratio)
AKT2 expression	1.67	0.67	6.162	1	.013	5.32
Lymphovascular invasion	1.49	0.68	4.789	1	.028	4.46
Constant	-1.69	0.63	7.100	1	.008	0.19
Test						
Hosmer-Lemeshow	-	-	0.002	2	.999	-
Goodness-of-Fit test						
Overall model evaluation	-	-	13.690	2	.001	-

LNM, lymph-node metastasis; IBC-NST, invasive breast carcinoma of no special type; SE, standard error; df, degree of freedom; e, euler number ≈ 2.718.

between AKT2 expression and LNM (p = .009). LVI also was significantly associated with LNM (p = .020). There was no significant association between patient age, tumor grade, or tumor size and LNM. Because both AKT2 expression and LVI showed significant associations with LNM, they were included in a multivariate regression model (Table 3).

Both AKT2 expression (odds ratio [OR], 5.32; 95% CI, 1.42 to 19.93) and LVI (OR, 4.46; 95% CI, 1.17 to 16.97) were significantly associated with LNM. Samples with high AKT2 expression were 5.32 times more likely to have metastases than were samples with low AKT2 expression, and samples with LVI were 4.46 times more likely to have metastases than were samples without LVI. We also calculated the metastatic probability based on the following formula [17]:

Table 4. Various probabilities for LNM based on model variables in IBC-NST

AKT2 expression	Lymphovascular invasion	Probability of LNM (%)
High	Yes	81.44
High	No	49.62
Low	Yes	45.18
Low	No	15.62

LNM, lymph-node metastasis; IBC-NST, invasive breast carcinoma of no special type.

$$P(Y) = \frac{e^{X1(1.67) + X2(1.49) - 1.69}}{1 + e^{X1(1.67) + X2(1.49) - 1.69}} \tag{2}$$

, where P(Y) is the probability of LNM, X1 represents AKT2 expression (high, 1; low, 0), and X2 represents LVI (yes, 1; no, 0). From this model, the probability of LNM can be calculated for various conditions (Table 4).

Model goodness-of-fit was adequate (Table 3). The Hosmer-Lemeshow test (p = .999) indicated that LNM numbers were not significantly different from those predicted by the model, and model predictions yielded satisfactory goodness-of-fit. Moreover, the difference between the overall model and a constant-only model was statistically significant (p = .001), indicating that the predictors reliably distinguished between LNM and non-LNM cases. The AUROC value for this model was 0.78, which indicates excellent discriminatory ability.

ROCs of AKT2 expression

The ability of AKT2 expression to discriminate against lymph-node metastases was assessed through ROC curve analysis (Fig.

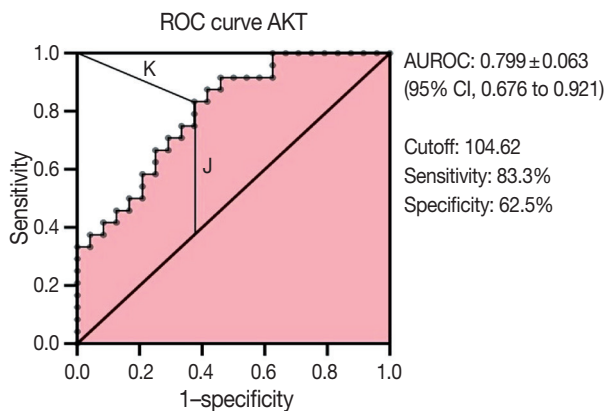


Fig. 3. Receiver operating characteristic (ROC) curve of AKT2 expression. J, Youden index; K, K-index; AUROC, area under the receiver operating characteristic; CI, confidence interval.

3). The AUC was 0.799 ± 0.063 (95% CI, 0.676 to 0.921). This area (approximately 0.8) showed excellent accuracy. The optimal cutoff point for AKT2 expression was 104.62 (H-score), which yielded the highest Youden Index (0.458) and lowest K-index (0.41) among all cutoffs. This H-score has 83.3% sensitivity and 62.5% specificity.

DISCUSSION

Biomarkers are objectively measured characteristics that indicate normal biological processes, pathological processes, pharmacological responses, or therapeutic interventions as proteins that function under specific conditions. AKT2, one of the AKT isoforms, has a role in cancer invasion and metastasis. Thus, AKT2 identification is important for assessing cancer cell characteristics that cause LNM [18]. There are various techniques for identifying AKT2 expression in cells, including polymerase chain reaction (PCR), fluorescence in situ hybridization (FISH), and other molecular methods. In this study, we used a relatively convenient and affordable technique, IHC staining, to identify AKT2. IHC is a common method to identify biomarkers using selective antibodies to bind to specific proteins in tumor cells. While other more advanced molecular methods, such as PCR and FISH, are increasingly used in clinical practice, they can be less practical than IHC [19].

Specific antibodies bind to AKT2 in the cell membrane and cytoplasm and, to visualize them, diaminobenzidine tetrahydrochloride was used as a chromogen to emit a brown color (Fig. 1). The higher was the intensity of the brown color, the higher was the expression of AKT2 in cells. Also, because AKT2 is located mainly in the cell membrane and cytoplasm, brown color can be

observed in those areas of the cell [5]. This is consistent with Trigka et al. [20], where 94.14% of their samples had immunoreactivity against AKT2 staining in cytoplasm and cell membranes. Research by Malik et al. [21] showed that the staining was localized to the membrane where AKT2 was observed to be active. These findings strengthen the value of IHC as a practical method for AKT2 detection.

To confirm AKT2 expression as a predictor of LNM, several known confounding factors had to be controlled [22], including patient race, additional histopathological diagnoses, tumor subtypes, and multiple comorbidities. We eliminated these factors through application of inclusion and exclusion criteria. Several other confounding factors, including age, tumor grade, tumor size, and LVI, were included in the model, but their association effect with LNM was controlled through bivariate and regression analyses. Among these confounding factors, only LVI has a significant relationship with LNM. After regression analysis to analyze the relationship between AKT2 expression and LNM, LVI was added as a covariate but did not change the effect of AKT2 expression on LNM. This suggests AKT2 expression as an independent predictor of LNM.

The association between AKT2 expression and LNM in IBC-NST is interesting. In the logistic regression model, AKT2 expression had a very high OR (5.32; 95% CI, 1.42 to 19.93), meaning that primary tumor samples with high AKT2 expression were 5.32 times more likely to have LNM than samples with low AKT2 expression. This relationship is due to underlying molecular mechanisms—as previously explained, AKT2 has a promigratory role in cell migration, invasion, and metastasis. AKT2, but not AKT1 or AKT3, enhances integrin $\beta 1$ -mediated attachment and invasion through collagen IV, which plays an important role in cell invasion and migration [23]. Furthermore, AKT2 directly interacts with PKC ζ , which activates adhesion-associated $\beta 1$ -integrin and the actin-polymerizing LIMK/Cofilin axis after epidermal growth factor stimulation [23]. Additionally, AKT2 stimulation by mammalian target of rapamycin in Ser473 causes glycogen synthase kinase-3 β degradation, which also triggers EMT [23]. This is consistent with Ye et al. [24], who found that AKT2 promoted breast cancer cell growth after G protein-coupled receptor stimulation. Chen et al. [25] also demonstrated an important role for AKT, finding that cPLA2 α mediates EMT via transforming growth factor β activation in the phosphoinositide 3-kinase/AKT pathway. All of these results support the role of AKT2 in inducing LNM.

We also found an association between LVI and LNM (OR, 4.46; 95% CI, 1.17 to 16.97), indicating that primary tumor

samples with LVI were 4.46 times more likely to show lymph-node metastases than samples without LVI. The molecular mechanisms underlying LVI are unclear. In their review, Kariri et al. [26] state that “understanding the role of cancer cell invasion and migration in the differentiation of LVI-related molecular alterations from these driving tumor cell invasion and migration as an early mechanism associated with malignancy is a ‘difficult’ but ‘beatable’ challenge.” However, several hypothetical mechanisms have been proposed. Ribelles et al. [27] suggested that genetic alterations can increase migratory potential. On the other hand, Melzer et al. [28] suggested that matrix metalloproteinases can disrupt primary tumor stability, inducing migration and, ultimately, LVI. Apart from the underlying molecular mechanisms, several studies have found associations between LVI and LNM. Research by Schoppmann et al. [29] indicates that LVI was associated significantly with a higher risk for developing LNM. In fact, Nathanson et al. [30] showed that LVI can predict systemic metastasis when regional lymph-node metastases are positive. All these findings explain the association between LVI and LNM identified in this study.

On the other hand, we calculated the probability of LNM by including a constant (β) to the model formula (2). In formula (2), the constant (β) is used as a multiplier of the related variable. This also shows that the variable with a greater constant (β) has a more dominant role in determining LNM probability, and vice versa. Therefore, it can be concluded that AKT2 expression is more dominant than LVI in determining LNM probability. Although no previous studies have examined these two components simultaneously, several correlational studies can explain this finding. Research by Wang et al. [31] demonstrated a positive correlation between AKT2 mRNA expression and LNM in breast cancer ($r = 0.46$, $p < .001$). Meanwhile, a meta-analysis by Zhang et al. [32] showed a correlation between LVI and lymph-node metastases. However, the correlation was low ($r = 0.24$; 95% CI, 0.19 to 0.28) [32], indicating that the role of LVI on LNM is less dominant.

The potential for AKT2 as an LNM predictor needs further elucidation. One approach uses LNM discrimination analysis on the ROC curve. The AUC ROC was 0.799 ± 0.063 (95% CI, 0.676 to 0.921), indicating excellent accuracy, in this study, AKT2 expression as a way to discriminate lymph-node metastases was very good. Therefore, we conducted an analysis to estimate an optimal cutoff as a guide for classifying high or low AKT2 expression.

As explained above, this study uses the median H-score to classify AKT2 expression. However, we are aware that use of a marker-

specific IHC cutoff assay is important for prediction of therapeutic response [33]. Therefore, we conducted an additional analysis to identify a potential cutoff for AKT2 expression, wherein we estimated an H-score of 104.62. This suggests that, if this cutoff is implemented in an IBC-NST AKT2 expression dataset, an H-score ≥ 104.62 can be classified as “high AKT2 expression.” On the other hand, values with an H-score < 104.62 can be classified as “low AKT2 expression.” Of course, this cutoff needs to be further explored and refined, but we expect it to help classify AKT2 expression in future studies.

In conclusion, AKT2 expression can be used as a predictor to determine LNM. LVI also can be used as a predictor, although it has a less dominant role. Both play a role in predicting LNM in IBC-NST. Moreover, AKT2 expression can be identified by IHC staining, a practical method, with an H-score cutoff of 104.62 for classifying high and low AKT2 expression. This cutoff can be used in future research regarding AKT2 expression in IBC-NST.

Ethics Statement

The experimental protocols were approved by the Ethics Committee of the Faculty of Medicine, University of Indonesia (protocol number 20-09-1169, July 2020). All participants provided written consent, and the study conforms with The Code of Ethics of the World Medical Association (Declaration of Helsinki).

Availability of Data and Material

The datasets generated or analyzed during the study are available from the corresponding author on reasonable request.

Code Availability

Not applicable.

ORCID

Primariadewi Rustamadji	https://orcid.org/0000-0003-2325-1091
Elvan Wiyarta	https://orcid.org/0000-0002-5676-7804
Kristina Anna Bethania	https://orcid.org/0000-0003-3548-0369
Kusmardi Kusmardi	https://orcid.org/0000-0003-4300-723X

Author Contributions

Conceptualization: PR, EW. Data curation: EW, KAB. Formal analysis: EW. Funding acquisition: PR. Investigation: PR, KAB. Methodology: PR, EW. Software: EW. Validation: PR. Visualization: EW. Writing—original draft: EW. Writing—review & editing: PR, KK. Approval of final manuscript: all authors.

Conflicts of Interest

The authors declare that they have no potential conflicts of interest.

Funding Statement

No funding to declare.

Acknowledgments

We would like to thank all the staff from Department of Anatomical Pathology Faculty of Medicine, Universitas Indonesia.

References

1. Bray F, Ferlay J, Soerjomataram IS, et al. Global cancer statistics 2018: GLOBOCAN estimates of incidence and mortality worldwide for 36 cancers in 185 countries. *CA Cancer J Clin* 2018; 68: 394-424.
2. Sharma GN, Dave R, Sanadya J, Sharma P, Sharma KK. Various types and management of breast cancer: an overview. *J Adv Pharm Technol Res* 2010; 1: 109-26.
3. Chiang AC, Massague J. Molecular basis of metastasis. *N Engl J Med* 2008; 359: 2814-23.
4. Roche J. The epithelial-to-mesenchymal transition in cancer. *Cancers (Basel)* 2018; 10: 52.
5. Song M, Bode AM, Dong Z, Lee MH. AKT as a therapeutic target for cancer. *Cancer Res* 2019; 79: 1019-31.
6. Yang ZY, Di MY, Yuan JQ, et al. The prognostic value of phosphorylated Akt in breast cancer: a systematic review. *Sci Rep* 2015; 5: 7758.
7. Riggio M, Perrone MC, Polo ML, et al. AKT1 and AKT2 isoforms play distinct roles during breast cancer progression through the regulation of specific downstream proteins. *Sci Rep* 2017; 7: 44244.
8. Xu H, Tian Y, Yuan X, et al. The role of CD44 in epithelial-mesenchymal transition and cancer development. *Onco Targets Ther* 2015; 8: 3783-92.
9. Rickham PP. Human Experimentation. Code of Ethics of the World Medical Association. Declaration of Helsinki. *Br Med J* 1964; 2: 177.
10. Rakha EA, Reis-Filho JS, Baehner F, et al. Breast cancer prognostic classification in the molecular era: the role of histological grade. *Breast Cancer Res* 2010; 12: 207.
11. O'Brien J, Hayder H, Peng C. Automated quantification and analysis of cell counting procedures using ImageJ plugins. *J Vis Exp* 2016; e54719.
12. Choudhury KR, Yagle KJ, Swanson PE, Krohn KA, Rajendran JG. A robust automated measure of average antibody staining in immunohistochemistry images. *J Histochem Cytochem* 2010; 58: 95-107.
13. Costa WH, Rocha RM, Cunha IW, Guimaraes GC, Zequi Sde C. Immunohistochemical expression of CD44s in renal cell carcinoma lacks independent prognostic significance. *Int Braz J Urol* 2012; 38: 456-65.
14. Sadeghi A, Roudi R, Mirzaei A, Zare Mirzaei A, Madjd Z, Abolhasani M. CD44 epithelial isoform inversely associates with invasive characteristics of colorectal cancer. *Biomark Med* 2019; 13: 419-26.
15. Ruopp MD, Perkins NJ, Whitcomb BW, Schisterman EF. Youden Index and optimal cut-point estimated from observations affected by a lower limit of detection. *Biom J* 2008; 50: 419-30.
16. Kallner A. Formulas. In: Kallner A, ed. *Laboratory statistics: methods in chemistry and health sciences*. 2nd ed. Cambridge: Elsevier, 2018; 1-140.
17. Peng CY, Lee KL, Ingersoll GM. An introduction to logistic regression analysis and reporting. *J Educ Res* 2002; 96: 3-14.
18. Wolf DM, Yau C, Wulffkuhle J, et al. Mechanism of action biomarkers predicting response to AKT inhibition in the I-SPY 2 breast cancer trial. *NPJ Breast Cancer* 2020; 6: 48.
19. Toren W, Ansari D, Andersson R. Immunohistochemical investigation of prognostic biomarkers in resected colorectal liver metastases: a systematic review and meta-analysis. *Cancer Cell Int* 2018; 18: 217.
20. Trigka EA, Levidou G, Saetta AA, et al. A detailed immunohistochemical analysis of the PI3K/AKT/mTOR pathway in lung cancer: correlation with PIK3CA, AKT1, K-RAS or PTEN mutational status and clinicopathological features. *Oncol Rep* 2013; 30: 623-36.
21. Malik SN, Brattain M, Ghosh PM, et al. Immunohistochemical demonstration of phospho-Akt in high Gleason grade prostate cancer. *Clin Cancer Res* 2002; 8: 1168-71.
22. Koniali L, Hadjisavvas A, Constantinidou A, et al. Risk factors for breast cancer brain metastases: a systematic review. *Oncotarget* 2020; 11: 650-69.
23. Hinz N, Jucker M. Distinct functions of AKT isoforms in breast cancer: a comprehensive review. *Cell Commun Signal* 2019; 17: 154.
24. Ye Y, Tang X, Sun Z, Chen S. Upregulated WDR26 serves as a scaffold to coordinate PI3K/AKT pathway-driven breast cancer cell growth, migration, and invasion. *Oncotarget* 2016; 7: 17854-69.
25. Chen L, Fu H, Luo Y, et al. cPLA2alpha mediates TGF-beta-induced epithelial-mesenchymal transition in breast cancer through PI3k/Akt signaling. *Cell Death Dis* 2017; 8: e2728.
26. Kariri YA, Aleskandarany MA, Joseph C, et al. Molecular complexity of lymphovascular invasion: the role of cell migration in breast cancer as a prototype. *Pathobiology* 2020; 87: 218-31.
27. Ribelles N, Santonja A, Pajares B, Llacer C, Alba E. The seed and soil hypothesis revisited: current state of knowledge of inherited genes on prognosis in breast cancer. *Cancer Treat Rev* 2014; 40: 293-9.
28. Melzer C, von der Ohe J, Hass R. Breast carcinoma: from initial tumor cell detachment to settlement at secondary sites. *Biomed Res Int* 2017; 2017: 8534371.
29. Schoppmann SF, Bayer G, Aumayr K, et al. Prognostic value of lymphangiogenesis and lymphovascular invasion in invasive breast cancer. *Ann Surg* 2004; 240: 306-12.
30. Nathanson SD, Kwon D, Kapke A, Alford SH, Chitale D. The role of lymph node metastasis in the systemic dissemination of breast cancer. *Ann Surg Oncol* 2009; 16: 3396-405.
31. Wang Y, Dang X, Zhang M, Wei C, Li X. The role and correlation analysis of PI3K/AKT pathway in breast carcinoma with lymph node metastasis. *J Immunopathol* 2018; 1: 4-7.
32. Zhang S, Zhang D, Yi S, et al. The relationship of lymphatic vessel density, lymphovascular invasion, and lymph node metastasis in breast cancer: a systematic review and meta-analysis. *Oncotarget* 2017; 8: 2863-73.
33. Pierceall WE, Wolfe M, Suschak J, et al. Strategies for H-score normalization of preanalytical technical variables with potential utility to immunohistochemical-based biomarker quantitation in therapeutic response diagnostics. *Anal Cell Pathol (Amst)* 2011; 34: 159-68.

Correlation of TTF-1 immunoeexpression and *EGFR* mutation spectrum in non–small cell lung carcinoma

Tripti Nakra¹, Varsha Singh^{1*}, Aruna Nambirajan^{1*}, Prabhat Singh Malik², Anant Mohan³, Deepali Jain¹

¹Department of Pathology, All India Institute of Medical Sciences, New Delhi;

²Department of Medical Oncology, Dr B.R. Ambedkar Institute Rotary Cancer Hospital, All India Institute of Medical Sciences, New Delhi;

³Department of Pulmonary Medicine and Sleep Disorders, All India Institute of Medical Sciences, New Delhi, India

Background: Thyroid transcription factor (TTF-1) is a diagnostic marker expressed in 75%–85% of primary lung adenocarcinomas (ACs). Activating mutations in the tyrosine kinase domain of the epidermal growth factor receptor (*EGFR*) gene is the most common targetable driver alteration in lung AC. Previous studies have shown a positive correlation between TTF-1 and *EGFR* mutation status. We aimed to determine the predictive value of TTF-1 immunoeexpression for underlying *EGFR* mutation status in a large Indian cohort. **Methods:** This retrospective designed study was conducted with medical record data from 2011 to 2020. All cases of primary lung AC and non–small cell lung carcinoma not otherwise specified (NSCLC, NOS) with known TTF-1 expression diagnosed by immunohistochemistry using 8G7G3/1 antibodies and *EGFR* mutation status diagnosed by quantitative polymerase chain reaction were retrieved, reviewed, and the results were analyzed. **Results:** Among 909 patient samples diagnosed as lung AC and NSCLC, NOS, TTF-1 was positive in 76.8% cases (698/909) and *EGFR* mutations were detected in 29.6% (269/909). A strong positive correlation was present between TTF-1 positivity and *EGFR* mutation status (odds ratio, 3.61; $p < .001$), with TTF-1 positivity showing high sensitivity (90%) and negative predictive value (87%) for *EGFR* mutation. TTF-1 immunoeexpression did not show significant correlation with uncommon/dual *EGFR* mutations (odds ratio, 1.69; $p = .098$). EGFR–tyrosine kinase inhibitor therapy was significantly superior to chemotherapy among EGFR mutant cases irrespective of TTF-1 status; however, no significant differences among survival outcomes were observed. **Conclusions:** Our study confirms a strong positive correlation between TTF-1 expression and common *EGFR* mutations (exon 19 deletion and exon 21 L858R) in advanced lung AC with significantly high negative predictive value of TTF-1 for *EGFR* mutations.

Key Words: *EGFR* mutation; Lung adenocarcinoma; Non–small cell lung carcinoma; Thyroid transcription factor-1; Uncommon mutations

Received: January 28, 2021 Revised: April 2, 2021 Accepted: May 10, 2021

Corresponding Author: Deepali Jain, MD, DNB, Department of Pathology, All India Institute of Medical Sciences, New Delhi 110029, India
Tel: +91-9868895112, Fax: +91-1126549200, E-mail: deepaljain76@gmail.com

*Varsha Singh and Aruna Nambirajan contributed equally to this work.

Thyroid transcription factor 1 (TTF-1) is a regulatory transcription factor for maintaining peripheral lung function and is required for normal lung morphogenesis [1]. It is expressed normally in type II pneumocytes and non-ciliated bronchiolar epithelial cells, and this expression pattern is retained in 75%–85% of primary lung adenocarcinomas (ACs) [2,3]. TTF-1 positivity is highly specific to lung AC among all non-neuroendocrine neoplasms of the lung and is used widely as an immunohistochemical (IHC) marker for diagnosis of AC of lung origin and in subtyping of non–small cell lung carcinoma (NSCLC) not otherwise specified (NOS) wherein TTF-1 positivity favors diagnosis of lung AC over that of squamous cell carcinoma [4].

AC is the most common histological subtype of lung carcinoma,

both worldwide and in India, with an increasing trend in incidence [5,6]. With discovery of mutations in the epidermal growth factor receptor (*EGFR*) gene in up to one-third of all ACs and the high response rates of these patients to EGFR tyrosine kinase inhibitor (EGFR-TKI) therapy, the latter is the first-line treatment of choice in patients with advanced non-squamous NSCLC harboring *EGFR* mutations. In accordance, any lung carcinoma sample diagnosed as AC, or NSCLC, NOS on histology with or without IHC should be subjected to molecular testing (MT) for targetable alterations in *EGFR*, anaplastic lymphoma kinase (*ALK*), or c-ros oncogene 1 (*ROS1*) genes at minimum [7].

One of the major constraints in diagnosis and clinical management of lung AC is the non-availability of adequate tumor

tissue for MT. With nearly 70% of all lung cancer patients presenting with advanced stage, small biopsies/cytology represent the major source of tumor tissue, and successful MT on such small samples requires triage of material by informed pathologists and trained technicians [8]. Further, in a developing country such as India, the majority of laboratories do not have facilities for MT, and the samples usually are deferred to a higher medical center, resulting in delay and difficulty in timely treatment decisions.

Unlike MT, IHC is a well-established technique practiced even in small laboratories, and IHC using the recommended TTF-1 8G7G3/1 mouse monoclonal antibody [9] is available in most laboratories. Limited studies have analyzed the correlation between TTF-1 expression and *EGFR* mutations in lung AC and have reported a positive correlation between the two. Further, like *EGFR* mutant ACs, TTF-1 positivity has been shown to be associated with longer overall survival (OS), especially in non-metastatic NSCLC [10-12]. This retrospective study was undertaken to assess the correlation of TTF-1 IHC with *EGFR* mutation status to understand whether TTF-1 expression status can be used as a guide for prioritizing *EGFR* MT and/or for treatment decisions in resource-limited settings.

MATERIALS AND METHODS

Case selection

The current study was of a retrospective design spanning over duration of 9 years (January 2011 to February 2020), approved by the institutional ethics committee (IECPG-480/29.08.2016).

All primary lung AC patients with available medical record data pertaining to both TTF-1 and *EGFR* mutation testing on surgical pathology samples were selected for this study. The present study cohort included patients from previously published data pertaining to *EGFR* mutation rate [13-15]. Histopathological slides were reviewed, and diagnosis was reconfirmed in accordance with *WHO classification of tumours of the lung, pleura, thymus and heart* (2015) [16]. Detailed histopathological examination and subtyping of all cases were performed. Clinicopathological data including age, sex, smoking status, specimen type, site of biopsy, IHC result of TTF-1, and *EGFR* mutation status were recorded from the histopathology requisition forms.

Immunohistochemistry for TTF-1

IHC for TTF-1 was performed on 4- μ m-thick, formalin-fixed, paraffin-embedded tissue sections as part of diagnostic work-up during routine clinical practice. Heat-induced epitope retrieval

was conducted in citrate buffer at pH 6, followed by a 3-hour incubation period with TTF-1 antibody (1:400, mouse monoclonal antibody, clone 8G7G3/1, Bio-SB, Santa Barbara, CA, USA). A universal-labeled streptavidin biotin kit was used as a detection system. Nuclear staining of weak or strong intensity in $\geq 5\%$ of tumor cells was considered positive for TTF-1 expression [4]. For every case, negative and positive internal controls (normal lung tissue) or external controls (absence of normal lung parenchyma) were used.

EGFR mutation analysis

Real-time polymerase chain reaction-based *EGFR* mutation testing was conducted using the *EGFR* RGQ PCR Kit (Therascreen, Cat No. 870111, Qiagen, Hilden, Germany) to detect 29 hotspot mutations in *EGFR* exons 18–21.

Statistical analysis

Data was analyzed using GraphPad Prism ver. 8 (GraphPad Software Inc., San Diego, CA, USA). Categorical variables were tabulated as frequency and percentage. The chi-square or Fisher exact tests were used to analyze the categorical variables between TTF-1 expression and *EGFR* mutations. Patient age was represented in mean values with standard deviations. A $p < .05$ was considered statistically significant.

RESULTS

A total of 909 patient samples were included in the study (Table 1). The mean age of the cohort was 57 years, with a male preponderance (male:female ratio of 2.4:1). Sample types were tumor resections ($n = 19$) and small biopsies ($n = 890$), the latter also including lymph node excision biopsies and Tru-Cut biopsies from metastatic sites. TTF-1 was positive in 76.8% cases (698/909) (Fig. 1) and was significantly more prevalent among non-smokers ($p < .001$); however, there was no difference in prevalence among sex or stage-based groups. *EGFR* mutations were detected in 29.6% of cases (269/909). *EGFR* mutations were significantly more frequent among NSCLC occurring in females (46% vs. 23% in males, $p = .001$), non-smokers (58% vs. 28% in smokers, $p < .001$), and in early stages of presentation (67% vs. 41% in late stages, $p = .011$). However, only a small proportion of our cases was diagnosed at earlier stages. The most common mutation detected was exon 19 deletion (146/269, 54.3%), followed by exon 21 mutation encoding the L858R amino acid change (exon 21 L858R; 65/269, 24.2%). Other less common mutations observed were in exon 21 L861Q (2/269, 0.7%), exon 20 inser-

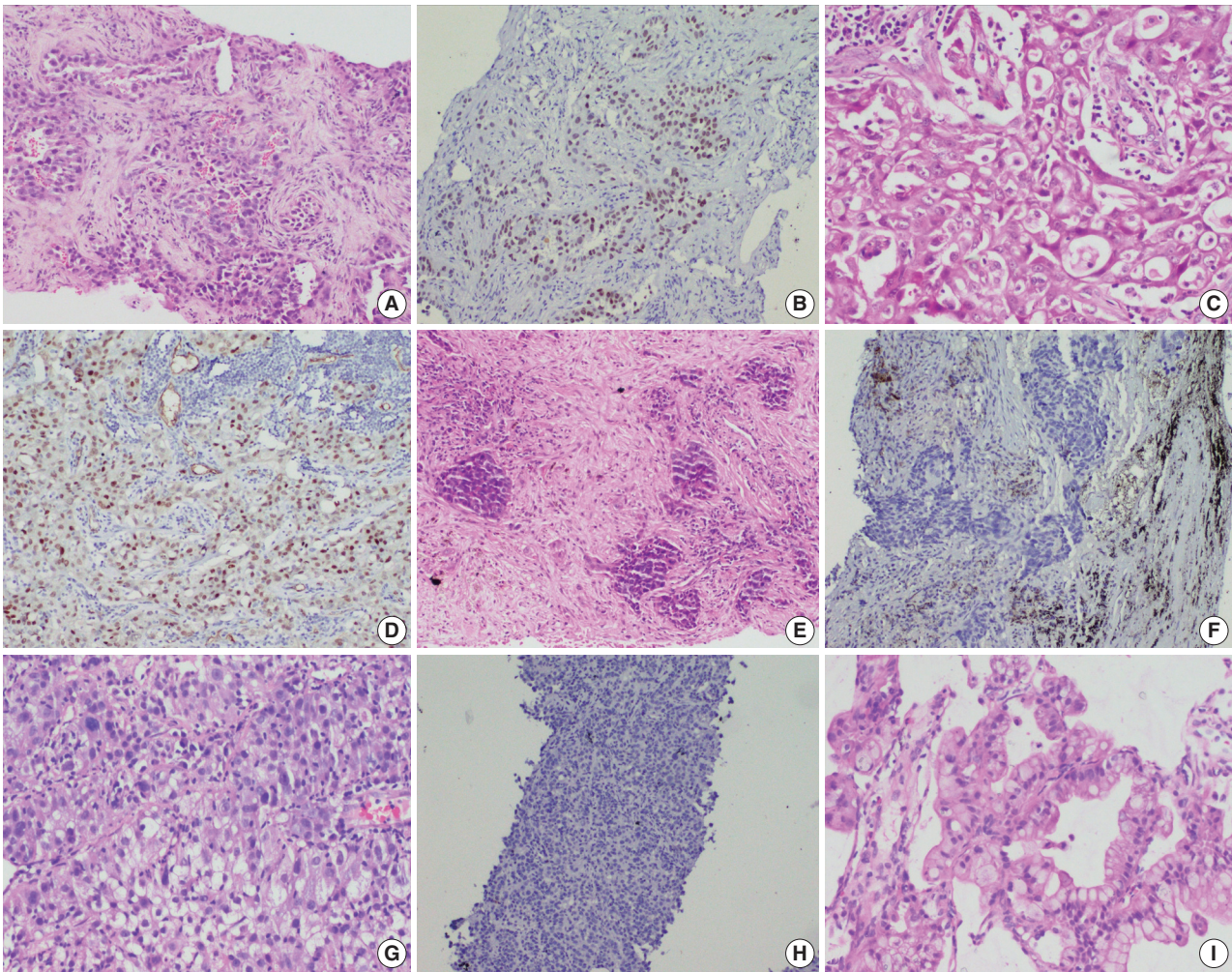


Fig. 1. Photomicrographs of non-small cell lung carcinoma (NSCLC). Epidermal growth factor receptor (*EGFR*) mutant lung adenocarcinoma with acinar and solid patterns (A) showing nuclear staining for thyroid transcription factor 1 (TTF-1) in tumor cells (B). *EGFR* wild type NSCLC with solid architecture (C) immunopositive for TTF-1 (D). Examples of *EGFR* mutant NSCLC not otherwise specified (NOS) (E) and *EGFR* wild type NSCLC, NOS (G) that are negative for TTF-1 (F, H); *EGFR* mutant invasive mucinous adenocarcinoma (I).

tion (4/269, 1.5%), exon 20 T790M (7/269, 2.6%), exon 20 S768I (3/269, 1.1%), and exon 18 G719X (3/269, 1.1%). Dual mutations involving multiple exons were detected in 39/269 cases (14.5%), the majority of which encoded the T790M amino acid change (17/39, 43.6%) in combination with other sensitive mutations. The rate of TTF-1 expression was lower among uncommon/dual mutations (84%, 49/58) compared to exon 19 deletion (91%, 133/146) and exon 21 L858R (92%, 60/65), although this did not reach statistical significance (Table 1).

Correlation between TTF-1 immunopositivity and *EGFR* mutation

Ninety percent of all *EGFR* mutant NSCLCs were TTF-1

positive, with TTF-1 positivity showing high sensitivity (90%) and negative predictive value (NPV; 87%) for *EGFR* mutations. However, only 30% of all TTF-1-positive ACs harbored *EGFR* mutations, showing low specificity (29%) and poor positive predictive value (PPV; 35%) (Table 2). Considering that the prevalence of *EGFR* mutations varies among clinicopathological subsets, in particular with sex and smoking status, we analyzed the correlation between TTF-1 and *EGFR* mutations in these subgroups separately. As expected, the PPV of TTF-1 positivity for *EGFR* mutations was highest among females (51%) and non-smokers (63%), which are the two clinical groups that show a higher prevalence of *EGFR* mutations. The lowest prevalence of *EGFR* mutations was among males (28%) and smokers (33%). Among individual types of mutations, PPV was higher with

Table 1. Clinicopathological features of patients included in the study

Parameter	No. (%)	TTF-1 immunohistochemistry			EGFR mutation status		
		Positive	Negative	p-value	Mutant	Wild type	p-value
Total No. of patients	909	698 (76.8)	211 (23.2)	-	269 (29.6)	640 (70.4)	-
Mean age at presentation (SD)	57 (12.3)	57 (12.4)	57 (12.3)	>.05	55 (12.2)	57 (12.4)	>.05
Sex							.001
Male	644 (70.8)	486 (75.5)	158 (24.5)	.082	148 (23.0)	496 (77.0)	
Female	265 (29.2)	212 (80.0)	53 (20.0)		121 (45.7)	144 (54.3)	
Smoking status (n=362)							<.001
Smoker	183 (50.6)	122 (66.7)	61 (33.3)	<.001	52 (28.4)	131 (71.6)	
Non-smoker	179 (49.4)	155 (86.6)	24 (13.4)		103 (57.5)	76 (42.5)	
Stage at presentation (n=358)							.011
I-III A	30 (8.4)	23 (76.7)	7 (23.3)	.594	20 (66.7)	10 (33.3)	
III B/IV	328 (91.6)	251 (76.5)	77 (23.5)		135 (41.2)	193 (58.8)	
First-line treatment (n=383)							-
EGFR-TKI	78 (20.4)	72 (92.3)	6 (7.7)		78 (100)	0	
Chemotherapy	305 (79.6)	222 (72.8)	83 (27.2)		89 (29.2)	216 (70.8)	
Tumor progression (n=397)				.061			.072
Yes	139 (35.0)	115 (82.7)	24 (17.3)		70 (50.4)	69 (49.6)	
No	258 (65.0)	192 (74.4)	66 (25.6)		105 (40.7)	153 (59.3)	
Tumor related deaths (n=397)				.502			>.990
Yes	30 (7.6)	25 (83.3)	5 (16.7)		13 (43.3)	17 (56.7)	
No	367 (92.4)	282 (76.8)	85 (23.2)		162 (44.1)	205 (55.9)	
Specimen type							-
Resections	19 (2.0)	16 (84.2)	3 (15.8)	-	5 (26.3)	14 (73.7)	
Small biopsies	890 (98.0)	682 (76.6)	208 (23.4)		264 (29.7)	626 (70.3)	
Histological diagnosis							-
AC/NSCLC, favor AC	815 (89.7)	698 (85.6)	117 (14.4)	-	261 (32.0)	554 (68.0)	
NSCLC, NOS	94 (10.3)	0	94 (100)		8 (8.5)	86 (91.5)	
EGFR mutation type							-
Exon 19 deletion	146 (16.1)	133 (91.1)	13 (8.9)	>.990	-	-	
Exon 21 L858R	65 (7.2)	60 (92.3)	5 (7.7)				
Uncommon/dual	58 (6.4)	49 (84.5)	9 (15.5)				
None	640 (70.4)	456 (71.3)	184 (28.7)				

TTF-1, thyroid transcription factor 1; EGFR, epidermal growth factor receptor; SD, standard deviation; TKI, tyrosine kinase inhibitor; AC, adenocarcinoma; NSCLC, non-small cell lung carcinoma; NOS, not otherwise specified.

common *EGFR* mutations (both exon 19 deletion and exon 21 L858R combined at 28%) than with uncommon/dual mutations (7%). The overall NPV of TTF-1 for *EGFR* mutations was 87%, was increased to 91% in males and for common *EGFR* mutations, and was highest for uncommon/dual mutations (96%).

We also calculated the diagnostic odds ratio (OR) within the entire cohort and within distinct clinicopathological subsets. OR denotes the ratio of the odds of TTF-1 being positive in an *EGFR* mutant tumor relative to the odds of TTF-1 being positive in an *EGFR* wild type tumor in this study and is independent of prevalence of *EGFR* mutations in the group under study. Overall, we found that TTF-1 was 3.6 times more likely to be positive in *EGFR* mutant tumors compared to *EGFR* wild type (OR, 3.61), with strong statistical strength ($p < .001$). This positive correlation between TTF-1 and *EGFR* mutation status remained sig-

nificant within all individual clinicopathological subsets except when only considering uncommon/dual *EGFR* mutations (Table 2, Fig. 2). The highest OR was observed in non-smokers (OR, 6.53) and among those with common *EGFR* mutations (OR, 4.09), with no significant difference in OR between the two common mutations, exon 19 deletion (OR, 3.59; 95% confidence interval [CI], 2.06 to 6.79; $p < .001$) and exon 21 L858R (OR, 3.88; 95% CI, 1.69 to 11.20; $p = .001$).

Histopathological subtyping based on TTF-1 and *EGFR* mutation status

TTF-1-positive *EGFR*-positive cases (n=242)

Most of these cases were classified as AC (n=235). Other rare subtypes included one case each of invasive mucinous AC and

Table 2. Correlation between TTF-1 immunohistochemistry and EGFR mutations

TTF-1 IHC/ EGFR mutation status	No. (%)		Sensitivity (%)	Specificity (%)	PPV (%)	NPV (%)	Odds ratio (95% CI)	p-value
	Mutation detected	No mutation detected						
Total								<.001
Positive	242 (90.0)	456 (71.2)	90	29	35	87	3.61 (2.38–5.68)	
Negative	27 (10.0)	184 (28.8)						
Females								<.001
Positive	108 (89.3)	104 (72.2)	89	28	51	75	3.19 (1.66–6.53)	
Negative	13 (10.7)	40 (27.8)						
Males								<.001
Positive	134 (90.5)	352 (71.0)	91	29	28	91	3.91 (2.26–7.31)	
Negative	14 (9.5)	144 (29.0)						
Non-smokers								<.001
Positive	98 (95.1)	57 (75.0)	95	25	63	79	6.53 (2.33–18.43)	
Negative	5 (4.9)	19 (25.0)						
Smokers								.045
Positive	40 (77.0)	82 (62.6)	77	37	33	80	1.99 (0.95–4.16)	
Negative	12 (23.0)	49 (37.4)						
Common EGFR mutations								<.001
Positive	193 (91.5)	505 (72.3)	91	28	28	91	4.09 (2.46–6.83)	
Negative	18 (8.5)	193 (27.7)						
Uncommon/dual EGFR mutations								.098
Positive	49 (84.5)	649 (76.3)	84	24	7	96	1.69 (0.82–3.51)	
Negative	9 (15.5)	202 (23.7)						

TTF-1, thyroid transcription factor 1; EGFR, epidermal growth factor receptor; IHC, immunohistochemistry; PPV, positive predictive value; NPV, negative predictive value; CI, confidence interval.

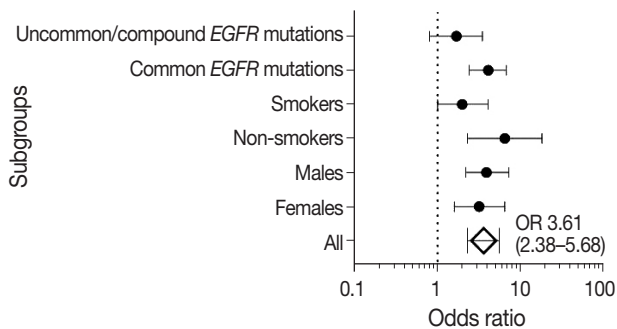


Fig. 2. Forest plot for correlation between thyroid transcription factor 1 and epidermal growth factor receptor (EGFR) mutation status in clinicopathological subgroups. Subgroup-specific odds ratios (ORs) are denoted by black dots (line width corresponding to 95% confidence intervals). Combined OR estimate for all patients is represented by a black diamond, where the width corresponds to 95% confidence intervals.

sarcomatoid carcinoma and five cases of adenosquamous carcinoma. The spectrum of EGFR mutations is shown in Fig. 3.

TTF-1–negative EGFR–positive cases (n=27)

Three cases were classified as invasive mucinous AC and one case as large cell carcinoma. Among the remaining cases, 16 cases classified as AC. EGFR mutations detected in these cases are

shown in Fig. 3. Among dual mutations, five were E20 T790M in combination with other activating mutations [exon 19 deletion (4) and exon 18 G719X (1)] and two were combination of exon 19 deletion with exon 21 L858R.

TTF-1–positive EGFR–negative cases (n=456)

The majority of this group showed AC (n = 435) with predominant patterns, as shown in Fig. 3. The following subtypes were identified: three cases of sarcomatoid carcinoma, four cases of invasive mucinous AC, and six cases of adenosquamous carcinoma. A few rare variants were noted (signet cell morphology in six, cribriform architecture in one, and hepatoid in one case).

TTF-1–negative EGFR–negative cases (n=184)

This group showed AC in 88 cases (Fig. 3), invasive mucinous AC in five cases, and adenosquamous carcinoma in three cases. One case showed AC with signet ring cell differentiation. A total of 87 cases with solid architecture and without evidence of glandular differentiation were classified as NSCLC, NOS.

Treatment details and survival analysis

Treatment details were available for 383 patients, where 305 patients received platinum-based chemotherapy and 78 patients

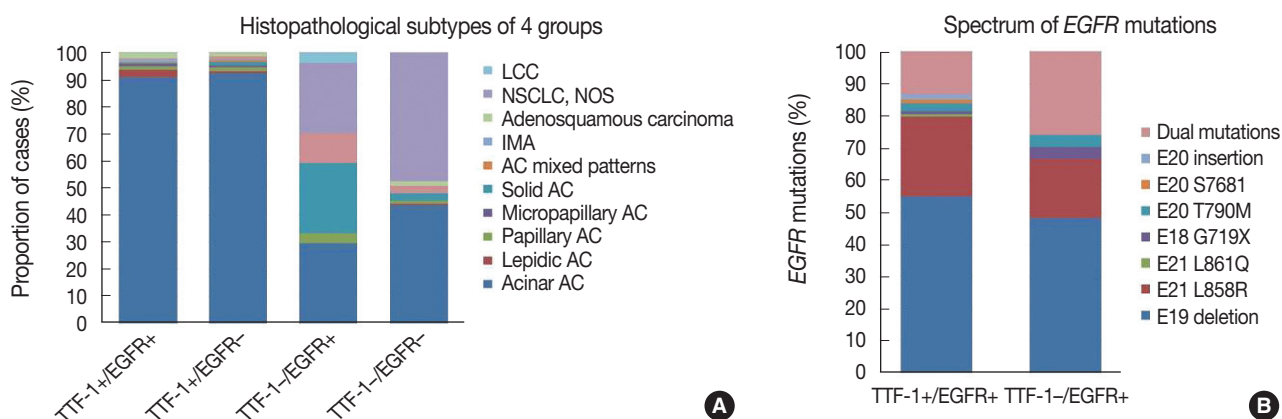


Fig. 3. Bar diagram showing histopathological subtyping of four groups based on thyroid transcription factor 1 (TTF-1) and epidermal growth factor receptor (*EGFR*) mutation status (A) and spectrum of *EGFR* mutations (B) in these groups. AC, adenocarcinoma; IMA, invasive mucinous adenocarcinoma; LCC, large cell carcinoma; NSCLC, non small cell lung carcinoma; NOS, not otherwise specified.

Table 3. Response to treatment with first-line *EGFR*-TKI treatment versus chemotherapy in the four patient groups

Parameter	TTF-1(+)/ <i>EGFR</i> mutant	TTF-1(+)/ <i>EGFR</i> wild type	TTF-1(-)/ <i>EGFR</i> mutant	TTF-1(-)/ <i>EGFR</i> wild type
Treatment, n (%)	114	83	14	38
1st line <i>EGFR</i> -TKI	49 (43.0)	0	4 (28.6)	0
1st line CT	65 (57.0)	83 (100)	10 (71.4)	38 (100)
First-line TKI, n (%)	49	0	4	0
Responders	35 (71.4)	0	3 (75.0)	0
Non-responders	14 (28.6)	0	1 (25.0)	0
First-line CT, n (%)	65	83	10	38
Responders	30 (46.2)	29 (34.9)	3 (30.0)	11 (28.9)
Non-responders	35 (53.8)	54 (65.1)	7 (70.0)	27 (71.9)
Odds ratio (TKI vs. CT)	2.9	1	6.9	1
95% CI	1.32–6.42	-	0.50–97.75	-
p-value	.008	-	.148	-
Median duration of follow-up (wk)	23.2	20.4	22.1	22.6
1-Year OS rate (%)	90.6	86.7	87.5	86.20
Median PFS (mo)	10.2	8.6	15.9	11.8
HR for PFS	1	1.07	0.83	0.92
95% CI	-	0.74–1.56	0.38–1.81	0.53–1.58
p-value	-	.694	.631	.754

EGFR, epidermal growth factor receptor; TKI, tyrosine kinase inhibitor; TTF-1, thyroid transcription factor 1; CT, chemotherapy; OS, overall survival; PFS, progression-free survival; HR, hazard ratio; CI, confidence interval.

received *EGFR*-TKI therapy as first-line treatment. A total of 29.2% of patients who received chemotherapy had *EGFR* mutated NSCLC, where treatment decisions were made before availability of *EGFR* mutation status results. Response to first-line therapy as per the Response Evaluation Criteria in Solid Tumors (RECIST) was available for 249 patients. Irrespective of TTF-1 and *EGFR* status, *EGFR*-TKI treatment resulted in superior response rates (71.7%, 38/53) compared to chemotherapy (37.2%, 73/196) (OR, 3.47; 95% CI, 1.84 to 6.53; 0.48, $p < .001$). For treatment response and survival analysis, patients were stratified into four groups based on TTF-1 expression and *EGFR* mutations: TTF-1+/*EGFR*+, TTF-1+/*EGFR*-,

TTF-1-/*EGFR*+, and TTF-1-/*EGFR*-. Response to treatment in these four groups is depicted in Table 3. Among *EGFR* wild type cases, patients receiving chemotherapy and harboring TTF-1-positive tumors responded better than patients with TTF-1-negative tumors. However, this difference did not reach statistical significance (OR, 1.32; 95% CI, 0.57 to 3.03; $p = .542$).

Survival data was available for 397 patients. The median duration of follow-up was 5.3 months. Overall, 35.01% of the patients experienced tumor progression during the course of therapy, and 7.6% of patients died. Patients with *EGFR* mutation and TTF-1 expression showed the best overall one-year survival rate (90.6%), while those who were double negative showed the

shortest (86.2%), although these differences did not reach statistical significance. Notably, the OS rates among patients with *EGFR* wild type tumors positive for TTF-1 (86.7%) and negative for TTF-1 (86.2%) were very similar. On the other hand, progression-free survival (PFS) was more homogenous and the PFS durations and hazard ratios for progression were comparable among the four groups.

DISCUSSION

Many observational studies over the years have reported strong positive correlation between TTF-1 expression and *EGFR* mutation status [17-22]. From a meta-analysis of 9,764 patients, Kim et al. [23] reported an OR of 5 between TTF-1 and *EGFR* mutations, and the OR was similar among European (OR, 4) and Asian (OR, 4) cohorts. The only previous study from India on a smaller South Indian cohort of 85 patients with advanced NSCLC reported an OR of 15 between TTF-1 and *EGFR* mutations [19]. In our single-institutional North Indian cohort of 909 patients, we found a similar strong correlation between TTF-1 and *EGFR* mutations (OR, 3.61) comparable to the results observed previously [17-23].

While *EGFR* mutations are more frequent in females and non-smokers [13,20,24], TTF-1 expression in NSCLC has shown inconsistent correlation with clinical parameters [21,25]. In the present study comprising predominantly of advanced stage non-squamous NSCLC diagnosed on small biopsies, TTF-1 expression was seen in approximately 77% of cases and was significantly more common among non-smokers but lacked association with age or sex, while *EGFR* mutations were detected in about 30% of all cases and significantly more frequent among females, non-smokers, and at early clinical stages. The frequency of *EGFR* mutation is similar to those reported in the Indian literature [13].

The correlation between TTF-1 and *EGFR* mutations in the present study remained significant irrespective of sex or smoking habit, indicating that the positive association is not merely due to increased prevalence of *EGFR* mutations in some demographic groups. Kim et al. [23] reported higher OR among females (OR, 4.87) compared to males (OR, 3.34), while Zhao et al. [21] reported lack of significant association between TTF-1 and *EGFR* mutations in males. In the present study, we observed comparable results between males and females, with ORs slightly higher among males (OR, 3.91) than females (OR, 3.19). Similarly, although non-smokers showed the highest ORs (6.53), there was significant positive correlation of TTF-1-*EGFR* among smokers as well, albeit with a lower OR of 1.99, as has been observed pre-

viously [21]. The degree of expression of TTF-1 (i.e., in > 50% of tumor cells or in 10%–50% of tumor cells) also does not appear to show significant difference in positive association with *EGFR* mutations, especially the exon 21 mutation [25]. In our study, we used a cutoff of > 5% tumor nuclei staining for positivity.

Morphological analysis of the TTF-1–negative cases harboring *EGFR* mutations showed histological evidence of AC in 70.4% of cases. On further subtyping of these cases, the association of *EGFR* mutations with predominant subtyping of the cases with TTF-1 negativity was akin to the published literature [26]. Acinar predominant AC showed higher propensity for *EGFR* mutations. A few cases of mucinous AC, which were mostly TTF-1 negative, also were positive for *EGFR* mutations.

The strength of correlation between TTF-1 and *EGFR* appears to vary according to type of mutation. While initial studies found significant association with exon 21 mutations and not with exon 19 deletion [21,25], others have found significant association of TTF-1 expression with both of these common mutations [23, 27,28]. We found strong association with both types of TKI-sensitive activating mutations, with an OR slightly higher for exon 19 deletion (OR, 4.63) than for exon 21 L858R (OR, 3.16). Interestingly, as has been observed in one previous study [27], we did not find significant correlation of TTF-1 with uncommon/dual mutations (OR, 1.69; $p > .05$).

The reported literature also states that more than 90% of *EGFR* mutated lung ACs are positive for TTF-1 [20-22,29]. In the present study, TTF-1 positivity showed 90% sensitivity for *EGFR* mutations, and the sensitivity was higher among males and non-smokers. Considering that TTF-1 positivity is not specific for *EGFR* mutations, with only 34.6% of all TTF-1 positive tumors harboring *EGFR* mutations, the NPV rather than the PPV becomes the important criterion in our assessment of the value of TTF-1 IHC as a screening tool for *EGFR* mutations. We found that TTF-1 IHC shows NPV of 87% for *EGFR* mutations, comparable to the NPVs of 88%–97% reported in published cohorts [17,19,23,30-32]. NPV varies with prevalence of *EGFR* mutations and sensitivity of TTF-1 IHC [33] and is likely to be higher in populations with lower prevalence of *EGFR* mutations, e.g., Western cohorts [30,31], and with the use of more sensitive TTF-1 IHC assays such as the SPT24 antibody clone (vs. 8G7G3/1) [9]. In line with these results, the highest NPVs in the present study were observed among males and among patients with uncommon/dual mutations.

EGFR mutation–specific antibodies have high specificity (94%–100%) and sensitivity (60%–100%) with high PPV and NPV for *EGFR* mutations compared to TTF-1 IHC. These an-

tibodies have shown high concordance rate compared to the gold standard molecular techniques [34]. However, its interpretation is highly variable due to differences in criteria for positivity, and its practical application is limited as these antibodies are meant to detect the two most common mutations (exon 19 deletion and exon 21 L858R), with significant numbers of false positive and false negative cases [34]. A molecular-based assay is needed to confirm *EGFR* mutation status, and screening of *EGFR* mutations by IHC seems not to be applicable [35]. TTF-1 is a diagnostic marker that can be used as a screening tool for *EGFR* mutations, but it cannot be replaced by *EGFR* mutation-specific antibodies.

The high NPV of TTF-1 for *EGFR* mutations has led some to suggest that patients with negative TTF-1 can be started on chemotherapy without MT in time- and resource-constrained settings [31]. We found, however, that approximately 13% of TTF-1–negative tumors harbored *EGFR* mutations, 50% of which were TKI-sensitive exon 19 deletion and exon 21 L858R mutations. Thus, until greater clarity is achieved on the tumor response rates of TTF-1–negative/*EGFR* mutant tumors for EGFR-TKI vs. chemotherapy, excluding patients for MT based on TTF-1 negativity should be discouraged.

Activating *EGFR* mutations are established as predictive biomarkers for TKI responsiveness in NSCLC and are known to confer a favorable prognostic effect on recurrence-free survival and OS irrespective of treatment arms [36,37]. Similarly, TTF-1 expression has been reported as a favorable prognostic biomarker in NSCLCs [11,12,38–40]. Transcriptional activation of TTF-1 has been shown to be necessary for *EGFR* downstream signaling in *EGFR* mutant tumors [41], and TTF-1 has been suggested to correlate with *EGFR* oncogene addiction in these tumors [28]. Tumors showing dual positivity for *EGFR* mutations and TTF-1 IHC have shown the best outcomes, while those negative for both carried the worst outcomes [12,21,28]. TTF-1 positive/*EGFR* wild type tumors and TTF-1 negative/*EGFR* mutant tumors show intermediate outcomes, with the former showing longer progression-free and OS than the latter in some studies [12,21,28]. In the present study, limited by availability of patient follow-up data, one-year OS was highest among TTF-1–positive/*EGFR* mutant cases and lowest for dual negative cases. TTF-1 positivity did not appear to alter the one-year OS or PFS among *EGFR* wild type tumors, as shown in previous studies [12,21,28]. The improved survival of TTF-1–positive/*EGFR* wild type cases can be attributed in part to the presence of other prognostically favorable alterations such as ALK or BRAF [42]; however, these alterations were not analyzed in our study.

TTF-1 positivity has been correlated with better response rates to chemotherapy [28,39,43] and EGFR-TKI [39], including some *EGFR* wild type tumors [28,38]. With regard to chemotherapy, we did observe slightly better response rates in TTF-1–positive/*EGFR* wild type cases compared to TTF-1–negative/*EGFR* wild type cases. However, with regard to EGFR-TKI, we found no differences in response rates between TTF-1–positive and TTF-1–negative *EGFR* mutant cases. None of our *EGFR* wild type cases received TKI treatment; hence, we could not analyze TKI response rates based on TTF-1 expression status. Nevertheless, our observations lack statistical significance, and observational trials including more patients are necessary to confirm or refute previous observations.

Conclusion

In agreement with previous studies, we found a strong positive correlation between TTF-1 expression and common *EGFR* mutations (exon 19 deletion and exon 21 L858R) in advanced lung AC. The strength of correlation was highest among non-smokers and lowest among those with uncommon/dual mutations. Despite a high NPV of TTF-1 IHC for *EGFR* mutations in the present study and previous studies, a better understanding of TTF-1–mediated modulation of treatment responses and its underlying biological mechanisms in *EGFR* mutant ACs is necessary before considering implementation of TTF-1 IHC as a surrogate for *EGFR* mutations.

Ethics Statement

Approval from the Institute Ethics Committee (IECPG-480/29.08.2016), All India Institute of Medical Sciences, was obtained to conduct this retrospective study on archival patient samples. Thus, the informed consent was waived due to the retrospective nature of this study.

Availability of Data and Material

The datasets generated or analyzed during the study are available from the corresponding author on reasonable request.

Code Availability

Not applicable.

ORCID

Tripti Nakra	https://orcid.org/0000-0001-9907-7531
Varsha Singh	https://orcid.org/0000-0002-2761-7102
Aruna Nambirajan	https://orcid.org/0000-0001-7589-537X
Prabhat Singh Malik	https://orcid.org/0000-0003-0205-8559
Anant Mohan	https://orcid.org/0000-0002-2383-9437
Deepali Jain	https://orcid.org/0000-0001-5315-9814

Author Contributions

Conceptualization: DJ. Data curation: TN, VS, AN, PSM, AM, DJ. Formal analysis: TN, VS, AN, DJ. Methodology: TN, VS, AN, DJ. Writing—original

draft: TN. Writing—review & editing: TN, VS, AN, PSM, AM, DJ. Approval of final manuscript: all authors.

Conflicts of Interest

D.J., a contributing editor of the *Journal of Pathology and Translational Medicine*, was not involved in the editorial evaluation or decision to publish this article. All remaining authors have declared no conflicts of interest.

Funding Statement

This work was supported by Department of Biotechnology (grant number N-1611) and The Lady Tata Memorial Trust (grant number N-1590).

References

1. Yatabe Y, Mitsudomi T, Takahashi T. TTF-1 expression in pulmonary adenocarcinomas. *Am J Surg Pathol* 2002; 26: 767-73.
2. Lau SK, Luthringer DJ, Eisen RN. Thyroid transcription factor-1: a review. *Appl Immunohistochem Mol Morphol* 2002; 10: 97-102.
3. Walia R, Jain D, Madan K, et al. p40 & thyroid transcription factor-1 immunohistochemistry: a useful panel to characterize non-small cell lung carcinoma-not otherwise specified (NSCLC-NOS) category. *Indian J Med Res* 2017; 146: 42-8.
4. Yatabe Y, Dacic S, Borczuk AC, et al. Best practices recommendations for diagnostic immunohistochemistry in lung cancer. *J Thorac Oncol* 2019; 14: 377-407.
5. Malik PS, Sharma MC, Mohanti BK, et al. Clinico-pathological profile of lung cancer at AIIMS: a changing paradigm in India. *Asian Pac J Cancer Prev* 2013; 14: 489-94.
6. Noronha V, Pinninti R, Patil VM, Joshi A, Prabhash K. Lung cancer in the Indian subcontinent. *South Asian J Cancer* 2016; 5: 95-103.
7. Lindeman NI, Cagle PT, Aisner DL, et al. Updated molecular testing guideline for the selection of lung cancer patients for treatment with targeted tyrosine kinase inhibitors: guideline from the College of American Pathologists, the International Association for the Study of Lung Cancer, and the Association for Molecular Pathology. *J Thorac Oncol* 2018; 13: 323-58.
8. Jain D, Iqbal S, Walia R, et al. Evaluation of epidermal growth factor receptor mutations based on mutation specific immunohistochemistry in non-small cell lung cancer: a preliminary study. *Indian J Med Res* 2016; 143: 308-14.
9. Inamura K. Update on immunohistochemistry for the diagnosis of lung cancer. *Cancers (Basel)* 2018; 10: 72.
10. Suda K, Mitsudomi T. Role of EGFR mutations in lung cancers: prognosis and tumor chemosensitivity. *Arch Toxicol* 2015; 89: 1227-40.
11. Berghmans T, Paesmans M, Mascaux C, et al. Thyroid transcription factor 1: a new prognostic factor in lung cancer: a meta-analysis. *Ann Oncol* 2006; 17: 1673-6.
12. Chung KP, Huang YT, Chang YL, et al. Clinical significance of thyroid transcription factor-1 in advanced lung adenocarcinoma under epidermal growth factor receptor tyrosine kinase inhibitor treatment. *Chest* 2012; 141: 420-8.
13. Nakra T, Mehta A, Bal A, et al. Epidermal growth factor receptor mutation status in pulmonary adenocarcinoma: multi-institutional data discussion at national conference of "Lung Cancer Management in Indian context". *Curr Probl Cancer* 2020; 44: 100561.
14. Singh V, Guleria P, Malik PS, et al. Epidermal growth factor receptor (EGFR), KRAS, and BRAF mutations in lung adenocarcinomas: a study from India. *Curr Probl Cancer* 2019; 43: 391-401.
15. Singh V, Nambirajan A, Malik PS, et al. Spectrum of uncommon and compound epidermal growth factor receptor mutations in non-small-cell lung carcinomas with treatment response and outcome analysis: a study from India. *Lung Cancer* 2020; 149: 53-60.
16. Travis WD, Brambilla E, Burke AP, Marx A, Nicholson AG. WHO classification of tumours of the lung, pleura, thymus and heart. 4th ed. Lyon: IARC Press, 2015.
17. Sheffield BS, Bosdet IE, Ali RH, et al. Relationship of thyroid transcription factor 1 to EGFR status in non-small-cell lung cancer. *Curr Oncol* 2014; 21: 305-8.
18. Carneiro JG, Couto PG, Bastos-Rodrigues L, et al. Spectrum of somatic EGFR, KRAS, BRAF, PTEN mutations and TTF-1 expression in Brazilian lung cancer patients. *Genet Res (Camb)* 2014; 96: e002.
19. Udupa KS, Rajendranath R, Sagar TG, Sundersingh S, Joseph T. Dual surrogate markers for rapid prediction of epidermal growth factor receptor mutation status in advanced adenocarcinoma of the lung: a novel approach in resource-limited setting. *Indian J Cancer* 2015; 52: 266-8.
20. Sun PL, Seol H, Lee HJ, et al. High incidence of EGFR mutations in Korean men smokers with no intratumoral heterogeneity of lung adenocarcinomas: correlation with histologic subtypes, EGFR/TTF-1 expressions, and clinical features. *J Thorac Oncol* 2012; 7: 323-30.
21. Zhao Q, Xu S, Liu J, et al. Thyroid transcription factor-1 expression is significantly associated with mutations in exon 21 of the epidermal growth factor receptor gene in Chinese patients with lung adenocarcinoma. *Onco Targets Ther* 2015; 8: 2469-78.
22. Gahr S, Stoehr R, Geissinger E, et al. EGFR mutational status in a large series of Caucasian European NSCLC patients: data from daily practice. *Br J Cancer* 2013; 109: 1821-8.
23. Kim HS, Kim JH, Han B, Choi DR. Correlation of thyroid transcription factor-1 expression with EGFR mutations in non-small-cell lung cancer: a meta-analysis. *Medicina (Kaunas)* 2019; 55: 41.
24. Travis WD, Noguchi M, Yatabe Y, et al. Adenocarcinoma. In: Travis WD, Brambilla E, Burke AP, Marx A, Nicholson AG. WHO classification of tumours of the lung, pleura, thymus and heart. 4th ed. Lyon: IARC Press, 2015; 46-51.
25. Shanzhi W, Yiping H, Ling H, Jianming Z, Qiang L. The relationship between TTF-1 expression and EGFR mutations in lung adenocarcinomas. *PLoS One* 2014; 9: e95479.
26. Dong YJ, Cai YR, Zhou LJ, et al. Association between the histological subtype of lung adenocarcinoma, EGFR/KRAS mutation status and the ALK rearrangement according to the novel IASLC/ATS/ERS classification. *Oncol Lett* 2016; 11: 2552-8.
27. Wei WE, Mao NQ, Ning SF, et al. An analysis of EGFR mutations among 1506 cases of non-small cell lung cancer patients in Guangxi, China. *PLoS One* 2016; 11: e0168795.
28. Park JY, Jang SH, Kim HI, et al. Thyroid transcription factor-1 as a prognostic indicator for stage IV lung adenocarcinoma with and without EGFR-sensitizing mutations. *BMC Cancer* 2019; 19: 574.
29. Vallee A, Sagan C, Le Loupp AG, Bach K, Dejoie T, Denis MG. Detection of EGFR gene mutations in non-small cell lung cancer: lessons from a single-institution routine analysis of 1,403 tumor samples. *Int J Oncol* 2013; 43: 1045-51.
30. Somaiah N, Fidler MJ, Garrett-Mayer E, et al. Epidermal growth factor receptor (EGFR) mutations are exceptionally rare in thyroid transcription factor (TTF-1)-negative adenocarcinomas of the lung. *Oncoscience* 2014; 1: 522-8.
31. Vincenten J, Smit EF, Vos W, et al. Negative NKX2-1 (TTF-1) as

- temporary surrogate marker for treatment selection during *EGFR*-mutation analysis in patients with non-small-cell lung cancer. *J Thorac Oncol* 2012; 7: 1522-7.
32. Jie L, Li XY, Zhao YQ, et al. Genotype-phenotype correlation in Chinese patients with pulmonary mixed type adenocarcinoma: relationship between histologic subtypes, TTF-1/SP-A expressions and *EGFR* mutations. *Pathol Res Pract* 2014; 210: 176-81.
 33. Lange K, Brunner E. Analysis of predictive values based on individual risk factors in multi-modality trials. *Diagnostics (Basel)* 2013; 3: 192-209.
 34. Gaber R, Goldmann T. Mini review: immunohistochemistry using *EGFR*-mutant specific antibodies in non-small cell lung carcinoma: accuracy and reliability. *J Cancer Treatment Diagn* 2018; 2: 17-23.
 35. Jiang G, Fan C, Zhang X, et al. Ascertain an appropriate diagnostic algorithm using *EGFR* mutation-specific antibodies to detect *EGFR* status in non-small-cell lung cancer. *PLoS One* 2013; 8: e59183.
 36. Gazdar AF. Activating and resistance mutations of *EGFR* in non-small-cell lung cancer: role in clinical response to *EGFR* tyrosine kinase inhibitors. *Oncogene* 2009; 28 Suppl 1: S24-31.
 37. Nan X, Xie C, Yu X, Liu J. *EGFR* TKI as first-line treatment for patients with advanced *EGFR* mutation-positive non-small-cell lung cancer. *Oncotarget* 2017; 8: 75712-26.
 38. Nakahara Y, Hosomi Y, Saito M, et al. Predictive significance of thyroid transcription factor-1 expression in patients with non-squamous non-small cell lung cancer with wild-type epidermal growth factor receptor treated with erlotinib. *Mol Clin Oncol* 2016; 5: 14-8.
 39. Sun JM, Han J, Ahn JS, Park K, Ahn MJ. Significance of thymidylate synthase and thyroid transcription factor 1 expression in patients with nonsquamous non-small cell lung cancer treated with pemetrexed-based chemotherapy. *J Thorac Oncol* 2011; 6: 1392-9.
 40. Tang X, Kadara H, Behrens C, et al. Abnormalities of the TTF-1 lineage-specific oncogene in NSCLC: implications in lung cancer pathogenesis and prognosis. *Clin Cancer Res* 2011; 17: 2434-43.
 41. Yamaguchi T, Yanagisawa K, Sugiyama R, et al. NKX2-1/TTF1/TTF-1-induced ROR1 is required to sustain *EGFR* survival signaling in lung adenocarcinoma. *Cancer Cell* 2012; 21: 348-61.
 42. Kret A, Clark C, Tennant S, Nicolson M, Kerr KM. Mutation analysis and association with TTF1 expression in lung non-squamous NSCLC. *Lung Cancer* 2015; 87(Suppl 1): S16.
 43. Gronberg BH, Lund-Iversen M, Strom EH, Brustugun OT, Scott H. Associations between TS, TTF-1, FR-alpha, FPGS, and overall survival in patients with advanced non-small-cell lung cancer receiving pemetrexed plus carboplatin or gemcitabine plus carboplatin as first-line chemotherapy. *J Thorac Oncol* 2013; 8: 1255-64.

Clinicopathologic features of cutaneous metastases from internal malignancies

Hyeong Mok Kwon^{1*}, Gyu Yeong Kim^{2**}, Dong Hoon Shin¹, Young Kyung Bae³

¹Department of Dermatology, Yeungnam University College of Medicine, Daegu;

²Yeungnam University College of Medicine, Daegu;

³Department of Pathology, Yeungnam University College of Medicine, Daegu, Korea

Background: Cutaneous metastasis (CM) is the spread of cancer cells from a primary site to the skin and is rarely the first sign of silent cancer. We investigated the clinicopathological characteristics of CM from internal malignancies in Korean patients treated at our institution over 20 years. **Methods:** The clinicopathological findings of 112 patients (62 females, 50 males) with CM diagnosed at Yeungnam University Hospital between 2000 and 2020 were retrospectively reviewed. **Results:** Mean patient age was 58.6 years (range, 26 to 87 years), and the most common primary cancer site was breast (74.2%) in women and lung (36.0%) in men. Ninety-six patients (85.7%) presented with CM after primary tumor diagnosis. CM from the lung or biliary tract usually occurred within 2 years of primary tumor diagnosis, whereas metastases from the breast and kidney occurred several years later. The chest, abdomen, and scalp were common sites of CM. Breast cancer usually metastasized to chest skin, while gastrointestinal tract cancers commonly metastasized to the abdomen. The scalp was a common location for CM from various tumors. The most common dermatologic presentations were nodules and masses. Immunohistochemical studies helped identify underlying malignancies when primary tumors were unknown. **Conclusions:** The relative frequency of CM parallels the overall incidence of primary malignant tumors, and CMs usually occur at anatomic sites close to the primary tumor. CM can be diagnosed based on clinical, radiological, and histological features; however, immunohistochemical study is required in some cases.

Key Words: Carcinoma; Metastasis; Skin, Immunohistochemistry

Received: February 25, 2021 **Revised:** April 22, 2021 **Accepted:** May 24, 2021

Corresponding Author: Young Kyung Bae, MD, PhD, Department of Pathology, Yeungnam University College of Medicine, 170 Hyeonchung-ro, Nam-gu, Daegu 42415, Korea
 Tel: +82-53-640-6755, Fax: +82-53-622-8432, E-mail: ykbae@ynu.ac.kr

*Hyeong Mok Kwon and Gyu Yeong Kim contributed equally to this work.

**Kyu Young Kim is currently an intern at Samsung Medical Center.

Cutaneous metastases (CMs) from internal malignancies are considered a sign of systemic cancer spread. However, CM can emerge at the same time as the internal malignancy and in rare cases can be the first clinical presentation of occult or unknown primary tumor. While single case reports of CM from various cancers have been reported in Korea [1-9], systematic reviews on the common clinical and morphological presentations and histological subtypes of CM are rare. A recent Korean study reviewed data from 401 patients with CM and reported that the two most common primary cancers were breast and lung cancer [10], and this finding was consistent with those of studies conducted in other ethnic groups [11-15].

This study was undertaken to document the clinicopathologic

features of CM from internal malignancies and primary tumor types, anatomic locations, times between primary tumor diagnoses and development of CMs, and immunohistochemical results of metastatic carcinomas from an unknown origin at the time of CM diagnosis. In addition, we sought to determine whether the frequency of CM reflects the incidence of corresponding primary tumors in Korean patients.

MATERIALS AND METHODS

Case selection

Consecutive cases with cutaneous metastatic carcinoma biopsied at Yeungnam University Medical Center (YUMC) between

January 2000 and July 2020 were selected for this study. CM presented as a tumor center in the dermis or subcutaneous tissue, and no features suggestive of primary neoplasm derived from skin appendages. When a patient had multiple synchronous CMs, the largest lesion was considered representative. Metastases from skin malignancies (melanomas or carcinomas), mammary Paget disease, sarcomas, hematolymphoid neoplasms, and/or carcinomas located in a biopsy scar or surgical wound site were excluded.

All histologic findings of hematoxylin and eosin- and immunohistochemically-stained slides of skin and corresponding primary tumors were reviewed. Medical records and pathology reports were reviewed for information about sites and dates of diagnoses of primary tumors and clinical presentations of CM. Anatomic locations of CM were classified into scalp, face, neck, chest, abdomen, back, perineum, upper extremity, or lower extremity. For cases with multiple CMs, anatomic location was categorized based on the largest lesion. Multifocality was defined as presence of multiple CMs in two or more anatomic locations.

Statistical analysis

Statistical analysis was performed using SPSS ver. 25.0 for Windows (IBM Corp., Armonk, NY, USA). The difference of time interval between primary tumor diagnosis and occurrence of CM according to tumor stage or histologic features was determined using Mann-Whitney or Kruskal-Wallis test followed by the Bonferroni method. Statistical significance was accepted for p -values $< .05$.

RESULTS

Incidence

A total of 112 patients (62 females, 50 males) with CM was included in this study. For diagnosis of CM, 79 (69.9%) patients underwent punch biopsy, and 34 (30.1%) underwent excision. Mean age at CM diagnosis was 58.6 years (median, 59 years; range, 26 to 87 years), and the mean age of women and men was 55.7 and 62.3 years, respectively. Primary tumor was confirmed histologically in 99 patients by surgical resection (64 patients at Yeungnam University Medical Center and 12 patients at other hospitals) or biopsy (23 patients). In 10 patients, presence of primary tumor was confirmed radiologically. Primary tumor was undetermined in two patients despite extensive work-up, and one patient refused further study. Breast (42.0%) was the most common primary cancer site, followed by lung (18.8%), stomach (10.7%), colon and rectum (5.4%), biliary tract (4.5%),

kidney (3.6%), and liver (2.7%) (Table 1). Breast cancer (74.2%) was the most common primary cancer in female patients, followed by stomach (6.5%), colorectal (4.8%), and lung (4.8%) cancer. In male patients, the most common primary cancer sites were lung (36.0%), stomach (16.0%), biliary tract (8.0%), and kidney (8.0%) (Table 1). Tumor stage, either pathologic or clinical, was available in 103 patients and distributed as follows:

Table 1. Underlying primary tumors according to sex and stage

Primary malignancy	Stage	Total	Female	Male
Breast		47 (42.0)	46 (74.2)	1 (2.0)
	I	5	5	0
	II	15	15	0
	III	22	22	0
	IV	4	4	0
	Unknown	1	0	1
Lung		21 (18.8)	3 (4.8)	18 (36.0)
	I	1	1	0
	II	1	0	1
	III	4	0	4
	IV	15	2	13
Stomach		12 (10.7)	4 (6.5)	8 (16.0)
	II	1	1	0
	III	8	2	6
	IV	3	1	2
Colorectum		6 (5.4)	3 (4.8)	3 (6.0)
	III	5	3	2
	IV	1	0	1
Biliary tract		5 (4.5)	1 (1.6)	4 (8.0)
	III	1	0	1
	IV	3	0	3
	Unknown	1	1	0
Kidney		4 (3.6)	0	4 (8.0)
	IV	2	0	2
	Unknown	2	0	2
Liver		3 (2.7)	1 (1.6)	2 (4.0)
	II	1	1	0
	III	1	0	1
	Unknown	1	0	1
Salivary gland		2 (1.8)	0	2 (4.0)
	III	1	0	1
	IV	1	0	1
Esophagus	Unknown	1 (0.9)	0	1 (2.0)
Lacrimal gland	II	1 (0.9)	0	1 (2.0)
Larynx	IV	1 (0.9)	0	1 (2.0)
Pancreas	IV	1 (0.9)	1 (1.6)	0
Paranasal sinus	IV	1 (0.9)	0	1 (2.0)
Prostate	IV	1 (0.9)	0	1 (2.0)
Thyroid	I	1 (0.9)	1 (1.6)	0
Tongue	III	1 (0.9)	1 (1.6)	0
Tonsil	IV	1 (0.9)	0	1 (2.0)
Unknown	Unknown	3 (2.7)	1 (1.6)	2 (4.0)
Total		112 (100)	62 (100)	50 (100)

Values are presented as number (%).

stage I in 7 (6.8%), stage II in 19 (18.4), stage III in 43 (41.7%), and stage IV in 34 (33.0%) patients. Six patients had no record of tumor stage (five patients underwent surgery at other hospitals and stage work-up was not performed in one patient), and primary tumors were unknown in three patients. Tumor stage according to primary site is listed in Table 1.

Histologic features of primary tumors

The histologic types of common primary tumors with CM are listed in Table 2. Primary breast cancers were invasive carcinoma of no special type (invasive ductal carcinoma) in 42 (89.4%) patients, invasive micropapillary carcinoma in two (4.3%), invasive lobular carcinoma in one (2.1%), metaplastic carcinoma

Table 2. Histologic type of most frequent primary tumors

Primary site	No.	Histologic type	No.
Breast	47	Invasive carcinoma, no special type	42
		Invasive micropapillary carcinoma	2
		Invasive lobular carcinoma	1
		Metaplastic carcinoma	1
		Unknown	1
Lung	21	Squamous cell carcinoma	10
		Adenocarcinoma	10
		Small cell carcinoma	1
Stomach	12	Adenocarcinoma	10
		Mucinous carcinoma	1
		Signet ring cell carcinoma	1
Colorectum	6	Adenocarcinoma	4
		Invasive micropapillary carcinoma	1
		Signet ring cell carcinoma	1

in one (2.1%), and unknown in one (2.1%). Breast molecular subtypes were luminal, triple-negative, human epidermal growth factor receptor 2-positive, and unknown in 21 (44.7%), 13 (27.7%), eight (17.0%), and five (10.6%) patients, respectively. Histologic grades were 1 in two (4.3%), 2 in 10 (21.3%), 3 in 30 (63.8%), and unknown in five (10.6%) patients. Presence or absence of lymphovascular invasion was available in 39 patients, 32 (82.1%) of whom showed lymphovascular invasion.

Of the 21 lung cancers with CM, 10 (47.6%) were squamous cell carcinomas, 10 (47.6%) were adenocarcinomas, and one (4.8%) was small cell carcinoma (Fig. 1). Of the 12 gastric adenocarcinomas with CM, eight (66.7%) were poorly differentiated, and the other four were either well differentiated, moderately differentiated, mucinous, or signet ring cell morphologies. For the six colorectal cancers, four were moderately differentiated adenocarcinomas, one was micropapillary carcinoma, and one was signet ring cell carcinoma.

All metastatic renal cell carcinomas were of the clear cell type (Fig. 2). The unusual CMs were from invasive ductal carcinoma from the lacrimal gland, adenoid cystic carcinoma from the submandibular gland, and papillary carcinoma from the thyroid gland. Four cases of squamous cell carcinoma of the esophagus, paranasal sinus, tongue, or tonsil developed CM.

Clinical presentation of CMs

Among the 112 patients, 96 (85.7%) presented with CM after primary tumor diagnosis (mean, 41.8 months; range, 1 to 325 months). In 12 patients (10.7%), CM was found at the same time as internal malignancies, and in four patients (3.6%), CM was the first sign of internal malignancy. Time between diagnosis of primary tumors and CM was greater for patients with

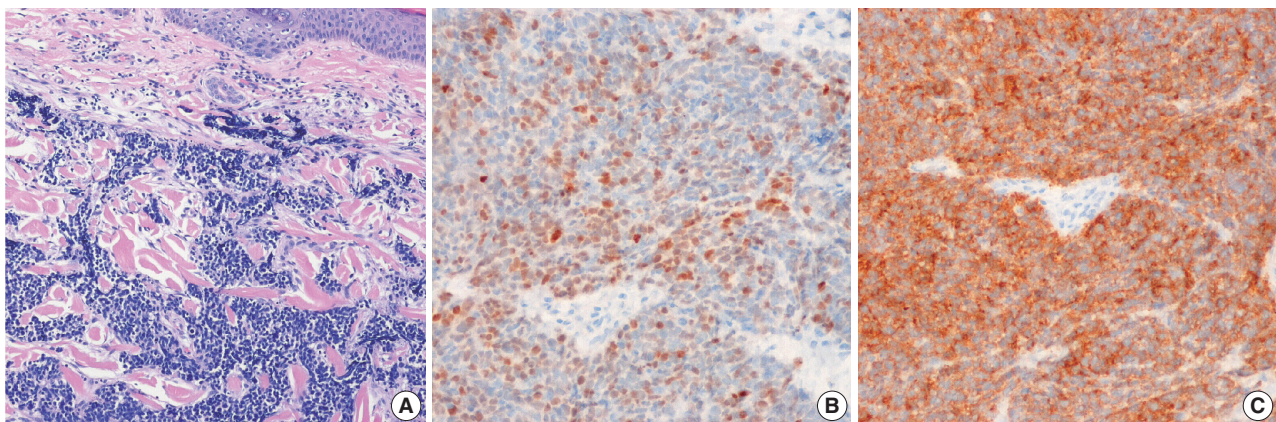


Fig. 1. Metastatic small cell carcinoma of the lung. (A) Tumor cells infiltrated dermal collagen bundles and were diffusely positive for thyroid transcription factor 1 (B) and synaptophysin (C).

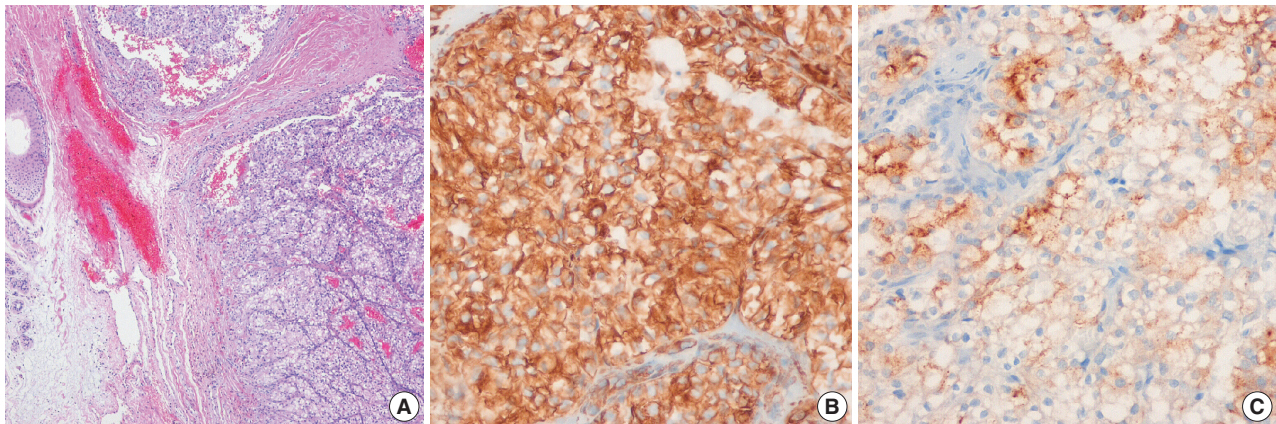


Fig. 2. Metastatic renal cell carcinoma. (A) The tumor was clear cell type, and tumor cells were positive for vimentin (B) and renal cell carcinoma (C).

breast or kidney cancer than for those with lung or biliary tract cancer (Table 3, Fig. 3). In breast cancer patients, tumor stage was significantly associated with time interval between primary tumor diagnosis and CM ($p < .001$). Stage II or III tumors showed a longer time interval between primary tumor diagnosis and CM than did stage IV tumors (Table 3). However, there was no statistical difference in time interval between diagnosis of breast cancer and CM according to presence or absence of lymphovascular invasion or histologic grade of the primary tumor (Supplementary Table S1). Due to the small number of patients, the same statistical analysis could not be performed for other primary tumors.

Forty-nine patients (43.4%) had multiple CM lesions, and 12 (10.7%) presented with multiple CMs at two or more anatomic locations (Table 4). About 70% of the 112 patients were asymptomatic, but others experienced tenderness (16.1%), oozing (6.3%), and pain (5.4%). The most common dermatologic presentations of CM were nodules (53.6%) or masses (19.6%), followed by papules (12.5%), plaques (9.8%), or ulcers (2.7%) (Table 4).

The common sites of CM were chest (35.7%), head and neck (34.8%; scalp, 16.1%; neck, 9.8%; face, 8.9%), and abdomen (17.9%) (Fig. 4). Breast cancer usually metastasized to the chest, lung cancer to the head and neck or chest, and gastrointestinal tract cancer to the abdomen or scalp.

Immunohistochemical markers that define primary sites

The primary tumor was unable to be confirmed histologically in 12 patients with CM. In these cases, primary tumor sites were identified based on immunohistochemical staining results of skin lesions and radiologic findings (Table 5).

Five patients had lung masses revealed by chest computed

tomography (CT) or positron emission tomography (PET)-CT. In four of these cases, the CM was adenocarcinomas; the other was squamous cell carcinoma. In all five patients, CMs were positive for cytokeratin 7 (CK7), four adenocarcinomas were negative for CK20, and two patients were positive for thyroid transcription factor 1 (TTF-1). Metastatic squamous cell carcinoma was positive for p63 and p40.

One patient had metastatic adenocarcinoma masses of the face and liver by PET-CT. Tumor cells in this patient were positive for CK7, CK19, and CK20 and negative for TTF-1 and caudal-type homeobox 2 (CDX2), which suggested biliary tract origin (Fig. 5). Interestingly, one female patient with metastatic carcinoma of the left chest skin was suspected of having breast cancer because tumor cells were positive for mammaglobin and progesterone receptor (PR) but negative for estrogen receptor (ER) and gross cystic disease fluid protein 15 (GCDFP-15). PET-CT of this patient depicted hypermetabolic areas in the left breast, axillary lymph nodes, and multiple bones.

One male patient with metastatic adenocarcinoma of the upper extremity skin had a prostatic mass and multiple lung and bone lesions. Tumor cells in a lung mass biopsy were positive for P504S but negative for TTF-1, although the metastatic adenocarcinoma was negative for P504S and prostatic specific antigen. Another patient with metastatic carcinoma in the abdominal skin that was morphologically consistent with clear renal cell carcinoma had a hypermetabolic mass on PET-CT in the right kidney. Tumor cells from the skin lesion were positive for paired box gene 8 (PAX8). In one female patient with metastatic adenocarcinoma of the scalp, PET-CT depicted multiple masses in the liver, adrenals, kidneys, ovaries, and omentum. Tumor cells from the scalp were positive for CK7, CK19, and PAX8 but negative for CK20, CDX2, TTF-1, WT-1, ER, and PR. In this patient,

Table 3. Time interval between diagnosis of primary malignancy and cutaneous metastasis in patients who developed cutaneous metastasis after diagnosis of primary malignancy

Primary site	Stage	No.	Time interval between diagnosis of primary tumor and occurrence of cutaneous metastasis ^a (mo)
Breast		46	1–325 (58.9±60.5)
	I	5	25–149 (84.0±58.4)
	II	15	11–188 (71.9±51.4)
	III	22	1–325 (48.1±70.1)
	IV	3	24–53 (36.0±15.1)
	Unknown	1	42
Lung		14	1–29 (12.5±9.5)
	I	1	3
	II	1	13
	III	4	2–26 (15.8±10.4)
	IV	8	1–29 (12.0±10.2)
Stomach		11	1–47 (20.8±17.9)
	II	1	31
	III	8	1–47 (19.9±19.1)
	IV	2	3–36
Colorectum	III	5	3–58 (26.4±21.5)
Kidney		4	4–180 (61.0±80.4)
	IV	2	4–35
	Unknown	2	25–180
Biliary tract		3	3–23 (13.3±10.0)
	III	1	23
	IV	1	3
	Unknown	1	14
Liver		3	
	II	1	64
	III	1	87
	Unknown	1	-
Salivary gland		2	
	III	1	30
	IV	1	25
Esophagus	Unknown	1	7
Lacrimal gland	II	1	39
Larynx	IV	1	30
Pancreas	IV	1	9
Paranasal sinus	IV	1	2
Thyroid	I	1	120
Tongue	III	1	17
Tonsil	IV	1	11
Total		96	1–325 (41.8±50.6)

^aValues are presented as range (mean±standard deviation).

a primary tumor originating from the ovary or biliary tract was suspected but not confirmed. Despite extensive work-up, primary cancer was not determined in one patient. Another patient refused further work-up aimed at identifying the primary site.

DISCUSSION

In this study, we retrospectively reviewed 112 cases with CM

from internal malignancies in patients treated over 20 years at our institution. Common primary tumor sites differed in female and male patients. Breast and stomach cancer were the most common primary tumors in female patients, while lung and stomach cancers were most common in male patients. Considering that the numbers of breast, gastric, lung, and colorectal cancer patients newly registered at our institution over the past 20 years (January 2000 to December 2020) were 10,890, 9,968, 8,409, and 8,188 patients, respectively, the incidence of CM might reflect the overall incidence of cancers. According to Korean cancer statistics for 2017 [16], the most common cancer sites were the stomach (12.8%), colorectum (12.1%), lung (11.6%), thyroid (11.3%), breast (9.6%), liver (6.6%), prostate (5.5%), pancreas (3%), biliary tract and gallbladder (2.9%), and kidney (2.3%). The most common sites by sex were breast (20.3%), thyroid (18.3%), colorectum (10.4%), and stomach (8.9%) in women and stomach (16.3%), lung (15.3%), colorectum (13.6%), and prostate (10.5%) in men. These results indicate that the incidence of CM is proportional to the overall incidence of cancer, with exceptions that lung cancer tended to metastasize more easily than stomach cancer, and that thyroid and prostate cancers rarely gave rise to skin metastases. In addition, the frequency of CM from breast cancer corresponded to the frequency of histologic and molecular subtypes of primary breast cancer. Previous studies on different ethnic groups, including a Korean study, reported similar results regarding correspondence between CM frequency and the overall incidence of primary malignant tumors [10,12–15,17,18].

However, time between primary diagnosis and development of CM varied considerably and depended on primary tumor type. For example, CM from lung and biliary tract cancers usually occurred within two years of primary diagnosis, whereas CM from breast cancer and hepatocellular and renal cell carcinoma occurred several years after primary diagnosis. Choi et al. [10] also reported that CM occurred several years (mean, 48.2 months) after diagnosis of hepatocellular carcinoma, while lung and pancreatic cancers metastasized to the skin within one year of primary diagnosis. Furthermore, it was reported in a Taiwanese study that CM occurred early in lung cancer (mean, 15.7 months; range, 1 month to 5 years) but several years after breast cancer excision (mean, 47.2 months; range, 1 month to 10 years) [13].

With regard to metastatic sites, any skin region might be involved, but the chest, head and neck, and abdomen were most affected by CM. In particular, breast cancer usually metastasized to the chest, whereas gastrointestinal tract cancers commonly metastasized to abdominal skin. These results support the notion that CM is usually found in an anatomic location close to the primary

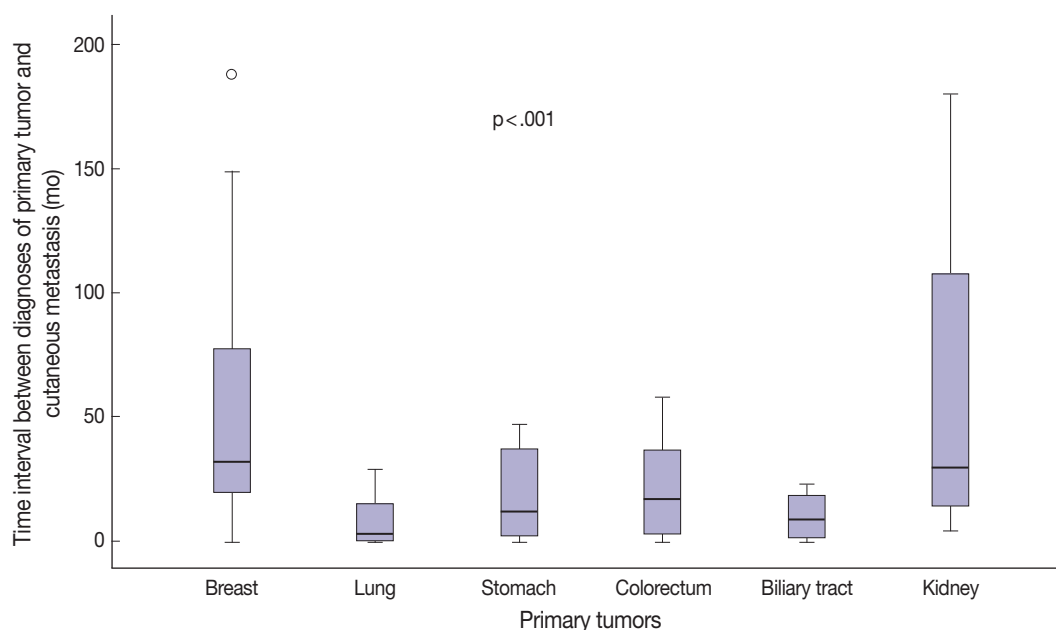


Fig. 3. Comparison of time interval between diagnosis of primary tumor and occurrence of cutaneous metastasis according to primary tumor site.

Table 4. Clinical presentation of cutaneous metastasis

Clinical presentation	No. of cases (%)
No. of lesions	
Single	63 (56.3)
Multiple	49 (43.8)
Focality	
Unifocal	100 (89.3)
Multifocal	12 (10.7)
Symptom	
Asymptomatic	78 (69.6)
Tenderness	18 (16.1)
Oozing	7 (6.3)
Pain/Tenderness	4 (3.6)
Pain	2 (1.8)
Itching	2 (1.8)
Bleeding	1 (0.9)
Dermatologic presentation	
Nodule	60 (53.6)
Mass	22 (19.6)
Papule	14 (12.5)
Plaque	11 (9.8)
Ulcer	3 (2.7)
Patch	1 (0.9)
Vesicle	1 (0.9)

tumor, presumably because epithelial cancer cells predominantly disseminate via lymphatic channels. However, some CMs occurred in regions distant from the primary tumors; for example, the scalp was a common CM location for various tumors. The possible mechanism as to why the scalp is a common destination

for CM is thought to be due to its high vascularity [19].

It has been reported that 2.9% to 21% of CMs are found prior to diagnosis of primary cancers [11,12]. In the present study, 11.5% of patients developed CM as the first manifestation of internal malignancy. In this clinical setting, pathologists can use morphologic examinations and immunohistochemical studies to identify underlying primary tumors and provide valuable information for subsequent clinical workup. In metastatic adenocarcinoma, positivity for CK7, TTF-1, and napsin A and negativity for CK20 indicate a pulmonary origin. Squamous cell carcinoma of the lung typically exhibits CK5/6 and p40 positivity, and small cell lung carcinoma is positive for TTF-1 but negative for CK7 and CK20 [20]. Metastatic small cell carcinoma of the lung and primary cutaneous Merkel cell carcinoma must be precisely differentiated as they share a neuroendocrine origin and have similar histologic features. CK20 and TTF-1 have been routinely used in this context because small cell lung carcinoma is usually CK20 negative but TTF-1 positive, while primary cutaneous Merkel cell carcinoma is CK20 positive (characteristically paranuclear dotlike) and TTF-1 negative in most cases [21,22]. However, about 10% of Merkel cell carcinomas are positive for TTF-1 and negative for CK20 [23].

The histologic features of metastatic breast cancer can be similar to those of primary cutaneous adnexal malignancies, and both are positive for CK7 and negative for CK20. ER, PR, mammaglobin, and GCDFP-15 are useful markers of breast origin

[21,24,25], but only 50% of metastatic breast carcinomas are ER positive and 65%–70% are mammaglobin positive. Gynecological malignancies occasionally exhibit ER and/or PR positivity

[26–28]. These findings indicate that immunohistochemical results should be considered alongside clinical and radiological findings. For gastrointestinal tract malignancies, CK7, CK20, and

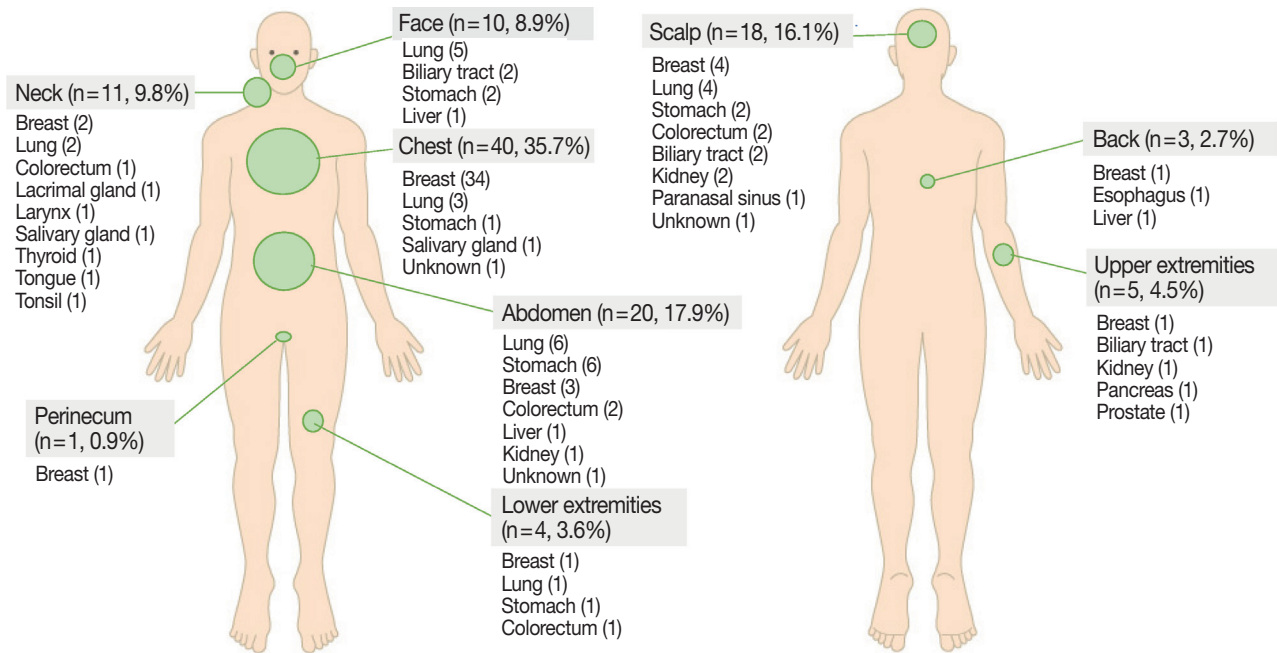


Fig. 4. Incidence of cutaneous metastasis by anatomic location and primary tumor site.

Table 5. Clinicopathologic features of cases with cutaneous metastasis in which the primary tumor was not confirmed histologically

No.	Age (yr)	Sex	Cutaneous metastasis			Radiologic findings	Suggested primary site
			Location	Histology	Immunohistochemical results		
1	62	M	Axilla	Adenocarcinoma	TTF-1+, CK7+, CK20-, CDX2-	Multiple masses in lungs, liver, bone, and LNs on PET-CT	Lung
2	61	M	Abdomen	Adenocarcinoma	TTF-1-, CK7+, CK20-, Napsin A-	Lung mass on CT	Lung
3	58	M	Scalp, Abdomen	Adenocarcinoma	TTF-1-, CK7+, CK20-	Lung mass on CT, suspicious metastases to hilar, subaortic, subcardinal LNs, and both adrenals	Lung
4	55	M	Scalp	Adenocarcinoma	TTF-1+, CK7+, CK20-	Lung mass on PET-CT, metastases to multiple LNs and bones	Lung
5	76	M	Chest	Squamous cell carcinoma	CK7 focal+, p63+, p40+	Lung mass on CT	Lung
6	68	M	Face	Adenocarcinoma	CK7+, CK19+, CK20+, TTF-1-, CDX2-	Liver masses on PET-CT without histologic confirmation	Biliary tract
7	58	F	Chest	Carcinoma	ER-, PR+, Mammaglobin+, GCDFP-15-	Left breast mass on PET-CT, metastases to bone and axillary LNs	Breast
8	72	M	Upper extremity	Adenocarcinoma	PSA-, P504S- Lung mass: TTF-1-, c-Met+, CK7+, P504S+, ERG-	Prostatic mass on PET-CT, multiple lung masses, metastases to multiple bones	Prostate
9	74	M	Abdomen	Renal cell carcinoma	PAX8+, RCC-	Right kidney mass on PET-CT, metastases to multiple bones	Kidney
10	36	F	Scalp	Adenocarcinoma	CK7+, CK19+, PAX8+, CK20-, CDX2-, TTF-1-, WT-1-, ER-, PR-	Multiple masses in liver, adrenals, kidneys, ovaries, and omentum on PET-CT	Unknown
11	67	M	Axilla	Carcinoma	GATA3+, CK7-, CK20-, PSA-, TTF-1-, CDX2-	No suggested primary tumor on PET-CT	Unknown
12	57	M	Trunk	Adenocarcinoma	CK7+, CK19+, CK20-, CDX2 focal+, TTF-1-	No further study	Unknown

M, male; TTF-1, thyroid transcription factor 1; CK, cytokeratin; LN, lymph node; PET-CT, positron emission tomography-computed tomography; ER, estrogen receptor; PR, progesterone receptor; GCDFP-15, gross cystic disease fluid protein 15; PSA, prostate specific antigen; RCC, renal cell carcinoma.

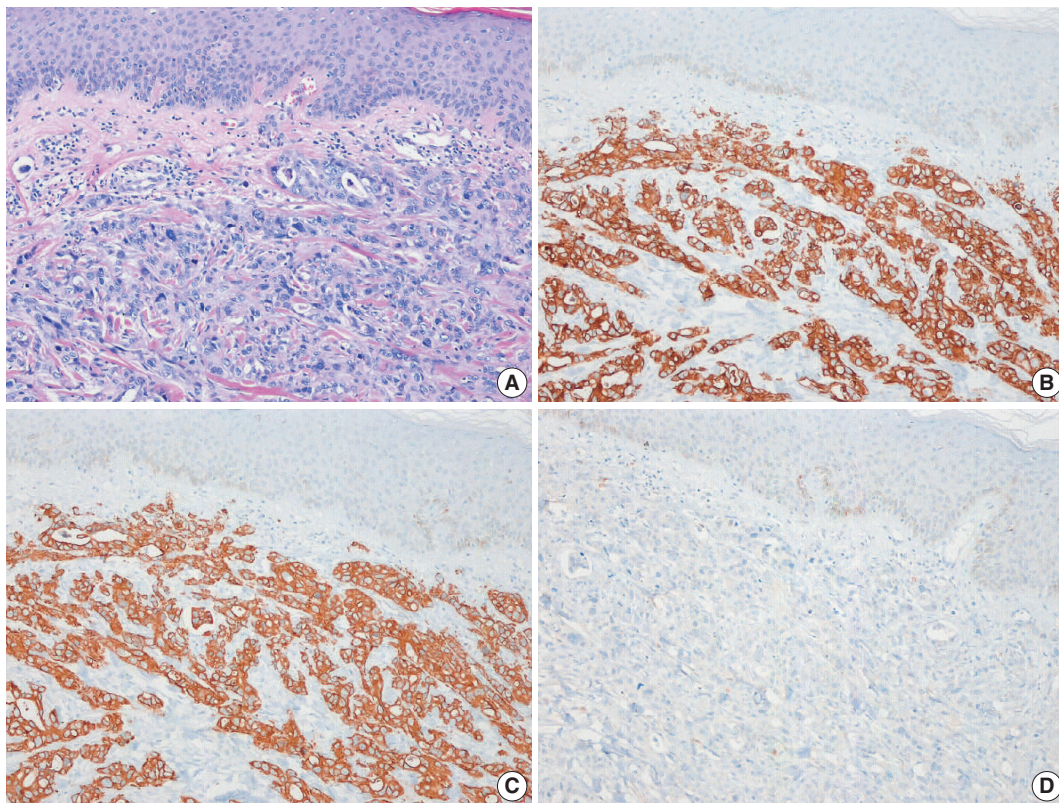


Fig. 5. Representative histologic features and immunohistochemical staining results for metastatic adenocarcinoma of the face. (A) Poorly differentiated adenocarcinoma was mainly located in the dermis. Tumor cells were positive for cytokeratin (CK) 7 (B) and CK19 (C) but negative for thyroid transcription factor 1 (D). Although no primary tumor was confirmed histologically, the metastatic adenocarcinoma was considered of biliary tract origin.

CDX2 can help determine tumor origin. Gastric cancer is generally positive for CK7 and CK20, whereas colorectal cancer is negative for CK7 and positive for CK20 and CDX2. In hepatocellular carcinoma, hepatocyte paraffin 1 (HepPar-1), arginase 1, and α -fetoprotein can help confirm diagnosis [20,29]. Renal cell carcinoma shows negativity for CK7 and CK20 and positivity for renal cell carcinoma marker and PAX8 [20]. Gynecological cancers exhibit a variety of immunohistochemical profiles and are generally positive for cancer antigens 125, CK7, and CK20 [21], though ovarian cancer and endometrial cancer are also PAX8 positive [30].

In conclusion, although CMs are rarely observed after diagnosis of primary internal malignancies, they occur at rates that are approximately proportional to the frequency of the primary tumor. The most common primary cancer sites in this retrospective study was breast in women and lung in men. Lung and biliary tract cancers usually metastasized to the skin within 2 years of primary cancer diagnosis, whereas metastases from breast cancer, hepatocellular carcinoma, and renal cell carcinoma occurred several years

later. Although metastasis to the skin can occur at any location, the chest, head and neck, and abdomen were most commonly affected. CM can be diagnosed by clinical, radiological, and histological examinations, although in some cases immunohistochemical studies are required.

Supplementary Information

The Data Supplement is available with this article at <https://doi.org/10.4132/jptm.2021.05.24>.

Ethics Statement

This study was approved by the Institutional Review Board (IRB) of Yeungnam University Medical Center (YUMC2020-06-092), with a waiver of the requirement for informed consent.

Availability of Data and Material

The data that support the findings of this study are available from the corresponding author upon reasonable request.

Code Availability

Not applicable.

ORCID

Hyeong Mok Kwon <http://orcid.org/0000-0002-1557-1370>
 Gyu Yeong Kim <http://orcid.org/0000-0003-4062-3184>
 Dong Hoon Shin <http://orcid.org/0000-0003-3130-3699>
 Young Kyung Bae <http://orcid.org/0000-0002-6689-9413>

Author Contributions

Conceptualization: YKB. Data curation: HMK, GYK. Formal analysis: GYK, YKB. Funding acquisition: YKB. Investigation: YKB, DHS. Methodology: HMK, GYK, DHS, YKB. Project administration: YKB. Validation: YKB. Writing—original draft: HMK, GYK, YKB. Writing—review & editing: HMK, GYK, DHS, YKB. Approval of final manuscript: HMK, GYK, DHS, YKB. Approval of final manuscript: all authors.

Conflicts of Interest

The authors declare that they have no potential conflicts of interest.

Funding Statement

This work was supported by the 2020 Yeungnam University Research Grant (220A480010).

References

- Moon JI, Park JY, Jeon TJ, et al. Non-umbilical cutaneous metastasis of pancreatic adenocarcinoma as the first clinical manifestation: a case report. *Korean J Gastroenterol* 2016; 68: 221-4.
- Kwon MJ, Ryu SH, Jo SY, et al. A case of hepatocellular carcinoma presenting as a gingival mass. *Korean J Gastroenterol* 2016; 68: 321-5.
- Song YW, Kim WS, Yun GY, et al. A case of early gastric cancer with nodular tumor-like scalp metastasis. *Korean J Gastroenterol* 2016; 68: 36-9.
- Yang HJ, Kang SY. Cutaneous metastatic renal cell carcinoma to the scalp. *Arch Craniofac Surg* 2019; 20: 392-6.
- Kim JH, Kim MJ, Sim WY, Lew BL. Alopecia neoplastica due to gastric adenocarcinoma metastasis to the scalp, presenting as alopecia: a case report and literature review. *Ann Dermatol* 2014; 26: 624-7.
- Kim MK, Kim SH, Lee YY, et al. Metastatic skin lesions on lower extremities in a patient with recurrent serous papillary ovarian carcinoma: a case report and literature review. *Cancer Res Treat* 2012; 44: 142-5.
- An MK, Park BW, Cho EB, Park EJ, Kim KH, Kim KJ. A case of cutaneous metastasis of nasopharyngeal carcinoma on the face. *Korean J Dermatol* 2019; 57: 80-3.
- Hong SG, Jo SY, Jeong HH, et al. Cutaneous metastasis originating from esophageal carcinoma: a case report. *Korean J Dermatol* 2020; 58: 269-72.
- Lee JY, Shin SJ, Yoo CS, Kil MS, Kim CW, Kim SS. A case of zosteriform cutaneous metastasis from lung cancer. *Korean J Dermatol* 2013; 51: 272-5.
- Choi ME, Jung CJ, Lee WJ, et al. Clinicopathological study of Korean patients with cutaneous metastasis from internal malignancies. *Australas J Dermatol* 2020; 61: e139-42.
- Brownstein MH, Helwig EB. Spread of tumors to the skin. *Arch Dermatol* 1973; 107: 80-6.
- Lookingbill DP, Spangler N, Sexton FM. Skin involvement as the presenting sign of internal carcinoma: a retrospective study of 7316 cancer patients. *J Am Acad Dermatol* 1990; 22: 19-26.
- Hu SC, Chen GS, Lu YW, Wu CS, Lan CC. Cutaneous metastases from different internal malignancies: a clinical and prognostic appraisal. *J Eur Acad Dermatol Venereol* 2008; 22: 735-40.
- Sittart JA, Senise M. Cutaneous metastasis from internal carcinomas: a review of 45 years. *An Bras Dermatol* 2013; 88: 541-4.
- Handa U, Kundu R, Dimri K. Cutaneous metastasis: a study of 138 cases diagnosed by fine-needle aspiration cytology. *Acta Cytol* 2017; 61: 47-54.
- Hong S, Won YJ, Park YR, et al. Cancer statistics in Korea: incidence, mortality, survival, and prevalence in 2017. *Cancer Res Treat* 2020; 52: 335-50.
- Gul U, Kilic A, Gonul M, Kulcu Cakmak S, Erinckan C. Spectrum of cutaneous metastases in 1287 cases of internal malignancies: a study from Turkey. *Acta Derm Venereol* 2007; 87: 160-2.
- Mok ZR, Yong AM, Leung AJ, Tan KB, Aw DC. Cutaneous metastasis: experience from a tertiary healthcare institution in Singapore. *Int J Dermatol* 2017; 56: 1497-8.
- Shah SR, Applebaum DS, Potenziani S, Huttenbach YT, Wolf J, Orenge IF. Cutaneous metastasis to the scalp as the primary presentation of colorectal adenocarcinoma. *Dermatol Online J* 2017 Nov 15 [Epub]. <http://dx.doi.org/10.5070/D32311037274>.
- Habermehl G, Ko J. Cutaneous metastases: a review and diagnostic approach to tumors of unknown origin. *Arch Pathol Lab Med* 2019; 143: 943-57.
- Hussein MR. Skin metastasis: a pathologist's perspective. *J Cutan Pathol* 2010; 37: e1-20.
- Yang DT, Holden JA, Florell SR. CD117, CK20, TTF-1, and DNA topoisomerase II-alpha antigen expression in small cell tumors. *J Cutan Pathol* 2004; 31: 254-61.
- Kervarrec T, Tallet A, Miquelostorena-Standley E, et al. Diagnostic accuracy of a panel of immunohistochemical and molecular markers to distinguish Merkel cell carcinoma from other neuroendocrine carcinomas. *Mod Pathol* 2019; 32: 499-510.
- Green AR, Young P, Krivinskas S, et al. The expression of ERalpha, ERbeta and PR in lobular carcinoma in situ of the breast determined using laser microdissection and real-time PCR. *Histopathology* 2009; 54: 419-27.
- Matsuoka K, Ohsumi S, Takashima S, Saeki T, Aogi K, Mandai K. Occult breast carcinoma presenting with axillary lymph node metastases: follow-up of eleven patients. *Breast Cancer* 2003; 10: 330-4.
- Gomez-Fernandez C, Daneshbod Y, Nassiri M, Milikowski C, Alvarez C, Nadjji M. Immunohistochemically determined estrogen receptor phenotype remains stable in recurrent and metastatic breast cancer. *Am J Clin Pathol* 2008; 130: 879-82.
- Liu H. Application of immunohistochemistry in breast pathology: a review and update. *Arch Pathol Lab Med* 2014; 138: 1629-42.
- Monaco SE, Wu Y, Teot LA, Cai G. Assessment of estrogen receptor (ER), progesterone receptor (PR), and human epidermal growth factor receptor 2 (HER2) status in the fine needle aspirates of metastatic breast carcinomas. *Diagn Cytopathol* 2013; 41: 308-15.
- Werling RW, Yaziji H, Bacchi CE, Gown AM. CDX2, a highly sensitive and specific marker of adenocarcinomas of intestinal origin: an immunohistochemical survey of 476 primary and metastatic carcinomas. *Am J Surg Pathol* 2003; 27: 303-10.
- Kandalaf PL, Gown AM. Practical applications in immunohistochemistry: carcinomas of unknown primary site. *Arch Pathol Lab Med* 2016; 140: 508-23.

Sarcomatoid urothelial carcinoma arising in the female urethral diverticulum

Heae Surng Park

Department of Pathology, Ewha Womans University Seoul Hospital, Seoul, Korea

A sarcomatoid variant of urothelial carcinoma in the female urethral diverticulum has not been reported previously. A 66-year-old woman suffering from dysuria presented with a huge urethral mass invading the urinary bladder and vagina. Histopathological examination of the resected specimen revealed predominantly undifferentiated pleomorphic sarcoma with sclerosis. Only a small portion of conventional urothelial carcinoma was identified around the urethral diverticulum, which contained glandular epithelium and villous adenoma. The patient showed rapid systemic recurrence and resistance to immune checkpoint inhibitor therapy despite high expression of programmed cell death ligand-1. We report the first case of urethral diverticular carcinoma with sarcomatoid features.

Key Words: Sarcomatoid carcinoma; Urothelial carcinoma; Urethral diverticulum

Received: March 9, 2021 **Revised:** April 16, 2021 **Accepted:** April 23, 2021

Corresponding Author: Heae Surng Park, MD, PhD, Department of Pathology, Ewha Womans University Seoul Hospital, Ewha Womans University College of Medicine, 260 Gonghang-daero, Gangseo-gu, Seoul 07804, Korea
 Tel: +82-2-6986-5253, Fax: +82-2-6986-3423, E-mail: turtle98p@naver.com

Urethral diverticular carcinoma (UDC) is extremely rare; the most common histological subtype is adenocarcinoma [1,2]. Sarcomatoid urothelial carcinoma (UC) is also unusual. Due to the scarcity of UDC and sarcomatoid UC, related studies have been limited to small series and single case reports. Herein, we report the first case of sarcomatoid UC of the female urethral diverticulum and her treatment response to immune checkpoint inhibitor therapy.

CASE REPORT

A 66-year-old woman with dysuria was referred to the urology department after visiting the emergency room and undergoing several urinary catheterization procedures. She was hospitalized for a cerebral infarction 7 months prior and had a history of cholecystectomy owing to acute cholecystitis 6 months before. A urethral diverticulum was identified through abdominopelvic computed tomography (CT) performed during admission for cholecystectomy (Fig. 1A), although no urological evaluation was conducted at that time. On presentation, abdominopelvic CT revealed a large mass involving the urethra, posterior wall of the

urinary bladder, and vagina with enlarged lymph nodes at both femoral, both inguinal, and both internal and external iliac areas (Fig. 1B). Ultrasound-guided transvaginal core needle biopsy of the urethral mass was performed, and histopathological examination revealed unspecified spindle cell sarcoma with stromal sclerosis. The patient underwent anterior pelvic exenteration with pelvic lymph node dissection.

The surgical specimen showed a 10-cm-sized, hard white mass in the urethra that had invaded the uterine cervix, anterior wall of the vagina, posterior wall of the urinary bladder, and perivesical fat (Fig. 2A). The cut surface of the mass showed central necrosis with cystic space formation. Histopathologically, the tumor was predominantly composed of pleomorphic spindle cells with moderate to severe nuclear atypia, brisk mitosis, and necrosis (Fig. 2B). The tumor nuclei were oval shaped and had vesicular chromatin and prominent nucleoli. The tumor occasionally produced abundant collagen, but neither specific mesenchymal differentiation nor a heterologous component was observed. Intratumoral lymphoplasmacytic infiltration was noted. The cystic space was focally lined by urothelial or glandular epithelium (Fig. 2C) and associated villous adenoma (Fig. 2D).

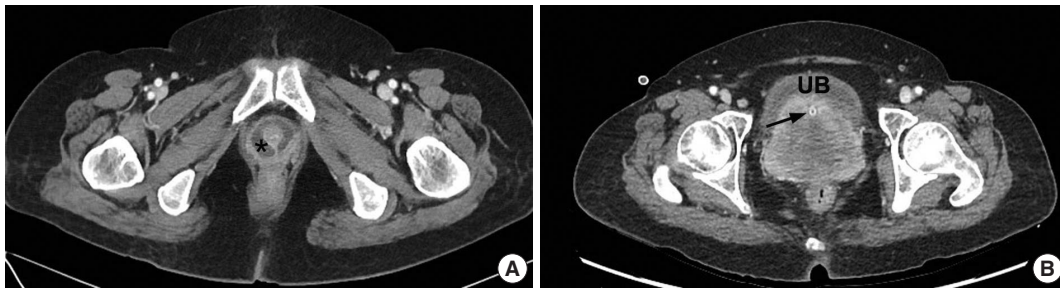


Fig. 1. Enhanced abdominopelvic computed tomography. (A) Axial image taken 7 months prior to presentation showed a urethral diverticulum (asterisk) at the level of the symphysis pubis. (B) Preoperative image revealed a large urethral mass (UB, urinary bladder; arrow, urinary catheter within the urethra).

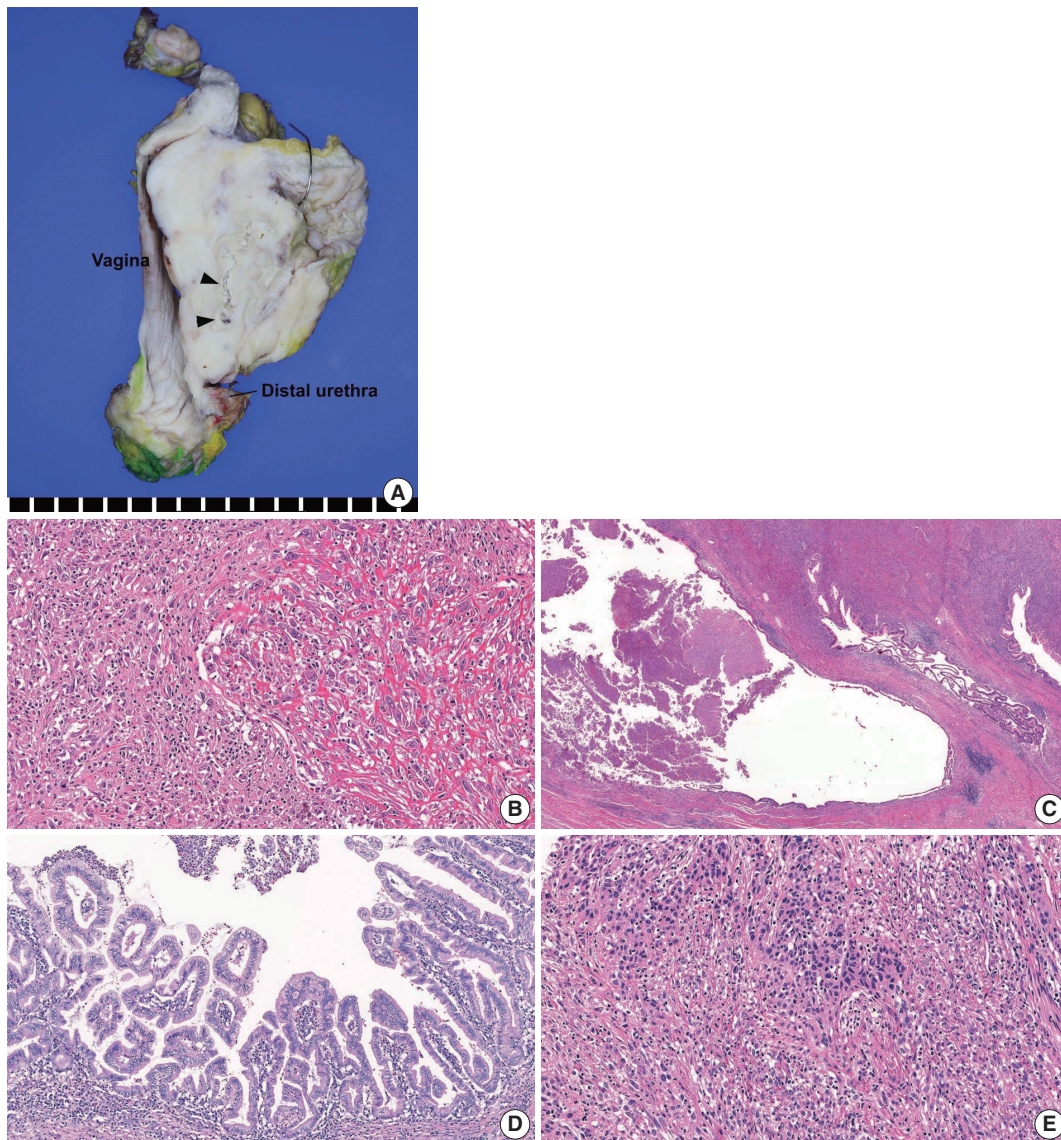


Fig. 2. Histopathological findings. (A) Gross examination revealed a 10-cm-sized, hard white urethral mass invading the uterus, vagina, urinary bladder, and perivesical fat. The cut surface showed necrosis and cystic space (arrowheads). (B) Microscopically, the majority of the tumor was composed of pleomorphic spindle cells with occasional collagen deposition. Intratumoral lymphoplasmacytic infiltration was noted. (C, D) The cystic space was lined focally by glandular epithelium (C) and associated villous adenoma (D). (E) A conventional urothelial carcinoma component was minimally present, and areas of epithelial-to-mesenchymal transition were noted.

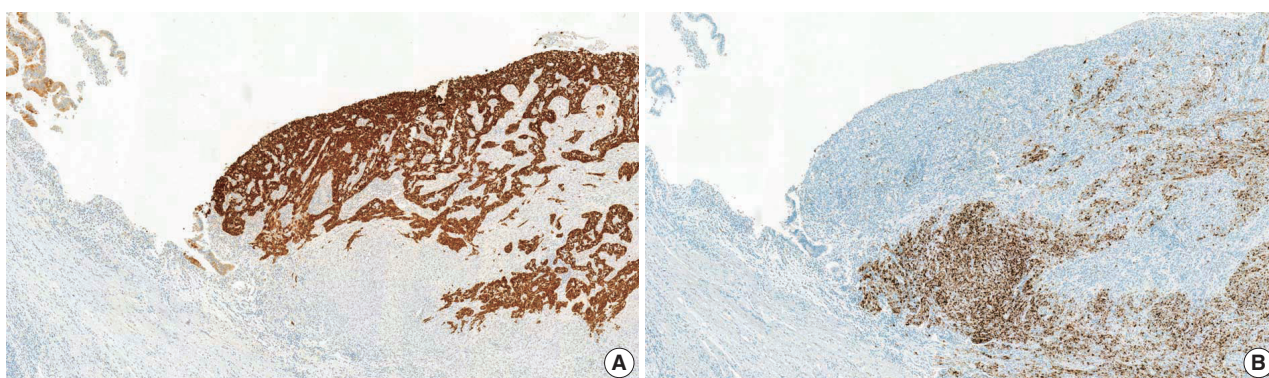


Fig. 3. Results of immunohistochemical staining. (A) Immunostaining for cytokeratin 7 highlighted the glandular epithelium (left side) and urothelial carcinoma component, whereas there was no staining of the sarcoma component. (B) Programmed death ligand-1 SP142 (Ventana Medical Systems, Tucson, AZ, USA) immunostaining showed diffuse positivity (90%) in tumor-infiltrating immune cells (ICs) of the sarcoma component, while ICs of the carcinoma component were negative.

The lining epithelium and premalignant lesion were juxtaposed with tumor tissue, suggesting tumor formation in the urethral diverticulum. A minimal conventional urothelial carcinoma component was present (less than 1%) near the diverticulum, and areas of epithelial-to-mesenchymal transition were noted (Fig. 2E). Although lymphovascular invasion was present, nodal metastasis was not identified among the 30 pelvic lymph nodes. Immunohistochemical staining for cytokeratin (CK) 7 highlighted the glandular epithelium and invasive carcinoma component (Fig. 3A). The invasive carcinoma component was positive for high molecular weight CK, p63, and GATA3, indicating a urothelial nature. Urothelial carcinoma in situ was not identified. Spindle cell component was negative for panCK, CK7, GATA3, p63, smooth muscle actin, myoglobin, anaplastic lymphoma kinase (clone, 5A4), S-100, and human melanoma black-45 immunostaining, but positive for vimentin. Programmed death ligand-1 (PD-L1) SP142 (Ventana Medical Systems, Tucson, AZ, USA) immunohistochemistry showed diffuse positivity (90%) in tumor-infiltrating immune cells (IC) of the sarcoma component, while no positive ICs were identified in the urothelial carcinoma component (Fig 3B). PD-L1 immunostaining was performed using three different tissue sections and the results were similar. The final pathological diagnosis was sarcomatoid UC arising from the urethral diverticulum (pT4N0).

During follow-up, multiple newly developed lung nodules were detected on chest CT 49 days postoperative. The patient underwent one cycle of palliative chemotherapy (adriamycin and cisplatin), but showed intolerance to the chemotherapeutic agent, and the disease progressed. She next underwent four cycles of atezolizumab and radiation therapy, but the disease continued to progress. She then received gemcitabine plus cisplatin, and the

tumor showed a partial response, but tumor progression occurred after 4 months of treatment. The patient next received weekly paclitaxel for 2 months and exhibited stable disease. Recently, she stopped chemotherapy temporarily and is alive 24 months postoperative.

DISCUSSION

Primary female urethral carcinomas are rare, and the most common histological subtype is urothelial carcinoma (45%), followed by adenocarcinoma (29%), squamous cell carcinoma (19%), and undifferentiated carcinoma (6%), according to a national urethral cancer survey conducted in the Netherlands [3]. UDC is very unusual, accounting for only 5% of all female urethral carcinomas [1,2]. More than 120 cases of UDC have been reported, and adenocarcinoma is the most common pathology (75%), while urothelial carcinoma (15%) and squamous cell carcinoma (10%) are less frequent [1,2].

UDC is hypothesized to arise from a periurethral gland or metaplastic epithelium with chronic irritation, and Gartner or mesonephric duct remnants [2]. UDC might contain premalignant lesions such as villous adenoma, intestinal metaplasia, or high-grade dysplasia [4]. The present case is suggestive of tumor origination from metaplastic change because of its relation to the glandular epithelium as well as villous adenoma.

The sarcomatoid variant of urothelial carcinoma is rare, but has been reported in the urinary bladder [5], bladder diverticulum [6], ureter [7], renal pelvis [8], and urethra [9]. As far as we know, this is the first case report of sarcomatoid UC arising from a urethral diverticulum. One meta-analysis showed that sarcomatoid urothelial carcinoma of the bladder tended to present as more

advanced disease than conventional urothelial carcinoma, which might lead to worse survival outcomes [5]. Sarcomatoid urothelial carcinoma is defined as a biphasic tumor composed of both malignant epithelial and mesenchymal elements, and the latter element is morphologically indistinguishable from sarcoma [10,11]. For most cases, the carcinomatous component is urothelial, but variable degrees of squamous cell carcinoma, adenocarcinoma, and small cell carcinoma components can be present [10,11]. The sarcomatous component is reported to constitute 20% to 100% of the tumor volume [12] and usually presents as undifferentiated high-grade sarcoma [11]. A heterologous component can be seen, most commonly osteosarcoma, followed by chondrosarcoma, leiomyosarcoma, rhabdomyosarcoma, liposarcoma, and angiosarcoma [10,11]. In tumors in the urinary system and those exclusively consisting of malignant spindle cells, the first differential diagnostic consideration should be sarcomatoid UC, since it can show a wide range of morphologies, and primary sarcoma of the urinary tract is rare. In such cases, extensive gross examination and immunohistochemistry must be performed to confirm the existence of a carcinoma component. In this case, transvaginal needle biopsy showed only high-grade sarcoma, suggesting primary urethral sarcoma. However, a very small urothelial carcinoma component was identified in the surgically resected specimen after extensive tissue examination.

Recently, immune checkpoint inhibitor therapy has demonstrated anti-tumor effects in advanced urothelial carcinoma. Atezolizumab is a Food and Drug Administration (FDA)-approved anti-programmed death-1/PD-L1 agent used for the treatment of advanced bladder cancer. PD-L1 SP142 immunohistochemistry was approved by the FDA as a companion diagnostic test in urothelial carcinoma patients based on the results of a phase 2 clinical trial, IMvigor210 [13]. However, a phase 3 randomized controlled trial, IMvigor211 [14], revealed higher PD-L1 SP142 expression ($\geq 5\%$ positivity in ICs) to be associated with response to both atezolizumab and chemotherapy in patients with platinum-treated locally advanced or metastatic urothelial carcinoma. Li et al. [15] evaluated PD-L1 SP142 expression in bladder UC and showed that the sarcomatoid variant was significantly associated with higher PD-L1 expression. In our case, the UDC showed high PD-L1 SP142 expression (IC 90%), but the tumor progressed despite atezolizumab administration. The PD-L1-negative urothelial carcinoma component could be the driver of progression in this patient, although the progressed lesion was not confirmed histologically. We report a very unusual case of sarcomatoid UC in the female urethral diverticulum, which showed aggressive behavior and resistance to atezolizumab therapy de-

spite high PD-L1 expression. Consideration of a broad range of histologic features is needed to diagnose sarcomatoid UC of the urinary system.

Ethics Statement

This study was approved by the Institutional Review Board (IRB) of Ewha Womans University Seoul Hospital (IRB No. 2021-02-23) and the need for informed consent was waived.

Availability of Data and Material

All data generated or analyzed during the study are included in this published article.

Code Availability

Not applicable.

ORCID

Heae Surng Park <https://orcid.org/0000-0003-1849-5120>

Conflicts of Interest

The author declare that they has no potential conflicts of interest.

Funding Statement

No funding to declare.

References

- Ahmed K, Dasgupta R, Vats A, et al. Urethral diverticular carcinoma: an overview of current trends in diagnosis and management. *Int Urol Nephrol* 2010; 42: 331-41.
- O'Connor E, Iatropoulou D, Hashimoto S, Takahashi S, Ho DH, Greenwell T. Urethral diverticulum carcinoma in females: a case series and review of the English and Japanese literature. *Transl Androl Urol* 2018; 7: 703-29.
- Derksen JW, Visser O, de la Riviere GB, Meuleman EJ, Heldeweg EA, Lagerveld BW. Primary urethral carcinoma in females: an epidemiologic study on demographical factors, histological types, tumour stage and survival. *World J Urol* 2013; 31: 147-53.
- Rajan N, Tucci P, Mallouh C, Choudhury M. Carcinoma in female urethral diverticulum: case reports and review of management. *J Urol* 1993; 150: 1911-4.
- Gu L, Ai Q, Cheng Q, et al. Sarcomatoid variant urothelial carcinoma of the bladder: a systematic review and meta-analysis of the clinicopathological features and survival outcomes. *Cancer Cell Int* 2020; 20: 550.
- Lembo F, Subba E, Lagana AS, Vitale SG, Valenti G, Magno C. Intradiverticular sarcomatoid carcinoma of the bladder: an overview starting from a peculiar case. *Urol J* 2016; 13: 2800-2.
- Wang Y, Liu H, Wang P. Primary sarcomatoid urothelial carcinoma of the ureter: a case report and review of the literature. *World J Surg Oncol* 2018; 16: 77.
- Rashid S, Akhtar M. Sarcomatoid variant of urothelial carcinoma of the renal pelvis with inferior vena cava tumour thrombus: a case report and literature review. *Case Rep Pathol* 2018; 2018: 1837510.
- D'Arrigo L, Costa A, Fraggetta F, Pennisi M, Pepe P, Aragona F. Carcinosarcoma of the female urethra. *Urol Int* 2016; 96: 370-2.
- Moch H, Humphrey PA, Ulbright TM, Reuter VE. WHO classifica-

- tion of tumours of the urinary system and male genital organs. 4th ed. Lyon: International Agency for Research on Cancer, 2016; 92.
11. Bostwick DG, Cheng L. Urologic surgical pathology. 3rd ed. Philadelphia: Saunders-Elsevier, 2014; 298-9.
 12. Sanfrancesco J, McKenney JK, Leivo MZ, Gupta S, Elson P, Hansel DE. Sarcomatoid urothelial carcinoma of the bladder: analysis of 28 cases with emphasis on clinicopathologic features and markers of epithelial-to-mesenchymal transition. *Arch Pathol Lab Med* 2016; 140: 543-51.
 13. Balar AV, Galsky MD, Rosenberg JE, et al. Atezolizumab as first-line treatment in cisplatin-ineligible patients with locally advanced and metastatic urothelial carcinoma: a single-arm, multicentre, phase 2 trial. *Lancet* 2017; 389: 67-76.
 14. Powles T, Duran I, van der Heijden MS, et al. Atezolizumab versus chemotherapy in patients with platinum-treated locally advanced or metastatic urothelial carcinoma (IMvigor211): a multicentre, open-label, phase 3 randomised controlled trial. *Lancet* 2018; 391: 748-57.
 15. Li H, Zhang Q, Shuman L, et al. Evaluation of PD-L1 and other immune markers in bladder urothelial carcinoma stratified by histologic variants and molecular subtypes. *Sci Rep* 2020; 10: 1439.

Metastatic gastric cancer of the testis diagnosed through urine cytology

Mee Sook Roh, Song-Hee Han

Department of Pathology, Dong-A University College of Medicine, Busan, Korea

Gastric carcinoma (GC) is the most common malignancy in Korea [1]. The common metastatic sites of GC include the regional lymph nodes, liver, peritoneum, bone marrow, and lung. Metastasis of GC to the male genital tract, including the testis, epididymis, scrotum, and spermatic cord, is exceptionally unusual in clinical practice [2]. Although previous studies have reported fewer than 30 cases in the past 70 years, detection of metastatic gastric adenocarcinoma in urine cytology is unique [2].

GC has varied histologic features, which causes problems with diagnosis through urine cytology. Our case emphasizes the importance of considering secondary lesions involving the testis in the urine cytology of relatively young patients. Although a clinical history of GC is a clue to diagnosis, this clinical information is not always available.

CASE REPORT

A 44-year-old male was admitted to our hospital with a history of swelling and pain in the left scrotum for 3 months. He was diagnosed with gastric tubular adenocarcinoma, moderately differentiated at another hospital in July 2016 (Fig. 1). He underwent radical subtotal gastrectomy for GC at another hospital and was classified as American Joint Committee on Cancer pathologic stage pT3N3. One year later, the patient received postoperative adjuvant chemotherapy with FOLFOX (oxaliplatin plus fluorouracil and leucovorin) for 14 cycles. The ensuing computed tomography scan suggested massive peritoneal seeding. Staging laparoscopic examination revealed intraperitoneal dis-

seminated nodules in the transverse and sigmoid colon and the liver. The patient received 21 courses of intraperitoneal chemotherapy for 20 months. Five months later, the patient presented with progressive scrotal pain and swelling. Scrotal ultrasonography revealed an ill-defined hypoechoic lesion and a large fluid collection in the left scrotal sac. His serum levels of lactate dehydrogenase (LDH), α -fetoprotein (AFP), and β -human chorionic gonadotropin (β -HCG) were normal. Routine voided urine cytology (ThinPrep, Hologic, Inc., Marlborough, MA, USA) revealed numerous, overlapping, 2-dimensional sheets with central lumina formation (Fig. 2A). The tumor cells showed vacuolated cytoplasm with moderate nuclear pleomorphism, coarse chromatin, and prominent nucleoli (Fig. 2B). Radical orchiectomy was performed at the same time. On gross examination, the testis was replaced partly by an infiltrating whitish mass measuring 3.4×1.6 cm (Fig. 1C). Histologically, the tumor showed irregularly distended or fused tubular or glandular structures in a background of atrophic testis (Fig. 1D). The cells exhibited variable amounts of intraluminal mucin with nuclear pleomorphism. Abundant lymphatic and vascular invasions were observed. Based on the pathologic features of the patient's previous original hematoxylin and eosin slide and his clinical history, a diagnosis of metastatic adenocarcinoma from urine cytology and surgical specimen was established. Although the patient subsequently received chemoradiotherapy, he died of complications two months later.

DISCUSSION

In cases with a clinical history of gastric cancer, diagnosis of metastasis based on cytology is uncomplicated and can be confirmed through review of hematoxylin and eosin-stained slides and immunohistochemistry. For cases that lack clinical history of a primary lesion, however, the differential diagnosis is difficult and supported by few features, especially in urine cytology.

Received: March 30, 2021 Revised: April 16, 2021
Accepted: April 19, 2021

Corresponding Author: Song-Hee Han, MD
Department of Pathology, Dong-A University College of Medicine, 32 Daesingongwon-ro, Seo-gu, Busan 49201, Korea
Tel: +82-51-240-2863, Fax: +82-51-243-7396, E-mail: pshsh625@gmail.com

The first consideration for differential diagnosis of abnormal cells on urine cytology is primary urinary bladder cancer, including high-grade urothelial carcinoma (HGUC) and adenocarcinoma [3,4].

The differential diagnosis should include non-urothelial neoplasms, such as metastases from other lesions and primary testis neoplasms either by direct invasion or lymphohematoge-

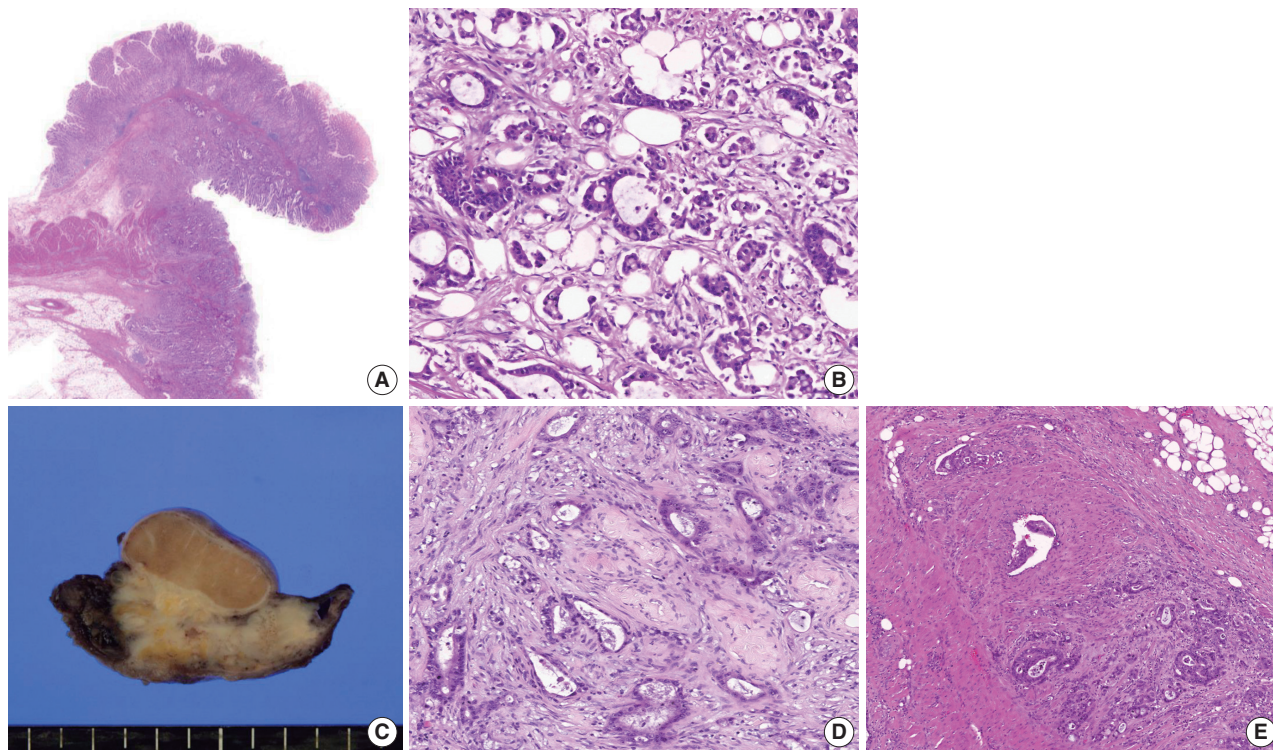


Fig. 1. Representative image of hematoxylin and eosin staining of a specimen from subtotal gastrectomy (A, B). In a radical orchiectomy specimen, an infiltrating whitish mass shows involvement of the testis (C). Histologically, this tumor is composed of an atypical glandular structure (D) that is frequently found in lymphovascular spaces (E), compatible with metastatic adenocarcinoma.

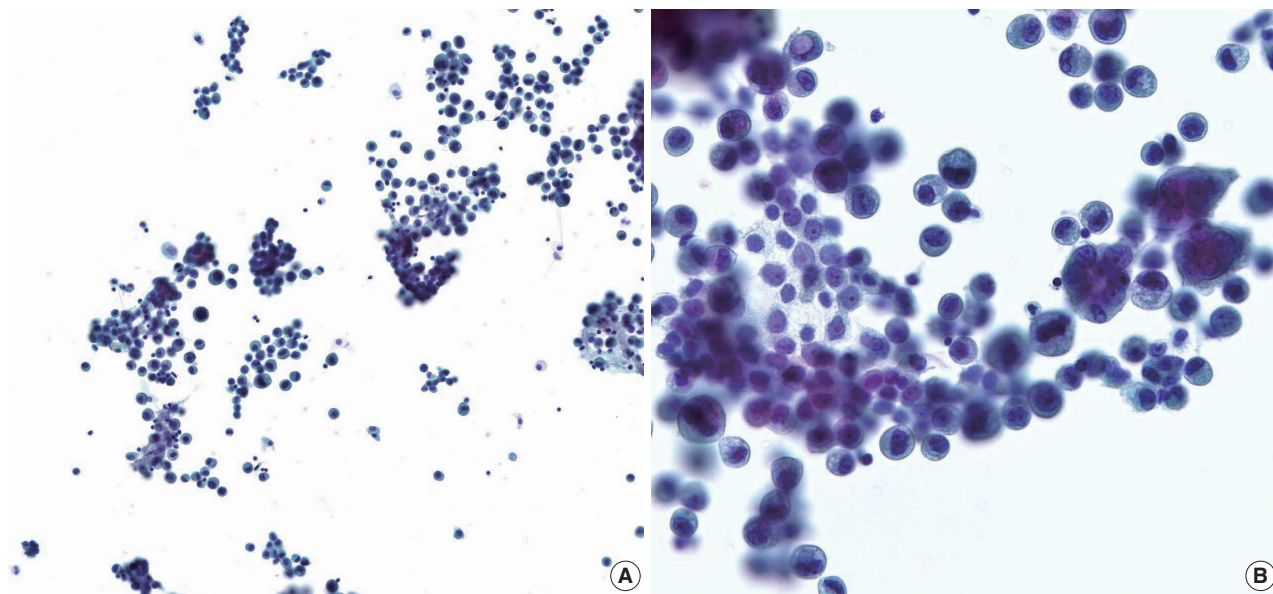


Fig. 2. Representative image of urine cytology on liquid-based preparation. (A) Voided urine cytology reveals numerous, crowded, overlapped clusters with occasional luminal formations. (B) Tumor cells show granular and vacuolated cytoplasm with moderate nuclear pleomorphism.

nous dissemination [3,4]. Relatively abundant and vacuolated cytoplasm is important in the differential diagnosis of HGUC. The absence of large uniform cells with dis-cohesion mixed with lymphocytes helps distinguish seminoma, the most common neoplasm of the testis [4]. However, metastatic adenocarcinoma and primary adenocarcinoma of the urinary bladder might be indistinguishable because they are fairly similar to their counterparts in organs such as the stomach, colon, and prostate [3,5]. When encountered with this diagnostic challenge, physicians can use certain clinical and morphological characteristics to differentiate metastatic lesions. The average age at diagnosis of metastasis to the testis is older than 50 years (range, 23 to 72 years) [2]. In contrast, patients with primary testicular tumors are rarely older than 40 years [6], and those with HGUC typically are older than 70 years [7]. Tumor markers in the serum also contribute to the differential diagnosis. Carbohydrate antigen 19-9 [8,9] and carcinoembryonic antigen [9] levels, related to GC, along with AFP, LDH, and β -HCG levels, related to primary tumors of the testis, are different according to clinical settings. Furthermore, metastatic symptoms include a palpable mass in the groin with or without pain, scrotal swelling, and hydrocele [2]. A review of the patient's clinical manifestations and histologic features can suggest metastatic lesions.

Progressive GC metastasis to the testis is extremely rare, has a poor prognosis, and is a diagnostic challenge [2]. For cases that include the possibility of metastasis, urine cytology can be a helpful screening method when correlated with clinical history of secondary lesions, especially in the testis.

Ethics Statement

This study was approved by Dong-A University Hospital Institutional Review Boards (DAUHIRB-TEMP-21-059) and informed consent was waived.

Availability of Data and Material

The datasets generated or analyzed during the study are available from the corresponding author on reasonable request.

Code Availability

Not applicable.

ORCID

Mee Sook Roh <https://orcid.org/0000-0002-5676-5569>
Song-Hee Han <https://orcid.org/0000-0002-4564-7014>

Author Contributions

Conceptualization: MSR, SHH. Data curation: MSR, SHH. Funding acquisition: SHH. Investigation: MSR, SHH. Writing—original draft: SHH. Writing—review & editing: MSR. Approval of final manuscript: all authors.

Conflicts of Interest

The authors declare that they have no potential conflicts of interest.

Funding Statement

No funding to declare.

References

- Hong S, Won YJ, Park YR, et al. Cancer statistics in Korea: incidence, mortality, survival, and prevalence in 2017. *Cancer Res Treat* 2020; 52: 335-50.
- Dai W, Liu D, Zuo J, et al. Metastatic tumor of male genital system from gastric cancer: a case report and review of literature. *Int J Clin Exp Pathol* 2017; 10: 8592-8.
- Bardales RH, Pitman MB, Stanley MW, Korourian S, Suhrlund MJ. Urine cytology of primary and secondary urinary bladder adenocarcinoma. *Cancer* 1998; 84: 335-43.
- Alsharif M, Aslan DL, Jessurun J, Gulbahce HE, Pambuccian SE. Cytologic diagnosis of metastatic seminoma to the prostate and urinary bladder: a case report. *Diagn Cytopathol* 2008; 36: 734-8.
- Tian Y, Yao W, Yang L, Wang J, Wazir R, Wang K. Primary adenocarcinoma of the rete testis: a case report and review of the literature. *Oncol Lett* 2014; 7: 455-7.
- Li B, Cai H, Kang ZC, Wu H, Hou JG, Ma LY. Testicular metastasis from gastric carcinoma: a case report. *World J Gastroenterol* 2015; 21: 6764-8.
- Hassan M, Solanki S, Kassouf W, et al. Impact of implementing the Paris system for reporting urine cytology in the performance of urine cytology: a correlative study of 124 cases. *Am J Clin Pathol* 2016; 146: 384-90.
- Kato K, Taniguchi M, Kawakami T, et al. Gastric cancer with a very high serum CA 19-9 level. *Case Rep Gastroenterol* 2011; 5: 258-61.
- Cainap C, Nagy V, Gherman A, et al. Classic tumor markers in gastric cancer: current standards and limitations. *Clujul Med* 2015; 88: 111-5.

